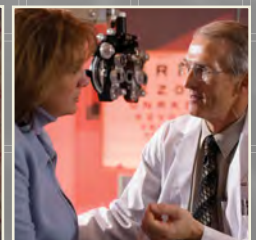
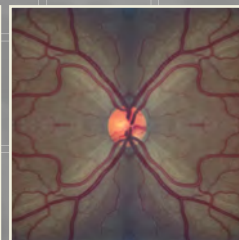
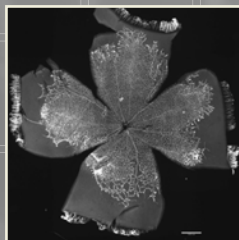
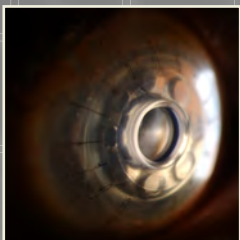
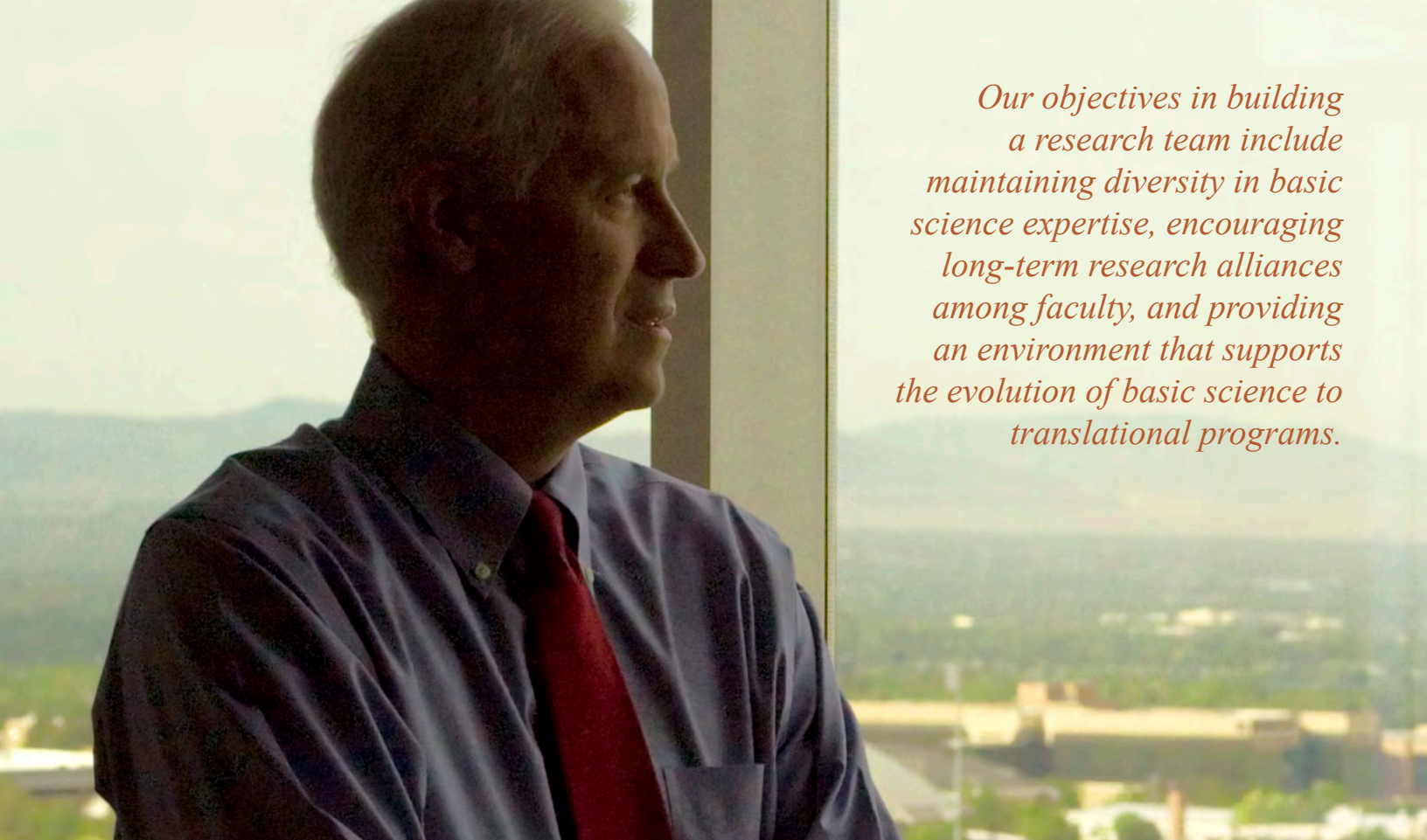




*The
John A. Moran
Eye Center*

Research and
Clinical Abstracts
2010 - 2011





Our objectives in building a research team include maintaining diversity in basic science expertise, encouraging long-term research alliances among faculty, and providing an environment that supports the evolution of basic science to translational programs.

Contents

- 2** ARVO 2011 Abstracts
- 30** Research at the Moran Eye Center
- 32** Retinal Research
- 47** Advanced Experimental Methods
- 48** **Highlight:** The Hartnett Laboratory
- 50** Visual Cortex Research
- 51** Developmental Research
- 54** **Highlight:** The Hageman Laboratory
- 56** Translational Research
- 64** **Highlight:** The DeAngelis Laboratory
- 66** Clinical Research: Anterior Segment
- 74** Clinical Research: Posterior Segment
- 77** Clinical Articles/Reports
- 82** **Highlight:** New Vision Institute
- 84** Donor Report



Photos Courtesy of Bryan William Jones.
Collaborators: Brenda Stringham, Greg Jones, Bryan William Jones, and Nathan Galli.

Randall J. Olson, MD

Professor, Chair and CEO of the John A Moran Eye Center;
Director of the University of Utah Vision Institute

The Department of Ophthalmology and Visual Sciences at the University of Utah School of Medicine continues to prosper. We were recently recognized by the state of Utah as their newest Institute (the third in the Health Sciences Center) with programs that extend well beyond the Department. The Vision Institute has programs that stretch from the Department of Obstetrics and Gynecology, Bioengineering and Computer Science to several out-of-state cancer hospitals and the Departments of Neuroscience and Anatomy and Human Genetics at our own University to name a few. Complex inquiry is no longer possible in a vacuum, and we consider this just a start with the Vision Institute a program that is not limited by our walls; just by our imagination and effort.

In the last year we have been very pleased to add two important researchers who bring mature programs of inquiry to the Vision Institute. Meg De'Angelis, PhD joined us from Harvard as a tenure track Associate Professor of Ophthalmology and Visual Sciences with expertise in the genetics of macular degeneration. She has joined Greg Hageman in aggressively pursuing this disease. Mining the information available in the Utah Population Database has required a team of investigators with its over eight million participants in large interlocking pedigrees. We are very excited about the new information that has been gleaned by Greg and Meg just in the short time they have been here.

ME Hartnett, MD has also joined us as a tenured Professor of Ophthalmology and Visual Sciences. She represents the true triple threat player and we are most fortunate to have her clinical skills, especially in Pediatric Retina as well as her research programs both in retinopathy of prematurity and macular degeneration. M. E. has already put together many collaborations both inside and outside our department. She has already proven herself a valuable addition to our faculty. So the Vision Institute research mission is alive, well and flourishing in Salt Lake City!

No matter our NIH funding level or number of publications, what is most important is how well we meet our translational mission. To this end we are dedicated and hope to be able to measure true success by making a difference in people's lives!

Sincerely,
Randall J Olson, MD

**Robert Marc, PhD**

Director of Research

The Moran Eye Center houses researchers whose studies span the development of the eye to the organization of cortex; the basis of phototransduction to the genetics of retinal diseases; the synaptology of the retina to neuroprosthetics. These efforts are enhanced by strong graduate programs and a tradition of interdepartmental collaboration. Our principles include maintaining basic science expertise, fostering research alliances, and accelerating the evolution of translational science programs.

**Paul Bernstein, MD, PhD**

Director of Clinical Research

The Clinical Research Group at the Moran Eye Center focuses on research that directly impacts the patient. Whether this means working with industry sponsors to run a clinical trial investigating a new drug or a clinician initiated study to systematically compare standard of care treatments, the Clinical Research Group is focused on finding the optimal in patient care. In this year alone, we have 45 clinical trials and research studies underway involving more than 550 patients. This work is shared with the global ophthalmic community in over 33 publications just this year.

**Gregory Hageman, PhD**

Director of Translational Research

The Moran Center for Translational Medicine (CTM) was recently created to expedite the pace at which basic scientific discoveries are translated into clinically effective diagnostics and therapies for the treatment of devastating eye disorders such as age-related macular degeneration and glaucoma, as well as other diseases. The conceptual framework for the CTM derived from a growing realization that seemingly disparate diseases likely share common etiologies and thus, common therapeutic targets. The CTM will draw upon the collective strengths and expertise of a collaborative team of cell biologists, molecular microbiologists, pathologists and clinicians to expedite its translational mission. The unique resources, clinical acumen and scientific expertise of the CTM will complement the core competencies of collaborating corporate and academic partners to insure its success.



ARVO 2011

VISIONARY GENOMICS

Short Hairpin RNA Delivered By Adeno-associated Virus Vectors (aav.shRNA) Induces Retinal Degeneration Via Extracellular And Intracellular TLR3

Ling Luo^{1,2}, Hironori Uehara^{1,2}, Subrata K Das^{1,2}, Bonnie Archer^{1,2}, Jacquelyn M. Simonis^{1,2}, Nirbhai Singh^{1,2}, Ying Liu¹, Thomas Olsen^{1,2}, Judd Cahoon¹, Balamurali K. Ambati^{1,2}. ¹Ophthalmology, University of Utah, Salt Lake City, UT. ²Salt Lake City VAHCS, Salt Lake City, UT

Purpose: To determine whether short hairpin RNA delivered by adeno-associated virus vectors (aav.shRNA) induces retinal neurotoxicity.

Methods: An adeno-associated viral vector encoding shRNA conjugated and green fluorescent protein (aav.siRNA.GFP, 0.3X10⁹GC/ul) was performed as treatment and the same concentration of adeno-associated viral vectors expressing GFP (aav.GFP) without shRNA or PBS were performed as controls. 10 days after intravitreal or subretina injection(1ul) in wild type or TLR3^{-/-} mice, fundi were examined in vivo by autofluorescence and optical coherence tomography (OCT) using the Heidelberg Spectralis. IFN-gamma and IL-12 levels were evaluated by ELISA. Retina was also observed in vitro by transmission electron microscope and stained by Tunnel staining. In situ hybridization was performed to show the shRNA localization. The primary human RPE cells

were transfected by the same set of aav.shRNA.GFP (1x10⁹GC/8cm²) and then the cytotoxicity was evaluated. The rescued experiment was performed by TLR3 antibodies and chloroquine. hRPE barrier function was tested by trans Epithelium Resistance(TER).

Results: Retinal degeneration and ruptured RPE layer RPE were easily found at 10 days after aav.shRNA. GFP treatment in wild type mice but not in controls and in TLR3^{-/-} mice. The levels of IFN-gamma and IL-12 treated with aav.shRNA.GFP increased significantly (n=8, P< 0.05) than the controls but no differences among each group in TLR3^{-/-}. Tunnel staining showed the photoreceptors apoptosis and retinal degeneration. TEM disclosed the increased vacuoles and pigments lost in RPE and abnormal junction between the PRE and disorganized segments. These abnormalities were only found in aav.siRNA.GFP treatment group but not in aav.GFP or PBS control in wild type mice. In situ hybridization showed shRNA localized in the outer nuclear layers primarily after intravitreal injection. The density of RPE cells dramatically decreased after aav.shRNA.GFP transfection 5 days than aav.GFP (n=6, p=3.2E-17) and PBS (N=6, P<3.4E-17). TLR3 antibodies & Chloroquine increased (1 hour) both extracellularly and intracellularly the density of RPE cells (n=6, p<0.0005). RPE barrier function dramatically and consistently decreased during one month after aav.shRNA.

GPF transfection.

Conclusions: aav.shRNA induces significant retinal neurotoxicity via activation of extracellular and intracellular TLR3.

Program#/Poster#: 10/A1
Presentation Time: Sunday, May 01, 8:30 AM -10:15 AM Session Number: 103 Session Title: Retina, Photoreceptors and RPE. Location: Hall B/C Reviewing Code: 354 retina/RPE: gene regulation/transcription - BI

An Enzymatically Switchable Sink in the Rod Inner Segments: A Model for Slow Return of Transducin to the Outer Segments

Wolfgang Baehr, Ryan Constantine, Houbin Zhang. Ophthal & Vis Sci Lab, Univ of Utah Sch of Med, Salt Lake City, UT.

Purpose: UNC119/HRG4 is a protein with sequence similarity to PrBP/ δ /Pde6 δ . A homolog of *C. elegans* UNC-119, it is expressed ubiquitously in multiple tissues, and abundantly in photoreceptor inner segments and synaptic terminals. We previously identified UNC119 as a novel acyl-binding protein with specificity for the transducin alpha subunit (T α). The purpose of this study is to study interaction of UNC119 with T α .

Methods: Isothermal titration mi-

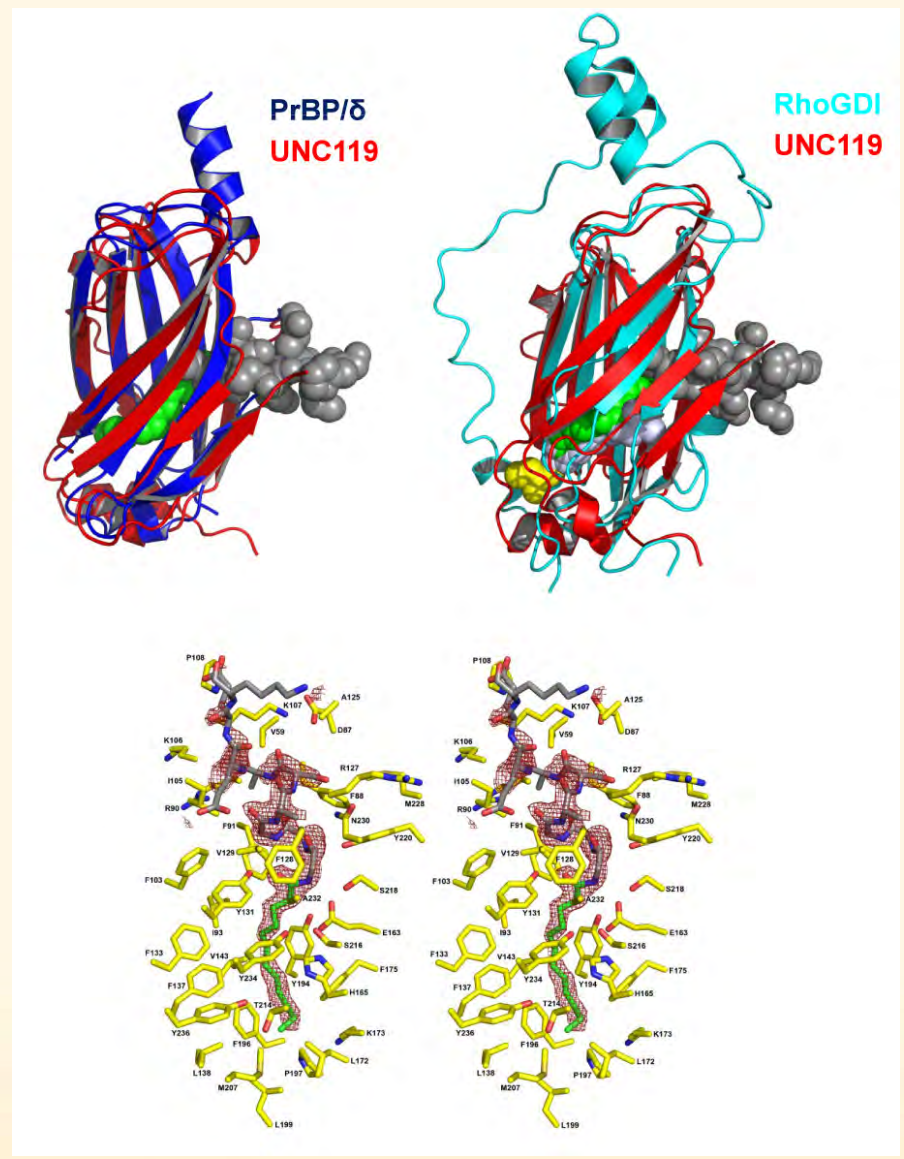
crocalorimetry (ITC), GTPase assay, co-crystallization of lauroyl-GAGAS-AEEKH ($T\alpha$ peptide) with UNC119, immunohistochemistry, diffusion model of UNC119/ $T\alpha$ -GTP.

Results: Isothermal titration calorimetry of UNC119 with an acylated N-terminal peptide of $T\alpha$ shows tight interaction ($K_d = 0.3 \mu M$). Reconstitution of purified transducin with depleted ROS membranes and UNC119 reveals that UNC119 inhibits the endogenous GTPase activity of $T\alpha$. Co-crystallization of UNC119 with acylated $T\alpha$ peptide demonstrates that the $T\alpha$ lipid chain is buried deeply into UNC119's hydrophobic cavity formed by an immunoglobulin-like β -sandwich fold. The UNC119 cavity is lined predominantly by hydrophobic residues (mostly Phe and Tyr) that mediate interaction with the lauroylated $T\alpha$ peptide primarily by Van der Waals forces, consistent with properties of a lipid binding site.

Interaction of UNC119 with full-length $T\alpha$ requires the $T\alpha$ GTP bound form. Translocation of $T\alpha$ to the inner segment during illumination is independent of UNC119, but full return to the outer segment during darkness is UNC119-dependent. Formation of the diffusible complex $T\alpha$ GTP/UNC119 requires GTP/GDP exchange on membranes in the inner segment in the absence of its GEF (rhodopsin). We suggest that slow GDP/GTP exchange and slow formation of $T\alpha$ GTP/UNC119 in the inner segment is a rate-limiting step in return of transducin to the outer segments in darkness.

Conclusions: We propose a model for the return of transducin to the outer segment by diffusion. The enzymatically switchable sink in the inner segments is controlled by slow GDP/GTP exchange in the absence of the GEF, rhodopsin, and low levels of UNC119 relative to transducin.

Program#/Poster#: 57/A48
 Presentation Time: Sunday, May 01, 8:30 AM -10:15am. Session Number: 103, Session Title: Retina, Photoreceptors and RPE. Location: Hall B/C



Gene Therapy For Gucy2d Leber Congenital Amaurosis (LCA1)

Shannon E. Boye^{1A}, Sanford L. Boye^{1A}, Thomas Conlon^{1B}, Kirsten E. Erger^{1B}, Jijing Pang^{1A}, Xuan Liu^{1A}, Sukanya Karan², Wolfgang Baehr², William W. Hauswirth^{1A}. ^AOphthalmology, ^BPediatrics, ¹University of Florida, Gainesville, FL; ²Ophthalmology, University of Utah, Salt Lake City, UT.

Purpose: We have previously shown that subretinal injection of serotype 5 Adeno-associated viral (AAV) vectors containing the murine GC1 cDNA driven by either the photoreceptor-specific human rhodopsin kinase (hGRK1) or the ubiquitous (smCBA) promoter were capable of restoring cone-mediated function and visual behavior and preserving cone photo-

receptors in the GC1KO mouse for at least three months. In the present series of experiments, we evaluated whether long term therapy was achievable in this mouse model. Additionally, we examined whether delivery of GC1 to photoreceptors of the GC1/GC2 double knockout mouse (GCdko), a model which exhibits loss of both rod and cone structure and function and phenotypically resembles human LCA1, would confer therapy to these cells.

Methods: Subretinal injections of AAV5-hGRK1-mGC1, AAV5-smCBA-mGC1 or the highly efficient capsid tyrosine mutant AAV8(Y733F)-hGRK1-mGC1 were performed in one eye of GC1KO or GCdko mice between postnatal day 14 (P14) and P25. Rod and cone photoreceptor function were assayed electroretinographically.

Localization of therapeutic GC1 expression and extent of cone photoreceptor preservation were determined by immunohistochemistry. Biodistribution studies were used to evaluate the presence of vector genomes in optic nerves and brains of treated animals.

Results: Cone photoreceptor function was restored in GC1KO mice treated with all vectors, with AAV8(733) being the most efficient. Responses were stable for at least 10 months post-treatment. Therapeutic GC1 was found in photoreceptor outer segments. By 10 months post-injection, AAV5 and AAV8(733) vector genomes were detected only in the optic nerves of treated eyes of GC1KO mice. AAV8(733)-vectored mGC1 restored function to both rods and cones in treated GCdko mice.

Conclusions: We demonstrate for the first time that long-term therapy is achievable in a mammalian model of GC1 deficiency, the GC1KO mouse. Importantly, therapy is also achievable in the GCdko mouse which mimics the LCA1 rod/cone phenotype. Our results provide proof-of-principle information for the development of an AAV-based gene therapy vector for treatment of LCA1.

Program#/Poster#: 493/D1140
Presentation Time: Sunday, May 01, 8:30 AM -10:15 AM Session Number: 117 Session Title: Nanomedicine, Nanopharmaceuticals, Tissue Bioengineering, Regenerative Medicine, and Nanodiagnosics. Location: Hall B/C Reviewing Code: 204 gene therapy - NT

Evaluation of the Capsular Bag Diameter with a Modified Capsular Tension Ring in Human Donor Eyes Using the Miyake-Apple Technique

Rakhi Jain¹, Liliana Werner², Nick Mamalis². ¹Implant R&D, Abbott Medical Optics Inc., Santa Ana, CA; ²Department of Ophthalmology, John A. Moran Eye Center, University of Utah, Salt Lake City, UT.

Purpose: The goal of this ex vivo

study was to compare the measurements of empty capsular bag diameter of human cadaver eyes using a modified capsular tension ring system and surgical calipers, using the Miyake-Apple technique.

Methods: A total of 9 human cadaver eyes (age range: 48 to 75 years) were used in this study. White-to-white diameter, equatorial diameter and axial length were measured and anterior chamber depth was measured using ultrasound biomicroscopy (UBM). The globes were prepared for surgery using the Miyake-Apple technique and, after removal of the cornea and iris, the capsular bag diameter was measured in two meridians with surgical calipers before and after lens extraction. After the modified capsular tension ring was implanted, the capsular bag was measured in two meridians using calipers as well as the ring measurement system.

Results: The mean natural lens diameter of the human eye was 9.57 mm (range: 9.2 - 9.95 mm). The mean capsule bag diameter increased slightly after lens extraction to 9.75 mm (range 9.6 - 9.85). The mean capsular bag diameter measured with the modified capsular tension ring using the ring measurement system/viscoelastic was 10.32 mm (range: 10.0 mm to 10.65 mm). There was no difference in the measurements (no measurement variation greater than 0.1 mm) of the empty capsular bag with the ring with and without viscoelastic. The capsular bag diameters measured with ring measurement system/viscoelastic were slightly larger than the measurements with surgical calipers (mean 10.11 mm, range: 9.9 - 10.4 mm).

Conclusions: It is difficult to measure the diameter of the evacuated capsular bag in vivo. The modified capsular tension ring system may be used to measure the capsular bag diameter intra-operatively. In the peer-reviewed literature, it is well understood that the sizing of accommodating intraocular lenses (IOLs) is a critical parameter in optimal performance. The modified capsular tension ring system may aid in the understanding of IOL sizing and optimization of accommodative am-

plitude.

Program#/Poster#: 23/D971
Presentation Time: Sunday, May 01, 11:15 AM - 1:00 PM. Session Number: 132. Session Title: Crystalline Lens, Presbyopia, Accommodation and Its Restoration Location: Hall B/C

Rap1 GTPase Is Involved In RPE Cell Barrier Function

Erika S. Wittchen¹, Keith Burridge¹, M Elizabeth Hartnett². ¹Cell and Developmental Biology, University of North Carolina, Chapel Hill, NC; ²Moran Eye Center, University of Utah, Salt Lake City, UT.

Purpose: To determine whether the small GTPase Rap1 regulates the formation and maintenance of retinal pigment epithelial (RPE) cell junctional barrier.

Methods: We utilized ARPE-19 cells as an *in vitro* cell culture model to study retinal pigment epithelial barrier properties. To dissect the role of Rap1 in this process, we used two techniques to inhibit Rap1 function: overexpression of RapGAP protein, which acts as a negative regulator of endogenous Rap1 activity, as well as treatment with engineered, adenovirally-transduced microRNAs designed to knockdown Rap1 protein expression. Transepithelial electrical resistance (TER) and real-time cellular analysis (RTCA) of electrical impedance were used as readouts for monolayer barrier properties. Immunofluorescence microscopy was used to visualize localization of cadherins, both under steadystate conditions, and during junctional reassembly following calcium switch. Choroidal endothelial cell (CEC) transmigration across RPE monolayers was quantified to assess choroidal neovascularization under conditions of Rap1 inhibition in RPE.

Results: Both knockdown of Rap1 or inhibition of its activity in RPE reduces steadystate TER and electrical impedance of ARPE-19 cell monolayers. The loss of barrier function is also reflected by the mislocalization of

cadherin and formation of gaps within the monolayer. TER measurement and immunofluorescent staining of cadherins after a calcium switch indicate that junctional reassembly kinetics are also impaired after the loss of Rap1 protein or its activity. Furthermore, CEC transmigration is significantly higher in Rap1-knockdown ARPE-19 monolayers compared to control.

Conclusions: Rap1 GTPase is an important cellular regulator of RPE cell-cell junctions, and is required for maintenance and formation of barrier function. Our observation that RPE monolayers lacking Rap1 allow greater transmigration of CECs suggests a possible role for potentiating choroidal neovascularization during the pathology of neovascular age-related macular degeneration.

Program#/Poster#: 863/A55
Presentation Time: Sunday, May 01,
3:15 PM - 5:00 PM. Session Number:
142 Session Title: RPE: Cell Biol-
ogy and Disease . Location: Hall B/C
Reviewing Code: 353 retina/RPE:
cell biology - RC

Effect Of Tissue-specific Disruption Of Porcupine On Mouse Eye Development

Sabine Fuhrmann^{1A}, Mary P. Colasanto^{1A}, Charles Murtaugh^{1B}, Elizabeth J. Bankhead^{1A}. ^AOphthal & Vis Sci, ^BHuman Genetics, ¹University of Utah, Salt Lake City, UT.

Purpose: During fetal development, the formation of the neural retina, retinal pigment epithelium (RPE) and anterior eye segment require highly coordinated tissue-tissue interactions and complex patterning events. The molecular signals that mediate these processes are not well understood. Excellent candidate signals are the Wnt ligands that control key processes during development and disease such as proliferation, cell fate decisions, tissue polarity and regeneration. The O-acyltransferase Porcupine (*Porcn*) is required for posttranslational modification regulating secretion and signaling activity of Wnts. PORCN deficiency in humans causes Focal Dermal Hypoplasia (FDH, Goltz Syndrome), an X-linked dominant multisystem birth

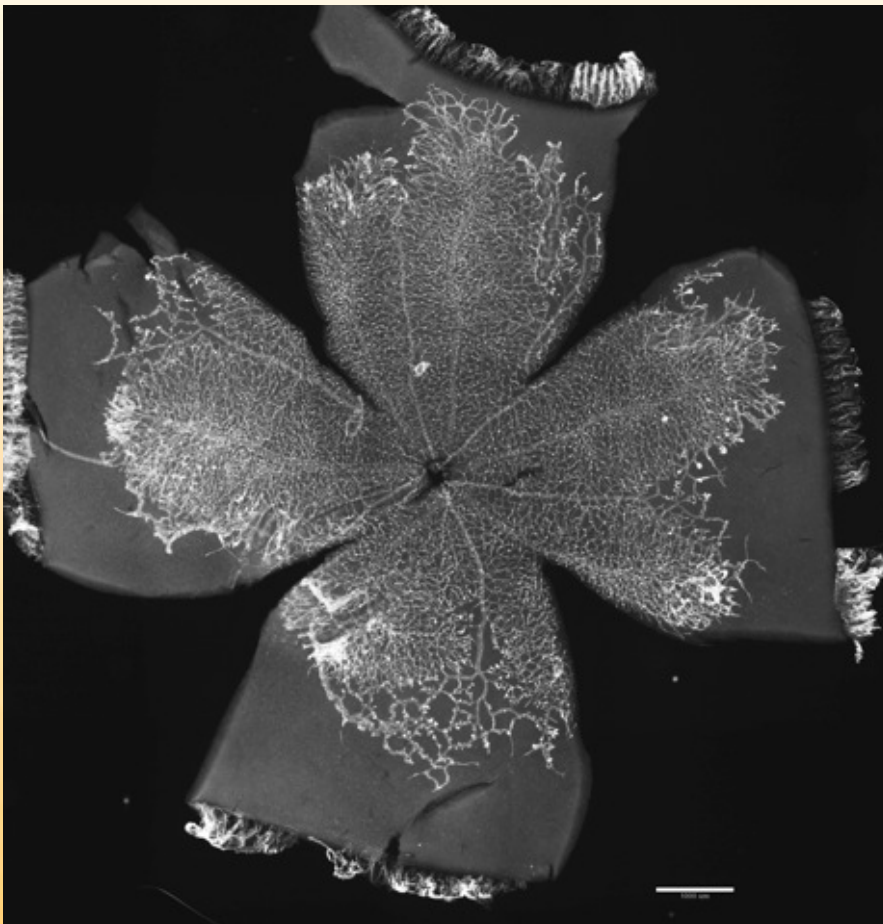
defect that is frequently accompanied with ocular abnormalities resulting in coloboma, microphthalmia or, in severe cases, in anophthalmia. To gain insight into the contribution of canonical and non-canonical Wnt signaling during eye development, we are conditionally disrupting the *Porcn* gene in mouse.

Methods: The conditional *Porcn* allele was generated by inserting loxP sites flanking exons 2-3. Thus, Cre-mediated recombination eliminates the start codon and the first 3 predicted transmembrane domains of the protein, likely producing a null or strong loss-of function allele. *Porcn* is disrupted in the developing mouse eye using tissue-specific Cre lines, and mutant eyes are analyzed by histological and immunohistochemical techniques.

Results: Eye-specific disruption of *Porcn* results in defects with variable frequency, such as microphthalmia, coloboma and shortened presumptive ciliary body. Initial immunohistochemical analysis showed that Otx1/2 antibody labeling is detectable in mutant RPE using different ocular Cre lines. However, our preliminary data suggest that retina-specific disruption of *Porcn* causes transdifferentiation of the dorsal RPE into retina.

Conclusions: Our studies indicate that expression of *Porcn* is critical for early eye development in mouse. Some of the observed defects are not detected upon interference with canonical Wnt signaling alone suggesting either a novel role for non-canonical Wnt signaling or a Wnt-independent function of *Porcn* during ocular development.

Program#/Poster#: 912/A104
Presentation Time: Sunday, May 01,
3:15 PM - 5:00 PM. Session Number:
143, Session Title: Retina and RPE
Cell Biology. Location: Hall B/C



Htra1 Transgenic Mice Manifest Polypoidal Choroidal Vasculopathy Phenotypes Identified In Human Genetic Association Studies

Alex D. Jones¹, Sandeep Kumar¹, Ning Zhang¹, Heather Fillerup¹, Chio Oka², Zhenglin Yang^{1,3}, Robert E. Marc¹, Balamurali K. Ambati¹, Kang Zhang⁴, Yingbin Fu¹. ¹Ophthalmology, University of Utah, Salt Lake City, UT; ²Division of Gene Function in Animals, Nara Institute of Science and Technology, Takayama, Ikoma, Nara, Japan; ³The Key Laboratory for Human Disease Gene Study of Sichuan Province, Changdu, China; ⁴Institute for Genomic Medicine and Shiley Eye Center, University of California San Diego, La Jolla, CA.

Purpose: Age-related macular degeneration (AMD) is the leading cause of irreversible blindness in the elderly. Wet AMD can be categorized by typical choroidal neovascularization (CNV) and polypoidal choroidal vasculopathy (PCV). The etiology and pathogenesis of CNV and PCV are not well understood. Genome-wide association studies have linked a multifunctional serine protease, HTRA1, to AMD. However, the precise role of HTRA1 in AMD remains unknown. To clarify the role of HTRA1 in AMD pathogenesis, we generated a mouse line (hHTRA1+) overexpressing human HTRA1 in mouse RPE.

Methods: The expression of human HTRA1 in hHTRA1+ mice was determined by real-time RT-PCR, western blotting and immunohistochemistry. The phenotypes of hHTRA1+ mice were examined by fluorescein angiography (FA), indocyanine green angiography (ICGA), fundus imaging, spectral-domain optical coherence tomography (SD-OCT), histology and electron microscopy (EM). The VEGF level was analyzed by western blotting and immunohistochemistry.

Results: Human HTRA1 was specifically expressed in the RPE of hHTRA1+ mice. On ICGA, hHTRA1+ mice exhibited cardinal features of PCV: polypoidal lesions resembling grape clusters and a network of branching abnormal vessels. In

late phase FA, senescent hHTRA1+ mice showed speckled hyperfluorescence with poorly demarcated leakage, resembling occult CNV. SD-OCT showed that the lesions were located beneath the RPE. Histology staining revealed serous exudation and abnormally dilated, thin-walled blood vessels in the choroid. These features are similar to histopathologic findings on surgically excised human PCV specimens. EM analysis showed that the tunica media and elastic laminae of choroidal arteries were severely degenerated or completely lacking. Both the RPE and photoreceptors showed atrophic changes. Another prominent feature of the hHTRA1+ mice was that the integrity of the Bruch's membrane was severely compromised as occurred in human CNV patients. Moreover, increased HTRA1 leads to the upregulation of VEGF in the RPE and choroid.

Conclusions: Our results demonstrate that increased HTRA1 is sufficient to cause PCV, and is a significant risk factor for CNV.

Program#/Poster#: 948/A140
Presentation Time: Sunday, May 01,
3:15 PM - 5:00 PM. Session Number:
144, Session Title: Age-related Macular Degeneration Animal Models.
Location: Hall B/C

Enzymatic And Regulatory Properties Of The Native Isozymes Of Retinal Guanylyl Cyclase, RetGC1 And RetGC2

Alexander M. Dizhoor¹, Elena V. Olshevskaya¹, Krzysztof Palczewski², Sukanya Karan³, Wolfgang Baehr³, Andrey B. Savchenko¹, Igor V. Peshenko¹. ¹Pennsylvania College of Optometry, Salus University, Elkins Park, PA; ²Case Western Reserve University, Cleveland, OH; ³University of Utah, Salt Lake City, UT.

Purpose: Retinal guanylyl cyclase (RetGC) in vertebrate photoreceptors is present as two isozymes, RetGC1 and RetGC2. Both RetGC1 and RetGC2 accelerate rod recovery from excitation when stimulated by Ca²⁺/Mg²⁺-binding guanylyl cyclase activating

proteins (GCAPs). However, the biochemical properties and the relative contribution of these isozymes to the overall cGMP synthesis in rod outer segments (ROS) are poorly understood. This study represents the first biochemical characterization of the native RetGC1 and RetGC2 isozymes in mouse ROS membranes.

Methods: *Gucy2F* or *Gucy2E* gene knockout mice were bred into GCAPs1,2^{-/-} double knockout background in order to functionally isolate RetGC1 or RetGC2, respectively. Mouse ROS were then purified by density gradient centrifugation and assayed for their GCAPs- and Ca²⁺-sensitive cyclase regulation.

Results: Basal RetGC activity measured at low free Ca²⁺ and physiological free Mg²⁺ in ROS isolated from GCAPs1,2^{-/-} mice was <3 nmol cGMP/min/mg rhodopsin, and GCAP1 and GCAP2 added at saturating concentrations increased the overall RetGC activity ~25 and 11-fold, respectively. Native RetGC1 was stimulated by GCAP1 and GCAP2 ~23 and 12-fold, whereas RetGC2 was stimulated at least 8 and 6-fold, respectively. Under the same conditions, the maximal activity of RetGC1 was ~5-times greater than RetGC2 activity. The native RetGC isozymes displayed similar apparent affinity for GCAP2 (1~2 μM), and RetGC1 displayed slightly higher (~1 μM) than RetGC2 (~4 μM) affinity for GCAP1. Calcium inhibited activation of each RetGC isozyme by GCAP1 and GCAP2 at EC₅₀ ~140 and 60 nM [Ca]_{free}, respectively, consistently with the GCAPs properties determined *in vitro* and *in vivo*. There was no detectable Ca²⁺-sensitive cyclase activity in the retinas lacking both RetGC1 and RetGC2.

Conclusions: Both GCAP1 and GCAP2 can efficiently stimulate native RetGC1 and RetGC2 isozymes *in vitro*. The affinity of GCAP1 for RetGC1 is slightly higher than for RetGC2, but both GCAPs stimulate RetGC1 and RetGC2 within the estimated range of the free GCAP concentrations in ROS. Ca²⁺-sensitivity of RetGC is determined by GCAP affinity for Ca²⁺, and does not depend on the

particular cyclase isozyme. RetGC1 contributes substantially more than RetGC2 to the total cGMP synthesis in rods, therefore, the reason why rods lacking RetGC1 are known to quickly recover from excitation remains to be determined.

Program#/Poster#: 1181/D1041
 Presentation Time: Sunday, May 01,
 3:15 PM - 5:00 PM. Session Number:
 153, Session Title: Photoreceptors.
 Location: Hall B/C

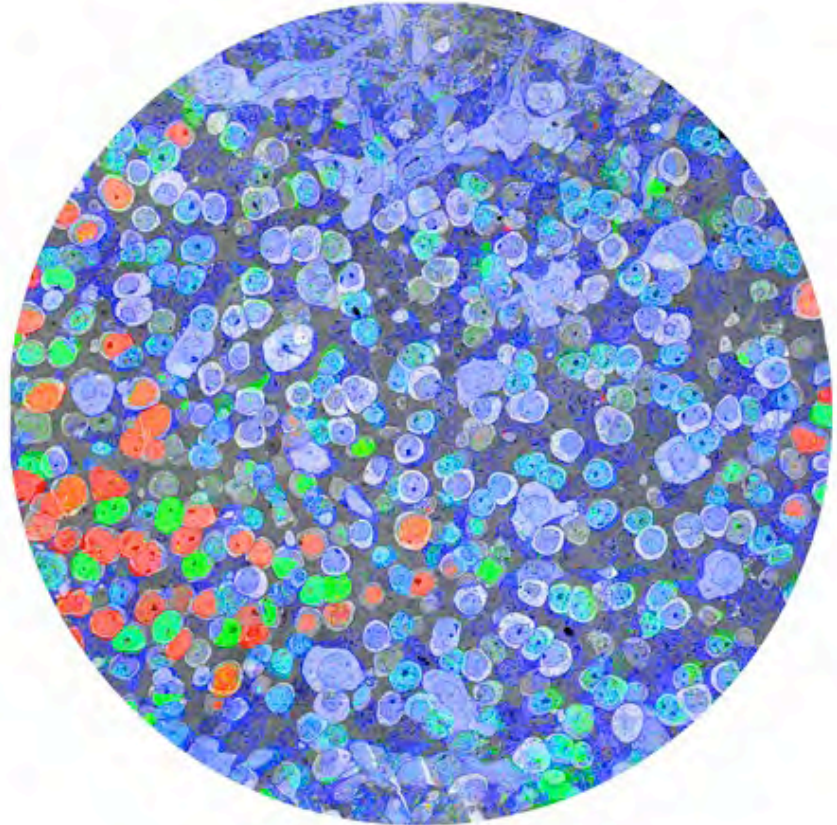
The Retinal Connectome: Amacrine-Amacrine Networks

Robert E. Marc, S. James Lauritzen,
 Bryan W. Jones, Carl B. Watt, Shoeb
 Mohammed, James R. Anderson.
 Ophthalmology-Sch of Med, Univ of
 Utah/Moran Eye Center, Salt Lake
 City, UT.

Purpose: Chains of amacrine cell (AC) synapses are abundant in the retinal inner plexiform layer (IPL). We sought to discover the cellular networks using these chains and explore the topologies of their signal processing roles by connectomics.

Methods: AC networks in the ultrastructural rabbit retinal connectome RC1 were annotated with the Viking viewer and explored by 3D rendering and graph visualization of connectivity (Anderson et al. 2011 The Viking viewer for connectomics: scalable multi-user annotation and summarization of large volume data sets. *J Microscopy*: [doi: 10.1111/j.1365-2818.2010.03402.x]). RC1 contains embedded small molecule signals, e.g. 4-aminobutyrate (γ) and glycine (G), enabling robust amacrine cell classification. Multiplicative gain was used to assess potency for each motif.

Results: Inhibitory AC-AC chains form at least four fundamental motifs. (1) Crossover is the major AC-AC motif and occurs between rod and cone as well as ON and OFF channels, involving over 30 crossover configurations, 80% of which engage GACs, including AI > AII AC and starburst AC (SAC) > AII AC chains. These data show that AI and AII cells have



more complex interactions than previously reported. (2) Nested feedback is prominent within channels in cone bipolar cell (BC) networks where two different γ ACs are postsynaptic to a BC and at least one is presynaptic to the other AC. (3) Veto channels are formed by GAC and giant γ AC synapses on AI AC dendrites in the OFF layer of the IPL. This architecture suggests global control of AI ACs at the near-somatic level. (4) Deeply nested, dense SAC > SAC chains are abundant. If they are inhibitory, they would constrain lateral signal propagation in the SAC network.

Conclusions: Complex AC-AC chains are a central mechanism in fine-grain control of receptive field networks. Crossover networks are abundant and heavily engage GACs. Nested feedback is common in cone but not rod-driven networks, suggesting that they are associated with tuning bipolar cell dynamics. Veto channel architectures, so far, are unique to OFF cone channels targeting AI ACs. Deep homocellular nesting by SACs may play a role in restricting excitation spread. These motifs account for the majority of AC-AC chains.

Program#/Poster#: 1607
 Presentation Time: Monday, May 02,
 2:15 PM - 2:30 PM. Session Number:
 251 Session Title: Inner Retinal
 Circuitry. Location: Room 305

A Novel Method for Determining Choroidal Neovascularization Volumes in vivo

Thomas D. Olsen^{1A}, Ling Luo^{1A},
 Bonnie Archer^{1A}, Kyle Jackman^{1A},
 Ying Liu^{1A}, Krysten Zygmunt^{1B}, Ross
 Whitaker^{1B}, Balamurali K. Ambati^{1A}.
^AMoran Eye Center, ^BScientific Computing and Imaging Institute, ¹University of Utah, Salt Lake City, UT.

Purpose: Choroidal neovascularization (CNV) volumes calculated by laser confocal microscopy combined with immunostaining is the most common method for CNV analysis. However, it only can be used in vitro and the CNV baseline cannot be evaluated. We developed new software, Seg3D, (University of Utah Center for Biomedical Computing) and determined if it can be used for in vivo CNV volume calculations.

Methods: Laser induced CNV and aav.shRNA.sftf subretinal injection induced CNV were developed in C57BL6/j mice as CNV models. After 2 weeks-6 months, CNV was imaged by OCT & FA using Heidelberg Eye Explorer Spectralis HRA+OCT II and subsequently exported into the Seg3D program. The scaling factors for each dimension, x, y & z ($\mu\text{m}/\text{pixel}$), were recorded and the corneal curvature standard was changed from 7.7 to 1.75. Each lesion area, on 2 dimensional images, was outlined using the provided polyline tool in Seg3D. The total number of voxels inside the identified regions were counted and reported by Seg3D. The volume of each OCT image stack was calculated and then normalized by multiplying the number of voxels by the scaling factors for each dimension. Mice were euthanized and prepared for IHC staining immediately after Spectralis images were taken. The same CNV lesions were calculated using scanning laser confocal microscope after immunohistochemistry staining (Isolectin alexa fluor@546, invitrogen), as usual. The same z stack step size was used on both methods. Microsoft Excel was used to analyze the volume calculations of each method as well as the correlation statistic and average difference.

Results: The CNV volume calculated using Seg3D ($3.03 \times 10^6 \mu\text{m}^3$) was, on average, 2.5 times larger than the volumes ($1.21 \times 10^6 \mu\text{m}^3$) calculated using the laser confocal microscope ($n=19$, $P=0.0006$). The correlation statistical analysis showed 0.76 correlation between these two methods.

Conclusions: Seg3D software is the singular method for CNV volume calculations in vivo to date. It can be used to analyze on the animal experiments with a normalized baseline requirement, as well as can be used to evaluate AMD in patients.

Program#/Poster#: 1687/A82
Presentation Time: Monday, May 02, 1:45 PM - 3:30 PM. Session Number: 259, Session Title: AMD Clinical Trials III. Location: Hall B/C

The Effect Of Laser-induced CNV In Rap1b-deficient Mice

Eiichi Nishimura¹, Manabu McCloskey¹, Yanchao Jiang¹, George W. Smith¹, Haibo Wang¹, Ryohei Koide², Mary E. Hartnett¹. ¹Ophthalmology, John A Moran Eye Center, University of Utah, Salt Lake City, UT; ²Ophthalmology, Showa University School of Medicine, Tokyo, Japan.

Purpose: Previous studies suggested that the RPE can encapsulate choroidal neovascularization (CNV) in some cases of AMD and reduce severe vision loss. We studied mice with a knockout to an isoform of Rap1 (Rap1b), which has been reported to be important in junctional assembly and integrity of epithelial cells, to address the question whether Rap1 was important in containing CNV.

Methods: We used a well accepted laser induced model for CNV. A 532nm OcuLight GL laser (0.1sec, 100um, 150mW) (Iridex, CA) was used to cause laser injury in adult Rap1b knockout or control C57B16 mice. Four to six laser spots were delivered to each eye. Retinal images were taken using a spectral domain optical coherence tomography unit (sd-OCT; Bioprogen, NC) prior to and 3 and 7 days following laser. Seven days following laser injury, animals were euthanized and choroidal flat mounts were dissected and stained using isolectin B4 (GS-1B4, Alexa Fluor 568, Invitrogen, CA). Confocal microscopy (Olympus, Japan) and image J were used to obtain CNV volumes for each lesion. The images were measured by two masked reviewers. Lesions with obvious hemorrhage or bridging of CNV were excluded from analysis. Lesions from each eye were averaged and analyzed using the Student t test.

Results: In both wild-type and knockout mice, disruption of the layers of the retina and Bruch's membrane/RPE layers were found by sd-OCT. Over the ensuing days, less edema was noticed. CNV volume was significantly larger in knockout mice (749009 ± 364063 pixels) as compared to wild type (236913 ± 143627 ; $P < 0.01$).

Conclusions: The volumes of laser induced CNV in Rap1b-deficient mice were larger than those in control wild type mice. Rap1b may be important in containing the size of CNV induced by laser injury and warrants further study.

Program#/Poster#: 1802/A332
Presentation Time: Monday, May 02, 1:45 PM - 3:30 PM. Session Number: 262, Session Title: Dry and Wet AMD: Diagnostics, Mechanisms, and Therapies. Location: Hall B/C.

Cone Opsin Determines The Time Course Of Cone Photoreceptor Degeneration In Leber Congenital Amaurosis

Tao Zhang, Ning Zhang, Wolfgang Baehr, Yingbin Fu. Department of Ophthalmology & Visual Sciences, Moran Eye Ctr, Univ of Utah, Salt Lake City, UT.

Purpose: Mutations in RPE65 or lecithin-retinol acyltransferase (LRAT) disrupt 11-*cis*-retinal recycling and cause Leber congenital amaurosis (LCA), the most severe retinal dystrophy in early childhood. The objectives were to investigate why ventral and central cones degenerate much more rapidly than dorsal cones in murine LCA models (*Rpe65^{-/-}* and *Lrat^{-/-}*) and to explore why blue cone function is lost early in LCA patients.

Methods: We used the *Lrat^{-/-}* mouse model to examine our hypothesis that mouse S-opsin and human blue opsin are more likely to cause cone degeneration than mouse M-opsin and human red/green opsins in LCA animal models and human patients, respectively. Subcellular localization of mouse M and S opsins was examined by immunohistochemistry. The mRNA and protein levels of cone opsins were analyzed by real-time RT-PCR and western blotting, respectively, at three stages of cone degeneration: 1) P14, pre-degeneration; 2) P18, early-stage degeneration; 3) P30, late-stage degeneration. We used a cell culture system to examine subcellular distribution various human cone opsins in the absence of 11-*cis*-retinal. Since rods and cones share similarities in

the synthesis and transport of visual pigments, we replaced rhodopsin with S-opsin in *Lrat*^{-/-} rods to see whether it would accelerate rod degeneration.

Results: Although both M and S cone opsins mistrafficked as reported previously, mislocalized M-opsin was degraded whereas mislocalized S-opsin accumulated in *Lrat*^{-/-} cones before the onset of massive ventral/central cone degeneration. Since S-opsin was expressed at a higher level in the ventral and central regions than in the dorsal region of the mouse retina, our results may explain why ventral and central cones degenerate much more rapidly than dorsal cones in murine *Rpe65*^{-/-} and *Lrat*^{-/-} LCA models. S-opsin in *Lrat*^{-/-} cones was phosphorylated and ubiquitinated, suggesting that LCA shares etiology with conformational diseases in the brain. In addition, human blue opsin and mouse S-opsin, but not mouse M-opsin or human red/green opsins, aggregated to form cytoplasmic inclusions in transfected cells. Replacing rhodopsin with S-opsin in *Lrat*^{-/-} rods resulted in mislocalization and aggregation of S-opsin in the inner segment and the synaptic region of rods and dramatically accelerated rod degeneration.

Conclusions: Our results demonstrate that cone opsins play a major role in determining the degeneration rate of photoreceptors in LCA.

Program#/Poster#: 1813/A343
Presentation Time: Monday, May 02, 1:45 PM - 3:30 PM. Session Number: 263, Session Title: Photoreceptor Degeneration: Genetic and Experimental Models. Location: Hall B/C

CompAng1 Increases VE-cadherin Stability, Decreases Vascular Leakage and Increases Soluble VEGF Receptor 1 in the Diabetic Mouse Retina

Judd M. Cahoon, Hiro Uehara, Ling Luo, Thomas Olsen, Anthony Radoshevich, Yang K. Cho, Jacquelyn M. Simonis, Bonnie Archer, Bala Ambati. Ophthalmology and Visual Sciences, University of Utah, Salt Lake City, UT.

Purpose: Diabetes Mellitus, a metabolic disease affecting nearly eight percent of the United States population, is the leading cause of new blindness among adults aged 20-74 years. The pathology behind diabetic retinopathy most likely involves vascular leakage. The angiopoietin ligands 1 and 2 acting on the Tie2 receptor are known to be important in vasculature leakage. In our study we used the Ins2 Akita mouse as an animal model of diabetes and used a stable, soluble form of angiopoietin 1 called CompAng1 expressed via adeno-associated virus (AAV2_CompAng1) in the retina of Akita mice to determine whether CompAng1 can reduce diabetic vascular hyperpermeability.

Methods: One month following intravitreal injection of AAV2_CompAng1 or control AAV2.AcGFP into diabetic Akita mice we assessed levels of CompAng1 in the retina by Western blot as well its effect on vascular leakage by Evans blue assay. Alpha-SMA staining was used to assess effect on pericytes, while VE-cadherin, VEGF and VEGF receptor expression were assessed by Western blotting and RT-PCR.

Results: AAV2_CompAng1 induced retinal CompAng-1 expression and reduced vascular permeability in diabetic Akita mice to levels comparable to wild-type C57Bl/6 mice. We did not find any changes in pericyte number but did find an increase in vessel area in those mice treated with AAV2_CompAng1 (30.5% increase over control) in the absence of neovascularization. AAV2_CompAng1 increased VE-cadherin protein but not mRNA expression. Although no difference was found in VEGF receptor 2 and VEGF-A expression between AAV2_CompAng1 and control, we did observe an increase in soluble VEGF receptor 1 expression in mice treated with AAV2_CompAng1 compared to control. To elucidate the relationship between AAV2_CompAng1 and soluble VEGF receptor 1 we assessed Ets-1, a transcription factor whose binding sequence is present in the VEGF receptor 1 promoter as well as whose expression is stimulated by the Tie2-Angiopoietin 1 signaling cascade. Ets-

1 mRNA was increased 2.5-fold over control by AAV2_CompAng1.

Conclusions: AAV2_CompAng1 increases VE-cadherin protein stability through the up-regulation of soluble VEGF receptor 1, which is known to sequester VEGF-A preventing it from signaling the degradation of VE-cadherin. Ets-1 may have an important role in this process. Thus, AAV2_CompAng1 may be increasing the stability of VE-cadherin protein without increasing its transcription.

Program#/Poster#: 2099
Presentation Time: Monday, May 02, 4:15 PM - 4:30 PM. Session Number: 276, Session Title: Diabetic Retinopathy. Location: Floridian BCD

Novel Gene Expression Signatures Associated With AMD And Its Risk Factors

Aaron M. Newman¹, Natasha Gallo¹, Lisa Hancox², Norma Miller³, Carolyn Radeke¹, Don Anderson¹, Gregory Hageman³, Lincoln Johnson¹, Monte Radeke¹. ¹Neuroscience Research Institute, University of California, Santa Barbara, CA; ²Microbiology, University of Iowa, Iowa City, IA; ³Ophthalmology and Visual Sciences, University of Utah, Salt Lake City, UT.

Purpose: Both genetic and environmental risk factors for AMD have been identified, however the molecular processes underlying the disease remain poorly characterized. Utilizing global transcriptional analysis of a large collection of human RPE-choroid tissue samples, we sought to identify novel gene expression profiles associated with both AMD and its risk factors.

Methods: Human RPE-choroid RNA was purified from the macular and extramacular regions of 31 normal and 35 AMD donor eyes ranging in age from 9-101 years. Eyes were graded by established morphological criteria to determine disease state. Transcriptome profiling was performed using Agilent 4x44K whole genome microarrays and statistical analyses were performed using a novel unsupervised

clustering algorithm (AutoSOME), two-class comparisons (permuted p-value t-tests), and gene ontology analysis (DAVID web tool).

Results: Whole-transcriptome cluster analysis revealed expression modules associated with known physiological states, including a large cluster enriched for RPE signature genes and clusters enriched in genes for local and lymphocyte-mediated inflammation. Unexpectedly, none of the clusters correlate with the AMD disease state, possibly reflecting its heterogeneous nature and inherent noise in postmortem tissues. To identify genes associated with specific disease states, we employed an exhaustive class comparison approach. We identified ~1000 genes differentially expressed between the macula and extramacula, hundreds of genes associated with the aging RPE-choroid, and importantly, many genes associated with various AMD disease states and with the CFH genotype. Consistent with a role for inflammation in AMD, nearly all AMD disease states show elevated expression of a unique set of chemokines, revealing an AMD inflammatory signature. Further, expression of angiogenesis-related genes is elevated in CNV and apoptosis-related genes are elevated in GA. Finally, we found novel gene expression modules associated with the CFH Y402H locus that show step-wise increases or decreases in expression levels from YY to YH to HH genotypes.

Conclusions: We completed global transcriptome analysis of the largest set of RPE-choroid tissue samples analyzed to date, and identified novel gene sets with potential relevance to AMD. These data have potentially significant utility for the design of new AMD therapeutics.

Program#/Poster#: 2333/A605
Presentation Time: Monday, May 02, 3:45 PM - 5:30 PM. Session Number: 286, Session Title: Molecular Biology of Age-related Macular Degeneration. Location: Hall B/C

Conditional Ablation of Retinal Elov14 Reveals a Key Role in Synthesis of VLC-PUFAs and Photoreceptor Light Responses

Peter Barabas¹, Aihua Liu¹, Wei Xing¹, ZongZhong Tong¹, Yun-Zheng Le², Robert Anderson², Kang Zhang¹, Paul S. Bernstein¹, David Krizaj¹.

¹Department of Ophthalmology, University of Utah, Salt Lake City, UT; ²Medicine, Univ of Oklahoma Hlth Sci Ctr, Oklahoma City, OK.

Purpose: To compare biochemical, physiological and behavioral phenotypes incurred by the genetic ablation of the Elov14 elongase and by Elov14 mutations that impair trafficking of the Elov14 protein in the transgenic mouse model for autosomal dominant Stargardt disease type 3 (STGD3).

Methods: Rod and cone conditional knockout (cKO) mice were generated using the pLox/Cre system. WT1 and TG2 lines carried the human wild type or the human mutant allele (de- Δ ACTT at 790-794) in two copies, respectively. RT-PCR and IHC were used to characterize expression and localization of Cre recombinase and Elov14. Visual acuity and outer retinal physiology were assessed using the optomotor head tracking response and electroretinographic (ERG) analysis, respectively. Gas chromatography coupled with mass spectrometry (GC-MS) was used to determine retinal levels of docosahexaenoic acid (DHA), eicosapentaenoic acid (EPA) and C₂₄-C₃₄ very long chain polyunsaturated fatty acids (VLC-PUFAs).

Results: DHA and C₂₄ lipid content of rod cKO retinas did not change whereas there was a ~ 50% decrease in C₃₀-C₃₄ VLC-PUFAs. In contrast, a 43.3% decrease in DHA and 66.5% decrease in C24:5n3 content was measured in TG2 retinas together with undetectable content of C₃₀-C₃₄ VLC-PUFAs. TG2 mice showed a severe visual phenotype with visual acuity that decreased from 0.380±0.006 cyc/deg at 1 month to 0.046±0.030 cyc/deg at 7 months of age. In cone cKO mice, the photopic ERG a- and b-wave decreased by 42.6±11.8% and by 19.2±2.3%, respectively. No ERG

changes were observed in rod cKO animals.

Conclusions: Our data shows that Elov14, expressed in rod photoreceptors, is required for synthesis of retinal VLC-PUFAs in the C₃₀-C₃₄ range, but is not required for biosynthesis of C₂₀, C₂₄ lipids. Elov14 elimination from cones compromised the photopic ERG. The phenotype of transgenic mice carrying the human mutant allele was markedly more severe than the phenotype of mice lacking the Elov14 protein. We conclude that cone but not rod, retinal signaling is impaired by loss of Elov14. Moreover, STGD3 may be associated with wider loss of PUFAs and vision loss than expected from a simple loss of Elov14 protein.

Program#/Poster#: 2361/D624
Presentation Time: Monday, May 02, 3:45 PM - 5:30 PM. Session Number: 287, Session Title: Genetics I. Location: Hall B/C

Characterization Of Retinal Ganglion Cell Loss In A Mouse Model With Elevated IOP

Chun Ding¹, Ning Tian², Luosheng Tang¹. ¹Ophthalmology, The Second Xiangya Hospital, Changsha, China; ²Ophthalmology & Visual Science, University of Utah, Salt Lake City, UT.

Purpose: To characterize the retinal ganglion cell (RGC) loss in a mouse model with elevated IOP using an in vivo imaging approach.

Methods: A mouse model with elevated IOP was induced in WT mice and Thy1-CFP mice aged 3 to 6 months by injecting the microbeads into the anterior chamber. Awake IOP was measured every other day using a Tonolab tonometer after microbead injection. The degree of RGC loss in WT mice with elevated IOP was assessed quantitatively using immunohistochemical staining (both Brn3b and DAPI) of RGCs in fixed retina 1, 2, 3, and 4 weeks after IOP elevation. In Thy1-CFP mice with elevated IOP, the number of CFP-positive RGCs in the same area of retina was assessed every week

in vivo using a confocal scanning laser microscope for 6 weeks. The results from in vivo imaging of Thy1-CFP mice were compared with the results from WT mice with immunohistochemical staining.

Results: A progressive loss of RGC was found after IOP elevation with 5.2%, 11.2%, 19.6%, 26.6% of RGCs at 1, 2, 3 and 4 weeks after IOP elevation using immunohistochemical staining. In Thy1-CFP mice with elevated IOP, the earliest decrease of CFP-positive RGCs was detected at 2 days after IOP elevation. Three weeks after the IOP elevation, CFP-positive RGCs were reduced by 21%. CFP-positive RGCs continued to decrease in number over time and, 6 weeks after IOP elevation, CFP-positive RGCs were reduced by 30%. These results are comparable with the results from immunohistochemical staining of WT mice with elevated IOP.

Conclusions: Anterior chamber injection of microbead effectively induced IOP elevation and a progressive RGC death. In vivo confocal scanning laser microscope imaging provides an effective and noninvasive approach to monitor the progress of RGC damage.

Program#/Poster#: 2462/D725
Presentation Time: Monday, May 02, 3:45 PM - 5:30 PM. Session Number: 289, Session Title: Glaucoma Models and Mechanisms. Location: Hall B/C

Interaction Of Whirlin And Espin Provides A Potential Link Between The Ush2 Complex And Actin Filaments

Le Wang¹, Junhuang Zou², Zuolian Shen², Jun Yang². ¹Ophthalmology, The First Affiliated Hospital of Jilin University, China and University of Utah, Salt Lake City, UT; ²Ophthalmology, John A Moran Eye Center, Salt Lake City, UT.

Purpose: Whirlin, *USH2A* and *VLGR1* are the three causative genes of Usher syndrome type II (USH2), a condition with both retinitis pigmentosa and congenital deafness. The proteins encoded by these genes form a

complex in photoreceptors. Disruption of this complex causes retinal degeneration. However, the composition and function of this complex are largely unknown. In this study, we identified a new component of this complex.

Methods: A yeast two-hybrid screen of a mouse retinal cDNA library was conducted using whirlin as a bait. The obtained whirlin-interacting candidate proteins were further examined by a series of biochemical and cellular assays in cultured cells, photoreceptors, and hair cells.

Results: Espin, an actin-binding and -bundling protein, was identified as a whirlin-interacting candidate by the yeast two-hybrid screen. The interaction between whirlin and espin was further confirmed by coimmunoprecipitation and colocalization in cultured cells. This interaction was shown to be mediated through the multiple domains in espin and in whirlin. In the retina, whirlin and espin was coimmunoprecipitated. In both photoreceptors and hair cells, these two proteins exhibited partial colocalization. The expression of espin was decreased in whirlin knockout hair cells.

Conclusions: This study demonstrates that espin is a novel component of the USH2 complex in both photoreceptors and hair cells. Based on the actin-binding and -bundling ability of espin, the interaction between whirlin and espin suggests that the USH2 complex may associate with actin filaments in cells. This interaction probably plays a more important role in hair cells than in photoreceptors.

Program#/Poster#: 2662/A143
Presentation Time: Tuesday, May 03, 8:30 AM -10:15 AM. Session Number: 313, Session Title: Retina: Cell Biology and Disease. Location: Hall B/C

Genetic Dissection Of p27-mediated Reactive Müller Gliosis

Felix R. Vazquez-Chona¹, Alyssa Lolofo¹, Dennis M. Defoe², Edward M. Levine³. ¹Ophthalmology, Univ of Utah, Salt Lake City, UT; ²Anatomy

& Cell Biology, ETSU College of Medicine, Johnson City, TN; ³Ophthalmology & Visual Science, University of Utah, Salt Lake City, UT.

Purpose: In an effort to identify key regulators of glial reactivity, we previously showed that global conditional inactivation of the cyclin-dependent kinase (CDK) inhibitor p27Kip1 induces Müller glia to proliferate, migrate, and upregulate intermediate filaments. Here, we address whether p27 inactivation acts cell autonomously to induce Müller glial reactivity, and whether p27 modulates Müller glial reactivity through its CDK/cyclin (CK) domain or through its phosphorylation state at serine-10 (S10).

Methods: We conditionally targeted the p27 coding region in adult mice harboring the *p27^{LoxP}* (*p27^{L+}*) mutation and expressing a tamoxifen-inducible Cre-recombinase under the control of a glial promoter, GLAST-CreER^{T2}. To determine which p27-domain modulates reactive gliosis we induced light damage in mice harboring either the CK- mutation or S10A knock-in mutation.

Results: Glial-specific p27 inactivation resulted in proliferative Müller glial reactivity. *p27^{+/-ck-}* retinas displayed enhanced levels of reactivity relative to the wild-type and *p27^{S10A/S10A}* retinas after light-induced retinal degeneration.

Conclusions: Preliminary data suggest that p27 regulates Müller glial reactivity through its CK domain. These findings also suggest that p27 is a key modulator of glial plasticity and its pathway represents a prime target to facilitate glial based regeneration and to modulate glial scar formation.

Program#/Poster#: 2674/A155
Presentation Time: Tuesday, May 03, 8:30 AM -10:15 AM. Session Number: 313, Session Title: Retina: Cell Biology and Disease. Location: Hall B/C

Low-Level Gestational Lead Exposure Induces Metabolomic Changes in Developing Mouse Retina

William D. Ferrell¹, Shawntay Chaney², Donald A. Fox^{2A}, Robert E. Marc³, Bryan W. Jones¹. ¹Ophthalmology, Moran Eye Center, Salt Lake City, UT; ^ACollege of Optometry, ²University of Houston, Houston, TX; ³Ophthalmology-Sch of Med, Univ of Utah/Moran Eye Center, Salt Lake City, UT.

Purpose: Low-level gestational lead exposure (GLE) increases retinal progenitor cell proliferation and rod photoreceptor and bipolar cell neurogenesis in mice. To determine the GLE-induced changes in cellular metabolism, we surveyed the small molecular metabolic signals in developing control and GLE retinas.

Methods: Female C57BL/6 mice were given tap water or water containing 55 ppm lead two weeks before mating, during pregnancy, and through postnatal day (PND)10 to produce a human-equivalent GLE model. Mice were sacrificed between 1000 and 1200 hours on PND2, PND6, PND10, and 4 weeks of age. Retinas were fixed with conventional aldehydes, plastic embedded, sectioned and processed for computational molecular phenotyping (CMP). Sections from control and GLE central retinas were examined and compared.

Results: Consistent with our previous studies, GLE mouse retinas had prolonged development compared to control. Between PND2 and PND10 there were metabolic variances in the molecular signals between GLE and controls for virtually every metabolite and protein examined: GABA, glycine, L-glutamate, L-glutamine, glutathione, arginine, L-aspartate, glutamate synthetase, CRALBP, GFAP, rod opsin and taurine. Notable changes in GLE retinas included an increased level of glutathione and GABA in the differentiated cell layer at PND2; an increased level of glutamate and aspartate, a decreased levels of glutamine and a delay in CRALBP expression in the Müller glial cell endfeet at PND6; and greater spacing between the progeni-

tor cell layer and differentiated cell layer, lowered overall taurine levels, and delayed rhodopsin development at PND10. The most pronounced changes in the 4 week-old GLE retinas included isolated cell classes with higher aspartate, glutamine, glutamate and GABA levels: especially in the GCL.

Conclusions: GLE-induced produced distinct metabolic differences during early postnatal retinal development. Differences in the metabolic envelopes of many retinal cell classes including horizontal cells, bipolar cells, amacrine cells, Müller glial and ganglion cells were observed. These findings suggest that alterations in retinal metabolism and the metabolic signatures of individual retinal cells may underlie the increased and prolonged cell proliferation and maturation of late-born rods and bipolar cells.

Program#/Poster#: 2688/A169
Presentation Time: Tuesday, May 03, 8:30 AM -10:15 AM. Session Number: 313, Session Title: Retina: Cell Biology and Disease. Location: Hall B/C

Intrinsic Mechanosensation In Mammalian Retinal Ganglion Cells Is Mediated By Trpv4

Daniel A. Ryskamp^{1,2}, Tunde Molnar², Peter Barabas², Wei Xing², David Krizaj^{1,2}. ¹Interdepartmental Program in Neuroscience, University of Utah, Salt Lake City, UT; ²Ophthalmology and Visual Science, University of Utah School of Medicine, Salt Lake City, UT.

Purpose: Retinal ganglion cells (RGCs) are immersed within a mechanically active environment in which they must constantly cope with and adapt to hydrostatic pressure and osmotic stress. The purpose of this project was to identify the molecular mechanism that underlies the mechanosensitive properties of mouse RGCs and to characterize the role of plasma membrane stretch in RGC Ca²⁺ homeostasis.

Methods: Retinas from C57BL/6J mice were used for calcium imaging

experiments, Western blotting, and fluorescent immunolabeling. RGCs expressing CFP driven by the *thy1* promoter or stained with Brn3 antibodies were included in the morphology analysis. TRPV4 signals were assessed with validated antibodies in wild type and knockout animals. RGC soma diameter measurements were performed using confocal and CCD camera-based microscope setups. [Ca²⁺]_i was measured in fura-2 loaded RGCs. Pressure stimuli were mimicked by hypotonic membrane stretch.

Results: Hypotonic saline elevated [Ca²⁺]_i in presumed RGCs by 439 ± 59 nM. The diameters of these cells (8.9 ± 1.3 μm) corresponded to diameters of dissociated thy1-CFP -positive cells (10.2 ± 1.8 μm), dissociated Brn3a-immunopositive cells (10.9 ± 0.9 μm), as well as Brn3a-positive RGCs in retinal slices (10.4 ± 2.0 μm). All Brn3a-immunopositive cells were immunopositive for TRPV4 (N = 81). Non-selective TRP channel blockers Ruthenium Red (10 μM) and gadolinium (100 μM) reduced the amplitude of stretch-induced responses (p < 0.0001 and p < 0.05, respectively) and TRPV4 agonist-induced [Ca²⁺]_i elevations. Cells responding to osmotic pressure were sensitive to stimulation with selective TRPV4 agonists whereas capsaicin, a TRPV1 agonist, had no effect on [Ca²⁺]_i in acutely dissociated RGCs (N > 110).

Conclusions: These results demonstrate that mouse RGCs are intrinsically mechanosensitive. Molecular transduction of mechanical stimuli involves TRPV4, a polymodal pressure- and osmosensitive channel which provides prominent modulation of RGC Ca²⁺ homeostasis and excitability. Our findings may have implications for blinding diseases associated with pathological changes in intraocular pressure.

Program#/Poster#: 3091/A107
Presentation Time: Tuesday, May 03, 2011, 1:45 PM - 3:30 PM. Session Number: 347, Session Title: Injury, Neuroprotection and Drugs in Glaucoma. Location: Hall B/C

Vegf Mediated Stat3 Activation Contributes To Retinal Avascularity In Rat Model Of Rop

Haibo Wang¹, Grace Byfield², Mary Elizabeth Hartnett¹. ¹Ophthalmology, John A. Moran Eye Center, The University of Utah, Salt Lake City, UT; ²Ophthalmology, University of North Carolina, Chapel Hill, NC.

Purpose: To investigate 1) whether upregulated vascular endothelial growth factor (VEGF) following repeated fluctuations in oxygen in the 50/10 oxygen-induced retinopathy (50/10 OIR) rat model contributes to avascular retina through activation of signal transducer and activator of transcription (STAT3), and 2) the molecular mechanisms involved.

Methods: Newborn rat pups were exposed to repeated fluctuations in oxygen between 50% and 10% inspired oxygen every 24 hours for 14 days. Pups were given the STAT3 inhibitor, AG490 (10mg/kg/d), or equal volume of PBS as control by daily intraperitoneal injections from postnatal day (P)3 to P13 or a neutralizing antibody to VEGF or non-immune IgG as control as an intravitreal injection on P12. Avascular area (AVA), expressed as a percentage of the avascular/total retinal areas, was measured in isolectin-stained retinal flat mounts. Phosphorylated STAT3, caspase 3, and erythropoietin (EPO) were measured by western blots and the amount of retinal VEGF protein was quantified by ELISA.

Results: Repeated fluctuations in oxygen in the 50/10 OIR model resulted in increased AVA ($p < 0.05$) with upregulation of VEGF expression ($p < 0.01$) and activation of STAT3 ($p < 0.01$) compared to room air raised pups. In the 50/10 OIR model, inhibition of STAT3 with AG490 decreased retinal AVA ($p < 0.05$) compared to PBS control and led to an increase in EPO expression without affecting the amount of cleaved caspase-3 or VEGF measured in whole retinas. Neutralizing VEGF activity significantly reduced phosphorylated STAT3 ($p < 0.001$) and increased EPO protein expression ($p < 0.05$) compared to control IgG.

Conclusions: The activation of STAT3 is associated with AVA at p14 in the 50/10 OIR model. In this signaling cascade, repeated oxygen fluctuations lead to increased VEGF, which induces downstream STAT3 phosphorylation that mediates retinal EPO expression. Further studies are needed to explore the molecular mechanisms by which STAT3 regulates EPO gene expression.

Program#/Poster#: 3126/A280
Presentation Time: Tuesday, May 03, 1:45 PM - 3:30 PM. Session Number: 349, Session Title: Retinopathy of Prematurity. Location: Hall B/C

Conjugation of Gadolinium Based Contrast Agent to Avastin for Pharmacokinetics with MRI

Randon M. Burr^{1A}, Sarah A. Molokhia^{1B}, Jacquelyn M. Simonis^{1B}, Nathan Gooch^{1A}, Barbara M. Wirostko², Balamurali K. Ambati³. ^ABioengineering, ^BOphthalmology, ¹University of Utah, Salt Lake City, UT; ²Ophthalmology, University of Utah, Park City, UT; ³Ophthalmology, John Moran Eye Center, Salt Lake City, UT.

Purpose: To conjugate Gd-DTPA to the drug Avastin®.

Methods: The use of zero length cross linkers was employed to derivatize Gd-DTPA (Sigma) to Avastin® (Genentech). Gd-DTPA was dissolved in MES of pH 6.0 at 1 mg/ml. EDC and S-NHS (Thermo Scientific) were added to the solution at concentrations of 2 mM and 5 mM respectively. The solution was gently spun for 30 minutes at room temperature. The pH was raised to approximately 7.0 - 7.4 by the addition of 5M NaOH. Immediately following, Avastin® is added to a concentration of 1 mg/ml and the solution is mixed for 24 hours at room temperature. The solution was diluted to 15 ml and then centrifuged at 4000 g for 20 minutes in a 30 kDa MWCO centrifugal filtrate unit (Millipore) to remove any unconjugated Gd-DTPA and unreacted maleamides. The same centrifugation process was repeated once more. SEC - HPLC was used to confirm the addition of the Gd-DTPA

with Superdex 200 10/30 GL column (GE Healthcare) and a mobile phase of PBS pH 7.0 at 0.5 mL/minute. ICP-OES was used to quantify the Gd content in solution and calculate a theoretical binding ratio of Gd-DTPA molecules per Avastin® molecule. Alterations to the binding affinity were identified using ELISA and integrity of the Avastin® was analyzed using IEX-HPLC with a bio MAB column (Agilent).

Results: We were able to detect peak shifts in retention time using SEC of approximately 1 - 2 minutes; the change in time depends upon the reaction conditions. After the use of the spin filter units the presence of Gd was detected. Our group has previously reported the development of a non-degradable drug delivery device for implantation in the capsular bag at the time of cataract surgery. We intend to develop a formulation with the derivatized Avastin® suitable for release from our drug delivery device.

Conclusions: The results suggest the addition of the Gd-DTPA to the Avastin® molecules. We intend to use this formulation to conduct pharmacokinetics analysis of Avastin® using MRI. Further characterization with mass spectrometry can confirm the exact number of Gd-DTPA molecules added per Avastin® molecule. Additional characterization using the combination of IEX and ELISA will be used to confirm the derivatized drug's stability.

Program#/Poster#: 3250/A498
Presentation Time: Tuesday, May 03, 1:45 PM - 3:30 PM. Session Number: 352, Session Title: Drug Delivery. Location: Hall B/C

Development And Viability Of A Novel, Sustained Release, Refillable, Intraocular Drug Delivery Device For Potential Multi Drug Use

Nathan Gooch^{1A}, Himanshu Sant¹, Michael Burr¹, Corey Bishop², Bruce Gale^{1B}, Balamurali Ambati^{1C}. ^ABioengineering, ^BMechanical Engineering, ^COphthalmology, ¹University of Utah, Salt Lake City, UT; ²Johns Hopkins

University, Baltimore, MD.

Purpose: To develop and determine viability of a novel, sustained release, refillable intraocular, drug delivery device which acts as a reservoir and delivery agent for potential multi drug use.

Methods: The capsule drug ring (CDR) prototypes were manufactured using a CO₂ VLS 3.60 (Versa Laser). The primary structural components for the device were made of Carbothane, a thermoplastic aliphatic polycarbonate-based polyether urethane. The device has been optimized using Avastin® and dexamethasone as the drugs of interest. Each component of the device has been evaluated for in vitro biocompatibility by testing for lens epithelial cell (B-3) migration and proliferation with Avastin® and dexamethasone, measuring Lipopolysaccharide (LPS) levels, and testing for the presence of pro-inflammatory cytokines (i.e. MIP-1 β , MIP-1 α , MCP-1, IL-1 β , TNF, TGF- β 1) after in vitro culture with macrophages (J774A.1) and fibroblasts (L-929).

Results: The design of the device was intended to maximize the volume available in the capsular bag without interfering with or impairing vision. The device was designed to be a circular ring shape and had a drug reservoir of 40 μ L. Prototype CDR designs have been manufactured. Two valves have been included in the design such that the reservoir would be refillable and also have potential for multi-drug delivery. The kinetics of drug release from the device have been shown to be near zero order. After manufacture, LPS was detected at levels below 0.0303 EU/mL. As each component of the device was specifically chosen because they are established medical grade biomaterials it was not unexpected that the device would be within acceptable biocompatibility limits.

Conclusions: The results show the successful manufacture of the CDR from established medical grade biomaterials. The drugs Avastin® and dexamethasone were used as drugs of interest to show that the device works as designed and delivers the drug in a

desirable way. The in vitro biocompatibility of the completed CDR and of the component materials was also assessed through a variety of tests and evaluation. The CDR shows great potential as an implantable ocular device for drug delivery.

Program#/Poster#: 3254/A502

Presentation Time: Tuesday, May 03, 1:45 PM - 3:30 PM. Session Number: 352, Session Title: Drug Delivery. Location: Hall B/C

Reflection - Based Quantification and Imaging of Macular Pigment in Human Infant Eyes Using the RetCam®

Mohsen Sharifzadeh¹, Robert O. Hoffman², Werner Gellermann¹, Paul S. Bernstein². ¹Physics, University of Utah, Salt Lake City, UT; ²Ophthalmology and Visual Sciences, Univ of Utah/Moran Eye Center, Salt Lake City, UT.

Purpose: We explore suitable optical and data processing possibilities of the RetCam® platform for the quantitative measurement of macular pigment (MP) in infant eyes. This will allow us to determine age-adjusted MP levels in a population of newborns, infants, and children.

Methods: Our method for the measurement of MP is based on the RetCam® platform, a video-based retinal imaging system widely used to inspect the infant retina. We have configured the instrument to permit reflection based imaging in a narrow spectral region overlapping the blue-green absorption range of the MP carotenoids. Two-dimensional pixel reflection intensity maps are obtained in which the MP is visible as a region of attenuated reflection. Using suitable software routines, we compare pixel reflection intensities from the peripheral retina and macular region, and in this way derive MP optical density levels as a quantitative measure for the MP concentration in the area of interest.

Results: A first-phase clinical trial involved 13 subjects aged 7 - 71 months. MP optical density levels ranged be-

tween 0.13 and 0.025. A plot of peak MP levels versus subject age reveals a highly correlated linear relationship ($R^2 = 0.77$). In subsets of subjects with nearly identical age, significant differences in MP levels were observed. In all cases, the spatial MP distributions peaked in the center (fovea) and featured a roughly circular symmetry.

Conclusions: The RetCam® platform can be optimized for the quantitative rapid measurement of MP levels and their spatial distributions in the human infant retina. Individual levels and distributions can vary significantly, while on the average, infant MP levels increase with age up to an as yet undetermined limit. While MP distributions in adults can vary drastically in shape, including, e.g., ring-like distributions with absence of central MP, all infant distributions measured so far exhibit high central levels and circular symmetry. RetCam® based MP measurements will make it possible to study MP uptake kinetics as well as spatial MP modifications while the retina matures, and as a function of external factors such as dietary modifications and stress factors.

Program#/Poster#: 3639/A631

Presentation Time: Tuesday, May 03, 3:45 PM - 5:30 PM. Session Number: 373, Session Title: Carotenoids and Retinoids (Macular Pigment and Visual Cycle). Location: Hall B/C

Carotenoids as Possible Interphotoreceptor Retinoid-binding Protein (IRBP) Ligands: A Surface Plasmon Resonance (SPR)-based Study

Preejith P. Vachali¹, Mary A. Garrlipp², Federico Gonzalez-Fernandez², Paul S. Bernstein¹. ¹University of Utah, Moran Eye Center, Salt Lake City, UT; ²Department of Ophthalmology and SUNY Eye Institute, Buffalo, NY.

Purpose: The transport of macular pigment carotenoids across the interphotoreceptor matrix may be mediated by a protein in the matrix, which could help as a carrier of these hydrophobic molecules from RPE/choroid to the retina. Interphotoreceptor retinoid-

binding protein (IRBP) is a candidate because it is abundant in the matrix and binds hydrophobic molecules such as visual-cycle retinoids and fatty acids. SPR-based biosensors have drawn attention in recent years because of their ability to analyze protein-ligand interactions rapidly and sensitively. In this study, we explored the binding interactions of various carotenoids with IRBP.

Methods: Bovine IRBP was purified to homogeneity by a combination of Con-A affinity, ion exchange, and size-exclusion chromatography. The protein at 10 $\mu\text{g/mL}$ in 10 mM sodium acetate, pH 4.5-5.0 was immobilized on the sensor chip surface using standard amine-coupling. Each of the five carotenoids was dissolved in sucrose monolaurate (SML) (Mitsubishi Chemicals, Japan) to achieve a high concentration, and 10 mM PBS (pH 7.4) with 0.01% Triton X-100 and 0.4 mM SML was used as the running buffer. The carotenoid concentration series was prepared as two-fold dilutions in running buffer. Typically, the carotenoid concentration series spanned 0.01-10 μM . All SPR measurements were recorded on a SensiQ SPR instrument (ICx Nomadics) at 25°C.

Results: The binding responses were analyzed using Qdat Software (ICx Nomadics). Out of the five carotenoids tested with bovine IRBP, lutein showed an affinity of 1.26 μM , while (3R, 3'R)-zeaxanthin and (3R, 3'S)-*meso*-zeaxanthin exhibited somewhat lower affinities with K_D values of \sim 1.82 and 2.4 μM , respectively. Beta-carotene had a relatively high affinity for IRBP with a K_D value of 0.873 μM . Astaxanthin showed the lowest affinity with a K_D value of 2.77 μM .

Conclusions: The results demonstrate that IRBP is able to bind carotenoids, although with relatively low specificity. Biosensor technology is useful to study carotenoid affinities with target proteins with high reliability and reproducibility. Biosensor-based SPR assays are promising approaches for the study of functional roles of IRBP, and they can likely be extended to other physiological ligands such as retinoids and fatty acids.

Program#/Poster#: 3640/A632
Presentation Time: Tuesday, May 03, 3:45 PM - 5:30 PM. Session Number: 373, Session Title: Carotenoids and Retinoids (Macular Pigment and Visual Cycle). Location: Hall B/C

Onset and Progression of Retinal Nerve Fiber Layer Myelination Associated With Optic Nerve Head Drusen

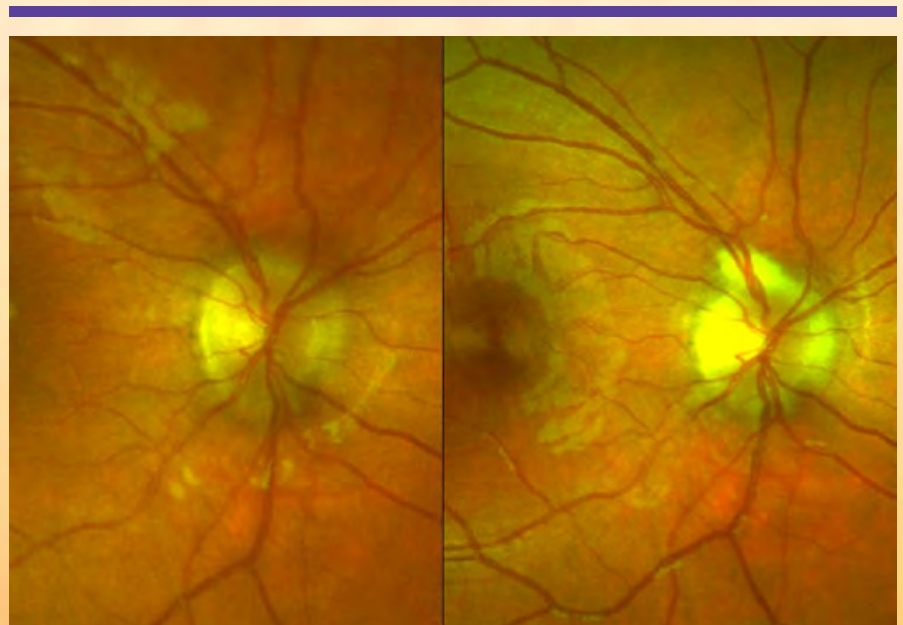
Sherry J. Bass¹, Jerome Sherman¹, Bradley J. Katz², Alfredo A. Sadun³, Allan Panzer⁴. ¹Clinical Sciences, SUNY College of Optometry, New York, NY; ²Department of Ophthalmology, John A. Moran Eye Center, University of Utah, Salt Lake City, UT; ³Neuro-Ophthal/Keck-USC Sch of Med, Doheny Eye Institute, Los Angeles, CA; ⁴Private Practice, Houston, TX.

Purpose: To report the onset and progression of retinal nerve fiber layer myelination (RNFM) in two young children with an associated finding of optic nerve head drusen.

Methods: A 7 year-old male (Case 1) and a 9 year-old female (Case 2) presented for routine ophthalmic care in two different practices and were followed 7 years and 4 years later, respectively. The 7 year-old had a family history of optic disc drusen.

Results: Case 1: Visual acuities were 20/20 in each eye at both visits. At the initial examination, the 7-year old was found to have peripapillary RNFM of the left eye only. When he was re-examined 7 years later, the myelination of the left eye had increased and there was new peripapillary myelination in the right eye. B-scan ultrasound was performed to rule out optic disc edema but instead revealed bilateral optic disc drusen. Automated perimetry revealed a full visual field in the right eye and an enlarged blind spot in the left eye with a mild, inferior arcuate scotoma in the left eye. **Case 2:** Visual acuities were 20/20 in each eye at both visits. At the initial examination, no abnormalities were noted in either eye. At the follow-up examination 4 years later, the optic nerve heads in both eyes were remarkable for blurred nasal borders. There was an onset of superior peripapillary RNFM off the optic nerve head of both eyes, greater in the right eye (Image). An SD-OCT of the optic nerve heads was commensurate with optic disc drusen. Visual fields were full in both eyes. Fluorescein angiography did not reveal any leakage from either disc. An MRI of the brain and orbits was normal.

Conclusions: Acquired and progressive peripapillary RNFM can be associated with optic nerve head drusen. It is hypothesized that in some cases, an increase in disc drusen may disrupt the lamina cribrosa and thereby break the



chemical barrier which would normally inhibit oligodendrocytes, resulting in myelination moving forward.

Program#/Poster#: 3873/D1105
Presentation Time: Tuesday, May 03,
3:45 PM - 5:30 PM. Session Number:
378, Session Title: Neuro-Ophthalmology II: Clinical Evaluation and Observations. Location: Hall B/C

Intrauterine Growth Restriction Alters Retinal IGF-1 Levels in Newborn Rats

M Elizabeth Hartnett^{1A}, Yanchao Jiang¹, Merica Hale², Haibo Wang¹, George W. Smith¹, Robert Lane².

^ARetina Service, ¹Moran Eye Center, Univ of Utah, Salt Lake City, UT;

²Department of Pediatrics, Univ of Utah, Salt Lake City, UT.

Purpose: Intrauterine growth restriction (IUGR) causes poor postnatal weight gain, which has been associated with low serum insulin-like growth factor-1 (IGF-1) and severe ROP in human infants. Still, the link between IUGR and ROP and mechanism for this observation remain unknown. We used a rat model of IUGR to test the hypothesis that IUGR affects retinal IGF-1 and receptor (IGF-1R) expression.

Methods: Prenatal bilateral ligation of the uterine arteries in timed pregnant dams induced uteroplacental insufficiency and IUGR in pups. Controls were dams placed under anesthesia without artery ligation. Two days following surgery, postnatal day (p)0 pups were delivered by Caesarian section. Pup retinas were dissected for growth factor mRNA or protein for IGF-1, IGF1-binding protein 3 (IGF-1BP3), IGF-1R, vascular endothelial growth factor (VEGF) and receptor 1 (VEGFR1), or flat mount labeling of the inner vascular plexus by lectin or ADPase.

Results: At p0, the inner retina was 4.5% vascularized. ADPase labeled cells preceded obvious blood vessels in both IUGR-induced and control pups. There were no differences in lectin stained retinal vascular/total ar-

teas between IUGR induced pups and controls ($p=0.65$). In IUGR induced male pups, there was significantly increased IGF-1 ($p=.02$) and IGF-1BP3 ($p=0.01$) mRNAs, whereas both male and female pups had reduced IGF-1R protein ($p<0.05$).

Conclusions: IUGR induced changes in IGF-1 and IGF-1R differentially in males and females, but did not affect VEGF or VEGFR1 expression or early inner plexus vascularization. Further studies are warranted to determine potential effects of IUGR on retinal angiogenesis and ROP.

Program#/Poster#: 3993/A60
Presentation Time: Wednesday, May 04, 8:30 AM -10:15 AM. Session Number: 411, Session Title: Angiogenesis I. Location: Hall B/C

Canonical Trp Channels (Trpc1 and Trpc3) Regulate Neurotransmission And Visual Acuity In The Mouse Retina

David Krizaj¹, Lutz Birnbaumer², Peter Barabas¹. ¹Ophthalmology and Visual Sciences, University of Utah School of Medicine, Salt Lake City, UT; ²NIH/NIEHS, Research Triangle Park, NC.

Purpose: To analyze light-evoked responses and visual behavior in mice lacking vertebrate homologs of the Drosophila TRP channel. TRP channels play a fundamental role in invertebrate photoreceptor signaling. Their canonical (TRPC) homologs have been implicated in ip-RGC phototransduction, however, expression and function of specific TRPC isoforms in vertebrate retinas is unknown.

Methods: RT-PCR was used to analyze the expression of Trpc1 -7 genes in wild type, KO and Pde6brd1 mice. Mouse lines lacking Trpc1 (TRPC1^{-/-}), Trpc3 (TRPC3^{-/-}) and Trpc1/Trpc3 (TRPC1/3^{-/-}) genes were tested for visual acuity and for light-evoked responses under photopic and scotopic conditions. Contrast sensitivity functions were obtained for optokinetic reflex (OKR) responses to moving sine-wave gratings using a virtual op-

tomotor apparatus (Optomotry) at optimal drift velocities for photopic and scotopic vision, respectively. Electoretinographic (ERG) analysis was performed in anesthetized mice under scotopic and photopic conditions.

Results: Trpc1 mRNA accounted for $78 \pm 15\%$ of the total canonical transcriptome in the mouse retina. Loss of rods in P90 Pde6brd1 retinas was associated with $77 \pm 7\%$ reduction in Trpc1 mRNA content. The amplitude of scotopic OKR responses in Sv129 wild type controls was 0.252 ± 0.003 cycles/degree. Scotopic acuity was increased in TRPC1^{-/-} (0.272 ± 0.009 c/deg) and TRPC3^{-/-} (0.292 ± 0.007 c/deg) animals. Given $88 \pm 10\%$ compensatory upregulation of Trpc3 mRNA in TRPC1^{-/-} retinas we generated TRPC1/3^{-/-} animals; their OKR was 0.308 ± 0.003 c/deg, significantly increased compared to controls ($P<0.001$). The scotopic a-wave was increased in TRPC1^{-/-} eyes at high flash intensities and in TRPC1/3^{-/-} eyes at all flash intensities ($P<0.01$). Increased b-wave amplitudes ($20 \pm 3\%$) were measured in double KO eyes. Photopic OKR responses in TRPC1^{-/-} and TRPC3^{-/-} animals were statistically indistinguishable from controls (0.412 ± 0.006 c/deg); however, a significant increase in photopic acuity was observed in TRPC1/3^{-/-} animals (0.442 ± 0.005 cycles/deg).

Conclusions: These results show that TRPC1 channels, possibly in heteromeric association with TRPC3, negatively regulate rod signaling and scotopic visual behavior in mice. Influx of calcium through TRPC1/3 channels appears to modulate the photosensitivity, neurotransmission and/or the dynamic range of light-evoked signals in wild type rods.

Program#/Poster#: 4121/A477
Presentation Time: Wednesday, May 04, 8:30 AM -10:15 AM. Session Number: 416, Session Title: Horizontal Cells and Bipolar Cells. Location: Hall B/C

Identifying a Clinically Meaningful Threshold for Change in Macular Edema in Patients with Uveitis

Jennifer E. Thorne¹, Elizabeth Sugar², Douglas A. Jabs³, Michael M. Altaweel⁴, Susan L. Lightman⁵, Nisha Acharya⁶, Albert T. Vitale⁷, MUST Research Group. ¹Ophthalmology, Johns Hopkins Wilmer Eye Inst, Baltimore, MD; ²Epidemiology, Johns Hopkins School of Public Health, Baltimore, MD; ³Ophthalmology, Mount Sinai School of Medicine, New York, NY; ⁴Ophthalmology & Visual Science, Univ of Wisconsin-Madison, Madison, WI; ⁵Ophthalmology, Moorfields Eye Hospital/Univ College London/Inst of Ophthalmology, London, United Kingdom; ⁶Ophthal-Proctor Foundation, Univ of California - SF, San Francisco, CA; ⁷Ophthalmology, Moran Eye Institute/University of Utah, Salt Lake City, UT.

Purpose: Optical coherence tomography (OCT) has become the gold standard for evaluating macular edema (ME). However, the threshold of change of retinal thickness (RT) that is clinically meaningful has yet to be identified. We sought to determine the threshold best able to predict clinically meaningful changes in visual acuity in the Multicenter Uveitis Steroid Treatment (MUST) Trial.

Methods: RT was measured at the central subfield with time domain OCT and visual acuity (VA) was measured with logarithmic (ETDRS) visual acuity charts at enrollment and six months. Participants were classified as having ME if the RT was $> 260\mu\text{m}$. The association between percentage change in RT and clinically meaningful VA thresholds (>5 , >10 letters or ≥ 15 letters) was evaluated.

Results: In the 75 eyes with ME at enrollment, a 20% improvement was optimal for predicting greater than 10-letter changes in visual acuity with a sensitivity of 75% and a specificity of 78%. Those with a 20% or greater reduction in retinal thickness had a mean 10.9 letter improvement (95% CI: 6.5 to 15.3) as compared to a -0.5 letter change (95% CI: -4.1 to 3.3) in visual acuity for those without a 20%

reduction ($p < 0.01$).

Conclusions: In addition to being above the level of measurement uncertainty, a 20% change in RT in patients with ME appears to be the optimal threshold for predicting clinically important changes in VA and may be considered as an outcome for clinical trials of treatments for uveitic macular edema.

Program#/Poster#: 4307/D1051
Presentation Time: Wednesday, May 04, 8:30 AM -10:15 AM. Session Number: 423, Session Title: Clinical and Translational Immunology. Location: Hall B/C

Bipolar Cell "Accessory ON" Input to Amacrine Cells in the OFF Inner Plexiform Layer

J.Scott Lauritzen, Bryan W. Jones, Carl B. Watt, Shoeb Mohammed, James R. Anderson, Robert E. Marc. Neuroscience, University of Utah, Salt Lake City, UT.

Purpose: Recent confocal studies report en passant ribbon synapses from inner plexiform layer (IPL) 4/5-stratifying ON Cone Bipolar Cells (ON-CBCs) onto dopaminergic amacrine cells (DACs), intrinsically photosensitive ganglion cells (ipRGCs) and bi-stratified diving ganglion cells (bsdGCs) in the OFF IPL of mammalian retina, thus comprising an "accessory on" input to the OFF layer. Our goal was to identify additional bipolar cell (BC) types suspected to participate in this accessory ON input, confirm the presence of en passant synapses with transmission electron microscopy (TEM), and identify the targets of such synapses.

Methods: BC networks in the ultrastructural rabbit retinal connectome RC1 were annotated with the Viking viewer, and explored via 3D rendering and graph visualization of connectivity (Anderson et al. 2011 The Viking viewer for connectomics: scalable multi-user annotation and summarization of large volume data sets. *J. Microscopy*: [doi:10.1111/j.1365-2818.2010.03402.x]). Small mol-

ecule signals embedded in RC1, e.g. 4-aminobutyrate (y), glycine (G), and L-glutamate (E), combined with morphological reconstruction allow for robust BC classification.

Results: Glycine positive bipolar cells (GBCs) with CBb3, CBb5, and Wide-Field morphology (MacNeil et al., 2004 classification scheme) form en passant ribbon synapses in IPL OFF layers, targeting either GABAergic amacrine cells (yACs), glycinergic amacrine cells (GACs), or both. TEM ultrastructural examination confirms the presence of both pre- and post-synaptic components necessary for functional synapses at the observed locations. Additional en passant ribbon synapses were confirmed with as yet unidentified targets, which may be the DACs, ipRGCs, and bsdGCs reported in the previous literature. Thus our results are consistent with and extend previous observations.

Conclusions: Multiple ONCBC types violate the IPL stratification rules, demonstrating a richer accessory ON network architecture than previously reported. yAC and GAC recipients of en passant synapses in the OFF layer represent novel targets of this accessory ON input, and GAC targets emerge as intriguing candidates for mediating crossover inhibition via accessory ON pathways.

Program#/Poster#: 4552/A491
Presentation Start/End Time: Wednesday, May 04, 1:45 PM - 3:30 PM. Session Number: 454, Session Title: Bipolar and Amacrine Cells; Retinal Cell Development. Location: Hall B/C

The Immune Protein CD3ζ Directly Regulates The Dendritic Morphology Of Rgcs In Mouse Retina

Ning Tian^{1A}, Li Jiang^{1B}, Ping Wang^{1A}, Wolfgang Baehr². ^AOphthalmology & Visual Science, ^BOphthalmology/Moran Eye Center, ¹University of Utah, Salt Lake City, UT; ²Ophthal & Vis Sci Lab #S6881, Univ of Utah Sch of Med, Salt Lake City, UT.

Purpose: Recent study suggests that

a key component of T-cell receptor (TCR), CD3 ζ , is expressed by retinal ganglion cells (RGCs) and that mice with a null mutation of CD3 ζ have impaired RGC dendritic morphology. The goal of current study is to determine whether CD3 ζ directly regulates the dendritic morphology of RGCs.

Methods: To determine whether expressing CD3 ζ by AAV2 virus in RGCs reverses the dendritic defects of RGCs of CD3 ζ ^{-/-} mice, we transfected retinas of Thy1-YFP/CD3 ζ ^{-/-} mice with self-complementary (sc) double-strained AAV2-CD3 ζ -mCherry vector at P3-5 and quantitatively examined the dendritic morphology of RGCs expressing both YFP and CD3 ζ -mCherry at P13-14. To determine whether CD3 ζ is intrinsically active in RGCs and regulates RGC dendrites directly, we knocked down CD3 ζ in retinas of Thy1-YFP mice with AAV2-virus expressing CD3 ζ specific shRNA and mCherry as a reporter at P3-5 and quantitatively examined the dendritic morphology of RGCs expressing both YFP and mCherry at P13-14.

Results: Our data showed that intraocular injection of AAV2 packed with sc CD3 ζ -mCherry or CD3 ζ specific shRNA-mCherry (3X10⁸ virus particles/eye) at P3-5 could effectively transfect a large number of retinal neurons at P13-14. The expression of CD3 ζ -mCherry fusion protein in RGCs of Thy1-YFP/CD3 ζ ^{-/-} mice significantly reduces the density of filopodia of RGCs at P13-14. However, RGCs not expressing CD3 ζ -mCherry fusion protein in transfected eyes have significantly higher density of filopodia in comparison with WT mice and mCherry-expressing RGCs of Thy1-YFP/CD3 ζ ^{-/-} mice. In addition, CD3 ζ specific shRNA-mCherry transfected RGCs in Thy1-YFP mice have much increased density of filopodia while the mCherry-negative RGCs in CD3 ζ specific shRNA-mCherry transfected eyes are not different from that of WT mice.

Conclusions: These results demonstrated that CD3 ζ -mCherry fusion constructs and CD3 ζ specific shRNA-mCherry constructs can be expressed by AAV2 virus *in vivo* in RGCs and

the expressed CD3 ζ protein and CD3 ζ specific shRNA are functional in the regulation of RGC dendrites. In addition, the dendritic defects of RGCs in CD3 ζ ^{-/-} mice are reversed by AAV2-induced expression of CD3 ζ . Furthermore, the effectiveness of CD3 ζ specific shRNA only in transfected RGCs of WT mice suggests that CD3 ζ is intrinsically active in RGCs and regulates RGC dendrites directly.

Program#/Poster#: 4559/A498
Presentation Time: Wednesday, May 04, 1:45 PM - 3:30 PM. Session Number: 454, Session Title: Bipolar and Amacrine Cells; Retinal Cell Development. Location: Hall B/C

Pharmaceutical Profile Of A Novel Rho Kinase (ROCK) Inhibitor ATS907 For Reduction Of IOP In Glaucoma

Muralitharan Kengatharan^{1A}, *Barbara M. Wiostko*^{1B}, *H Umeno*², *Henry H. Hsu*^{1C}. ^AResearch and Development, ^BClinical, ^CClinical Research, ¹Altheos, South San Francisco, CA; ²Research and Development, Asahi Kasei Pharma, Tokyo, Japan.

Purpose: To investigate the pharmaceutical profile of ATS907, studies were conducted to evaluate potency and selectivity, cell permeability, absorption and metabolism.

Methods: Standard protocols were used to assess: (i) kinase inhibitor profile of ATS907 (parent) and its primary metabolite, ATS907M1, against 18 kinases in isolated enzymes *in vitro*; (ii) cell permeability in caco-2 cells *in vitro*; (iii) generation of ATS907M1 in S9 fraction of liver homogenates from human (H), *cynomolgus* monkeys (NHP), dogs, and Japanese white rabbit (JWR) using LC-MS; and (iv) pharmacokinetic profile of ATS907 and ATS907M1 in aqueous humor following topical administration to rabbits.

Results: The Ki (in nM) of ATS907 (parent) and ATS907M1 (metabolite) on ROCK1 was 36.0 and 7.8, and on ROCK2 was, 37.0 and 7.5 nM, respectively. Against other 16

kinases, ATS907 was less potent (i.e. >10X relative to ROCK in terms of IC50) in all but 2 kinases (relative potencies vs ROCK in terms of IC50 were PKA, 4.5X; PKC theta, 4.0X). ATS907M1 was selective against the 16 kinases (relative potency vs ROCK >100X in terms of IC50). The major metabolite in the S9 fraction from livers of H, NHP and JWR was ATS907M1, while M1 was largely absent in dogs. Metabolism profile of H and NHP were comparable. In JWR, a larger quantity of ATS907M1 was observed. Cell permeability (x10E-6 cm/sec) of ATS907 was 38.2 and of ATS907M1 was 9.8. Following topical dosing in JWR, aqueous levels of both ATS907 and ATS907M1 reached Tmax within 1 hour, reflecting rapid penetration into the anterior chamber. ATS907 declined rapidly in the aqueous while ATS907M1 declined more slowly over 8 hrs. Plasma levels of metabolite were low and the parent ATS907 was undetectable.

Conclusions: Following topical administration, ATS907 is rapidly converted to a more potent and selective metabolite, ATS907M1. The rapid cellular penetration and conversion of the parent to ATS907M1 may offer advantages in providing a wider therapeutic index. This unique pro drug-like property of ATS907 makes it an attractive IOP lowering agent.

Program#/Poster#: 3106/A122
Presentation Time: Tuesday, May 03, 1:45 PM - 3:30 PM. Session Number: 347, Session Title: Injury, Neuroprotection and Drugs in Glaucoma. Location: Hall B/C

Targeting Mueller Cell-derived VEGF With Short Hairpin RNA

*George W. Smith*¹, *W. David Culp, Jr.*², *Grace Byfield*³, *Tal Kafri*⁴, *John Flannery*⁵, *Mary Elizabeth Hartnett*¹. ¹Ophthalmology, John A. Moran Eye Center, University of Utah, Salt Lake City, UT; ²Affnery, Inc., Durham, NC; ³Research Triangle Institute International, Research Triangle Park, NC; ⁴Microbiology and Immunology, University of North Carolina, Chapel Hill, NC; ⁵Helen Wills Neuroscience

Institute, University of California, Berkeley, CA.

Purpose: Mueller cells often overexpress angiogenic factors in pathologic conditions. We designed HEK reporter cell lines that constitutively express either VEGF120 or VEGF164 to test the degree of silencing of VEGF using short hairpin RNAs, fashioned as microRNAs, with the goal of silencing Mueller cell-derived VEGF in vivo.

Methods: HEK cells were transduced with lentiviral vectors containing either rat VEGF120 to target VEGFA or rat VEGF164 cDNA and a GFP reporter to assess efficiency of several VEGF shRNA silencing plasmids. The lentiviral transfer vectors of the reporter HEK cells contained two CMV promoters, one driving production of viral elements and the other expression of the desired VEGF splice variant followed by an IRES element and blasticidin/GFP selection/reporter. The GFP in this construct allows for visualization of transfection efficiency while the blasticidin allows for selection of only VEGF expressing cells. The shRNA target sequences (two each for VEGFA and VEGF164) were cloned into expression plasmids containing a red fluorescent reporter gene driven by the CMV promoter. Both HEK VEGF reporter cell lines were transfected with each of the silencing plasmids and flow cytometry was used to determine the percent silencing of VEGF protein expression. Similarly, four commercially available shRNAs each packaged into a lentiviral transfer vector were used to transduce HEK rat VEGF120 and VEGF164 reporter cell lines. VEGFA mRNA silencing was measured 48 hours later by real-time PCR.

Results: Two VEGF164 shRNAs silenced VEGF164 protein expression by 13 and 36 percent and did not silence protein expression in the VEGF120 cell line. Two VEGFA shRNAs silenced VEGF120 protein expression by 13 and 33 percent and VEGF164 by 38 and 47 percent. In HEK rat VEGF164 cells, the four shRNAs silenced VEGFA mRNA by 34, 64, 46, and 30 percent, while in HEK rat VEGF120 cells they silenced

VEGFA mRNA by 0, 74, 11, and 50 percent.

Conclusions: Selective silencing of VEGF splice variants or VEGFA is possible using shRNAs on HEK rat VEGF reporter cell lines. Silencing specific VEGF splice variants may prove useful when inhibiting a growth factor like VEGF, which has physiologic and pathologic effects depending on concentration and signaling.

Program#/Poster#: 4865/A109
Presentation Time: Wednesday, May 04, 3:45 PM - 5:30 PM
Session Number: 472, Session Title: Angiogenesis II. Location: Hall B/C

Membrane Bound Vegf Receptor2 Can Be Shifted To Soluble Vegf Receptor2 Using Morpholino Antisense Oligomer, Which Suppresses Angiogenesis And Lymphangiogenesis In Murine Corneal Suture Models

Hironori Uehara^{1,2}, *Judd Cahoon*¹, *Ling Luo*^{1,2}, *YangKyung Cho*¹, *Jackie Simonis*^{1,2}, *Bala Ambati*^{1,2}. ¹Moran Eye Center, University of Utah, Salt Lake City, UT. ²Salt Lake City VAHCS, Salt Lake City, UT.

Purpose: Vascular endothelial growth factor-A (VEGF-A) is a potent initiator of angiogenesis and VEGF receptor-2 (VEGFR2) is its primary angiogenic receptor. In addition to membrane-bound VEGFR2 (mb-VEGFR2), the VEGFR2 gene produces a soluble isoform protein, which contains only partial extracellular domain, because of alternative polyadenylation. Soluble VEGFR2 (sVEGFR2) is known to bind VEGF-C and exert anti-lymphangiogenesis. We tried to shift mRNA expression of mb-VEGFR2 to sVEGFR2 using morpholino-oligomer to manipulate splicing.

Methods: We designed morpholino-oligomer targeted to exon13-intron13 junction (VEGFR2e13_MO). Using human umbilical vein endothelial cells, we assessed expression of mb-VEGFR-2 and sVEGFR-2 by real-time RT-PCR, flow cytometry and western blot. We determined a

polyadenylation site induced by VEGFR2e13_MO using 3'RACE. Furthermore, we tested potential anti-angiogenic effects of VEGFR2e13_MO in murine corneal suture angiogenesis. CD31 and LYVE-1 stains were used to evaluate neovascularization and lymphangiogenesis.

Results: VEGFR2e13_MO increases sVEGFR2 mRNA 17 times ($p<0.001$) and decreases mb-VEGFR2 35% ($p<0.05$) compared with the controls. Flow cytometry showed VEGFR2e13_MO reduced VEGFR2 positive cells 44% compared to the controls. In western blot for sVEGFR2, we detected sVEGFR2 protein from the culture medium of VEGFR2e13_MO transfected cells, but not control cells. By 3'RACE, we confirmed that one of the polyadenylation sites is induced by VEGFR2e13_MO. VEGFR2e13_MO injection reduced neovascularization 50% compared to the controls ($p<0.001$) one week after corneal suture injury, and reduced lymphangiogenesis 30% compared to the controls ($p<0.05$) two weeks after corneal suture injury.

Conclusions: A morpholino targeting the exon13-intron13 junction of the VEGFR2 gene preferentially promoted expression of sVEGFR2, while suppressing mb-VEGFR2 and angiogenesis in corneal injury models. By modifying splicing factors, we can activate a latent polyadenylation signal and produce a different isoform of the target protein. This may become a new approach for developing for anti-angiogenic drugs.

Program#/Poster#: 4868/A112
Presentation Time: Wednesday, May 04, 3:45 PM - 5:30 PM. Session Number: 473, Session Title: Angiogenesis II. Location: Hall B/C

Anti- Angiogenesis Effect Of Morpholino Antisense Oligomer In Murine Corneal Suture Model

YangKyung Cho, *Hironori Uehara*, *Ling Luo*, *Bala Ambati*. Ophthalmology, University of Utah, Moran Eye Center, Salt Lake City, UT.

Purpose: VEGF receptor 1(VEGFR1) is known to be one of the main receptors for VEGF-A. VEGFR1 gene produces two kinds of isoform, soluble and membrane bound VEGFR1. By stimulation of VEGF-A, membrane bound VEGFR1 leads angiogenesis. On the other hand, soluble VEGFR1 sequestered VEGF-A activity by binding to VEGF-A, so results in anti-angiogenetic effect. These isoforms are generated by alternative splicing. Previously, we succeeded to convert membrane VEGFR1 to soluble VEGFR1 by blocking splicing event with morpholino antisense oligomer(sVEGFR1_MO, Flt morpholino) using culture cells. In this study, we examined Flt morpholino can inhibit angiogenesis in vivo murine corneal suture model

Methods: We used a murine corneal suture model to investigate the effect of morpholino promoting sFlt in suppressing neovascularization and lymphangiogenesis. In an inhibition experiment, we placed 3 corneal sutures on day 0, and then injected Flt morpholino, nonspecific(STD) morpholino, and PBS into corneal stroma of each group on day 1 and 4. On day 7, we harvested the cornea. In a regression experiment, we placed 3 corneal suture on day 0 and we injected Flt morpholino, STD morpholino, and PBS into corneal stroma of each group on day 7 and 10 and then we harvested corneas on day 14. After staining of vessels(CD31) and lymphatic vessels(LYVE1) of cornea, we checked with fluorescent microscope and digitally quantified neovascularization.

Results: In analysis of angiogenesis(in regression experiment), we can find significant difference between groups(mean area of angiogenesis/triangular corneal area around suture is 0.262 ± 0.182 in Flt morpholino group(N=22), 0.535 ± 0.256 in STD morpholino group(N=29), and 0.364 ± 0.184 in PBS group(N=28)). Flt morpholino group showed less neovascularization than STD morpholino group($p=0.000$). In analysis of lymphangiogenesis(in both inhibition and regression experiment), we can find significant difference between

groups(in inhibition, mean area of lymphangiogenesis/triangular corneal area around suture is 0.272 ± 0.181 in Flt group(N=29), 0.470 ± 0.206 in STD group(N=20), and 0.347 ± 0.194 in PBS group(N=30)). Flt morpholino group showed less lymphangiogenesis than STD morpholino group($p=0.002$ in inhibition, $p=0.000$ in regression)

Conclusions: Morpholinos promoting sFlt reduced angiogenesis and lymphangiogenesis compared with nonspecific morpholino and had a tendency of reducing angiogenesis and lymphangiogenesis compared with control PBS

Program#/Poster#: 4875/A119
Presentation Time: Wednesday, May 04, 3:45 PM - 5:30 PM. Session Number: 473, Session Title: Angiogenesis II. Location: Hall B/C

p63+ Cells Can Be Isolated From Cadaver Corneas Up To 6 Weeks After Death

Jacquelyn M. Simonis¹, Hironori Uehara¹, YangKyung Cho¹, Subrata K. Das¹, Bonnie Archer¹, Romulo Albuquerque², Balamurali K. Ambati¹. ¹Moran Eye Center, University of Utah, Salt Lake City, UT; ²Ophthalmology, University of Kentucky, Lexington, KY.

Purpose: To evaluate the proportion of stem cells derivable from cadaver corneas long after time of preservation. Currently, tissue for transplant is only suitable for a short period of time. Determining the duration of stem cell survival could indicate that donor corneas are viable for longer periods of time.

Methods: Human donor corneas were received from the Utah Lion's Eye Bank. Limbal cells were isolated from the corneas by fine dissection and treatment with 0.25% trypsin-EDTA, and plated on a feeder layer of lethally irradiated 3T3-J2 cells (ATCC). One week later the cells were harvested and immunofluorescence was performed using antibodies for p63-a limbal stem cell marker and DAPI. Confocal microscopy was performed

to evaluate the localization of p63 and DAPI positive cells.

Results: Cells were successfully cultured from three donor corneas (M&F, age > 65) which had been harvested 6 weeks previously. Upon assessing p63 & DAPI co-localization it was found that approximately 10% of cultured cells were both p63 & DAPI positive.

Conclusions: Stem cells remain viable up to 6 weeks after preservation of donor cadaver corneas and can be successfully isolated, identified, and cultured in vitro.

Program#/Poster#: 5127/D826
Presentation Time: Wednesday, May 04, 3:45 PM - 5:30 PM. Session Number: 481, Session Title: Stem Cell and Bioengineering. Location: Hall B/C

Assessing Susceptibility to Age-Related Macular Degeneration with Genetic Markers and Environmental Factors

Yuhong Chen¹, Jiexi Zeng², Chao Zhao³, Kevin Wang³, Elizabeth Trood³, Jeanette Buehler⁴, Matthew Weed³, Daniel Kasuga³, Paul Bernstein⁴, Kang Zhang³. ¹Ophthalmology, Eye and ENT hospital, Fudan University, Shanghai, China; ²Ophthalmology, Department of Ophthalmology, 2nd Xiangya Hospital, Central South University, Changsha, China; ³Ophthalmology, Shiley Eye Center, University of California San Diego, San Diego, La Jolla, CA; ⁴Ophthalmology, Department of Ophthalmology & Visual Sciences, Moran Eye Center, University of Utah School of Medicine, Salt Lake City, CA.

Purpose: To evaluate the independent and joint effects of genetic factors and environmental variables on advanced forms of age related macular degeneration (AMD) including geographic atrophy (GA) and choroidal neovascularization (CNV), and to develop a predictive model with both genetic and environmental factors included.

Methods: Demographic information, including age of onset, smoking status

and body mass index (BMI), was collected in 1844 participants. Genotypes were evaluated for eight variants in five genes related to AMD. Unconditional logistic regression analyses were performed to generate a risk predictive model.

Results: All genetic variants showed strong association with AMD. Multivariate odds ratios (ORs) were 3.52 (95% CI: 2.08-5.94) for *CFH* rs1061170 CC, 4.21 (95% CI: 2.30-7.70) for *CFH* rs2274700 CC, 0.46 (95% CI: 0.27-0.80) for *C2* rs9332739 CC/CG, 0.44 (95% CI: 0.30-0.66) for *CFB* rs641153 TT/CT, 10.99 (95% CI: 6.04-19.97) for *HTRA1/LOC387715* rs10490924 TT and 2.66 (95% CI: 1.43-4.96) for *C3* rs2230199 GG. Smoking was independently associated with advanced AMD after controlling for age, gender, BMI and all genetic variants.

Conclusions: *CFH* confers more risk to the bilaterality of GA whereas *LOC387715/HTRA1* contributes more to the bilaterality of CNV. *C3* confers more risk for GA than CNV. Risk models with combined genetic and environmental factors together have notable discrimination power. Early detection and risk prediction of AMD could help to improve the prognosis of AMD and reduce the outcome of blindness. Targeting high risk individuals for surveillance and clinical interventions may help reduce disease burden.

Program#/Poster#: 5228/D1112
Presentation Time: Wednesday, May 04, 3:45 PM - 5:30 PM. Session Number: 483, Session Title: Genetics of Age-related Macular Degeneration. Location: Hall B/C

Role Of Heterogeneous Nuclear Ribonucleoprotein G (hnRNP-g) In Cornea

Nirbhaj Singh^{1,2}, *Michelle Tiem*^{1,2}, *Christian Bowers*¹, *Balamurali Ambati*^{1,2}. ¹Ophthalmology-University of Utah, John Moran Eye Center, Salt Lake City, UT. ²Salt Lake City VAHCS, Salt Lake City, UT.

Purpose: To determine if Heterogeneous nuclear ribonucleoprotein G (hnRNP-G) regulates sFlt-1 expression in cornea

Methods: Full length (hnRNP-G) was cloned into pCMV vector. pCMV-hnRNP-G and empty pCMV was transfected into HUVEC cells. After 72 hrs cell were harvested and Real Time PCRs were performed for soluble FLT1 (sFLT-1) and membrane FLT-1 (mFLT-1) gene expression. Real time PCR was performed using primers designed against N-terminal region present in soluble NRP-1 and C-terminal end present in membrane NRP-1 only. RNA-binding protein immunoprecipitation (RIP) was performed using anti-hnRNP-G antibody. Bound RNA was extracted and analyzed.

Results: pCMVhnRNP-G over expression in HUVEC lead to 2.5 fold increase in sFLT-1 while there was no significant change in mFLT-1 levels. hnRNP-G was found to bind to FLT-1 mRNA.

Conclusions: hnRNP-G binds to FLT-1 mRNA and over expression leads to changes in sFLT-1 levels.

Program#/Poster#: 5306
Presentation Time: Thursday, May 05, 9:45 AM -10:00 AM. Session Number: 506, Session Title: Corneal Wound Healing II. Location: Floridian BCD

Visual Outcomes Based on Preoperative Keratometry in Moderate Myopic LASIK

Steven M. Christiansen, Shameema Sikder, Majid Moshirfar, John A. Moran Eye Center, University of Utah, Salt Lake City, UT.

Purpose: To evaluate the efficacy of myopic laser in situ keratomileusis (LASIK) based on preoperative keratometry (K).

Methods: One hundred fifty patients (216 eyes) with preoperative spherical equivalent (SE) ranging from -2.00 to -5.99 diopters (D) underwent LASIK using the VISX STAR S2/S3 Excimer

Laser Platform. Seventy-two patients (108 eyes) with a preoperative K value less than 42.0 D (Group 1) were compared with 78 patients (108 eyes) with a preoperative K value greater than or equal to 46.0 D (Group 2). Eyes were matched for preoperative age, spherical equivalent, cylinder, and preoperative pachymetry prior to statistical analysis. Primary outcome measures were uncorrected (UDVA) and corrected (CDVA) distance visual acuities, keratometry, and manifest refraction at 1, 3, 6, and 12 months postoperatively.

Results: Moderately myopic eyes with flat corneas preoperatively had significantly better LASIK outcomes compared to eyes with steep corneas. The mean 6-month SE in group 1 was -0.19 ± 0.47 and in group 2 was -0.37 ± 0.50 (p-value=0.007). Eighty-three percent of eyes in group 1 were within 0.25 D of plano, compared to 59% in group 2. Furthermore, one eye in group 1 lost one line of CDVA compared to eight eyes in group 2.

Conclusions: Moderate myopes with flatter corneas preoperatively have significantly better postoperative visual outcomes when compared with eye whose corneas are steeper prior to myopic LASIK.

Program#/Poster#: 5784/D1069
Presentation Time: Thursday, May 05, 8:30 AM -10:15 AM
Session Number: 524. Session Title: Refractive Surgery. Location: Hall B/C

The Proneural Target Gene *Sbt1* Regulates Neurogenesis By Governing Proliferation In The Xenopus Retina

*Kathryn B. Moore*¹, *Mary A. Logan*², *Issam Al Diri*¹, *Monica L. Vetter*¹. ¹Neurobiology and Anatomy, University of Utah, Salt Lake City, UT; ²Jungers Center for Neurosciences Research Department of Neurology, Oregon Health and Science University, Portland, OR.

Purpose: Proneural basic helix-loop-helix (bHLH) transcription factors are

key regulators of retinal neurogenesis, activating the expression of target genes that execute a program of neuronal differentiation within progenitors. Our study focuses on understanding this differentiation program in *Xenopus* retinal progenitors by examining the function of bHLH target genes.

Methods: We performed a screen for proneural target genes, identifying a novel gene called *sbt1* (shared bHLH target 1). *sbt1* encodes a novel protein with no conserved functional motifs that is conserved across vertebrate species. We used in situ hybridization and gain and loss of function approaches to elucidate the spatial and temporal expression of *sbt1* and to gain insight into its function during retinal development.

Results: In situ hybridization analysis showed that *sbt1* is transiently expressed in late proliferating and early differentiating cells in the *Xenopus* retina and is localized both at the membrane and in the nucleus. Overexpression of either mouse or *Xenopus sbt1* in progenitors promoted differentiation of early born retinal neurons, and also enhanced the ability of the bHLH factor Ath5 to promote neurogenesis. Conversely, inhibition of SBT1 translation in *Xenopus* retinal progenitors by injection of antisense morpholino into cleavage-stage blastomeres prevented/delayed retinal neuron differentiation, resulting in an increase in Müller glia and progenitors. Loss of function of *sbt1* in retinal progenitors blocked the expression of markers for differentiated retinal neurons suggesting that it is required for full proneural function. In addition, overexpression of *sbt1* caused a reduction in mitotic cells in the optic vesicle as measured by phospho-histone H3 staining. We performed a yeast 2-hybrid screen for SBT1 interactors and have isolated several potential protein partners, including proteins involved in cell cycle regulation.

Conclusions: Based on these results, we propose that *sbt1* is expressed in retinal progenitors as they initiate neuronal differentiation, and may function in regulating cell cycle exit downstream of proneural bHLH fac-

tors during retinal development.

Program#/Poster#: 6012/A161
Presentation Time: Thursday, May 05, 11:15 AM - 1:00 PM. Session Number: 539, Session Title: Epigenetics, Stem Cells and Ocular Development. Location: Hall B/C

Identification Of Novel Sflt-1 Regulators Through Genome Wide Expression Analysis

Derick G. Holt¹, Leah Owen¹, Helen Huang^{1,3}, Subrata K. Das^{1,3}, Jacquelyn Simonis^{1,3}, Balamurali K. Ambati^{2,3}. ¹Ophthalmology & Visual Sciences, University of Utah, Salt Lake City, UT; ²Ophthalmology, John Moran Eye Center, Salt Lake City, UT. ³Salt Lake City VAHCS, Salt Lake City, UT.

Purpose: Corneal neovascularization (KNV) is a central feature in the pathogenesis of many blinding corneal disorders. We have previously demonstrated that the soluble form of VEGF receptor 1 (sFlt-1) is the main preserver of corneal avascularity. In order to identify novel genes involved in the regulation of KNV, we have utilized genome-wide microarray analysis of three mice strains who share the same genetic background but have differing susceptibility to KNV. Statistical analysis was performed to identify groups of genes according to their expression patterns and functional properties. Further, we utilize knock-down techniques to investigate whether candidate genes of interest may act through regulation of sFlt-1.

Methods: Microarray data obtained from corneal samples derived from MRL/MpJ, C57/B6, and Pax6+/- mice were analyzed using genome-wide clustering and Sequential Bonferroni analyses. Reverse-transcriptase PCR was utilized to independently confirm the expression patterns of specific genes of interest. Knock-down experiments using target-specific siRNAs were carried out in a cell culture system.

Results: Differentially expressed genes fell into several important func-

tional classes including extracellular matrix regulators, angiogenesis factors, transcription factors, and regulators of alternative splicing. The expression pattern of several candidate genes was confirmed using quantitative RT-PCR. Raver2 and SamHD1 were identified as candidate positive and negative regulators of sFlt-1 expression, respectively. Knock down experiments using plasmids expressing shRNA suggest that two novel factors may act to regulate sFlt-1 levels.

Conclusions: Genome-scale microarray analysis across a spectrum of murine models has identified several promising candidate regulators of corneal avascularity, including two factors which may act by modulating the expression of the key regulator sFlt-1.

Program#/Poster#: 6409/D873
Presentation Time: Thursday, May 05, 11:15 AM - 1:00 PM. Session Number: 552, Session Title: Inflammation and Neovascularization. Location: Hall B/C

Diagnosis of Macular Edema in Patients with Uveitis

John H. Kempen¹, Elizabeth A. Sugar², Nisha Acharya³, James P. Dunn, Jr.⁴, Susan G. Elner⁵, Glenn J. Jaffe⁶, Susan L. Lightman⁷, Jennifer E. Thorne⁸, Albert T. Vitale⁹, Michael M. Altaweel¹⁰. ¹Ophthalmology/Biostatistics&Epidemiology, Scheie Eye Inst/Univ of Penn, Philadelphia, PA; ²Biostatistics/Epidemiology, Johns Hopkins Bloomberg School of Public Health, Baltimore, MD; ³Ophthal-Proctor Foundation, Univ of California - SF, San Francisco, CA; ⁴Ophthalmology, Wilmer Eye Inst/ Johns Hopkins School of Medicine, Baltimore, MD; ⁵Ophthalmology, Univ of Michigan-Kellogg Eye Ctr, Ann Arbor, MI; ⁶Ophthalmology, Duke University Eye Center, Durham, NC; ⁷Clinical Ophthalmology, Moorfields Eye Hospital/Univ College London/Inst of Ophthalmology, London, United Kingdom; ⁸Ophthalmology, Johns Hopkins Wilmer Eye Inst, Baltimore, MD; ⁹Ophthalmology, Moran Eye Institute/University of Utah, Salt Lake City, UT; ¹⁰Oph-

thalmology & Visual Science, Univ of Wisconsin-Madison, Madison, WI.

Purpose: Diagnosis of macular edema (ME) is a high priority in uveitis. We compared methods of diagnosing ME in eyes of Multicenter Uveitis Steroid Treatment (MUST) Trial participants, who had active or recently active intermediate, posterior or panuveitis.

Methods: Eyes were assessed for ME by Reading Center gradings of stereo fluorescein angiograms (FA) and Stratus OCT-3 Fast Macular Thickness scans (OCT) obtained at the same visit. Macular thickening (MT) was defined as retinal thickness ≥ 240 μm by OCT and macular leakage (ML) was defined by the presence of leakage on FA in the central macula. Kappa (κ) and McNemar's test (MNT), and predictive probabilities assessed agreement between methods.

Results: Among 481 eyes with uveitis (255 patients), OCT and FA images were collected and graded for 90% and 76% of eyes, respectively ($p < 0.001$). Agreement between MT by OCT and ML by FA was modest ($\kappa = 0.36$). The disagreement was driven primarily by the presence of ML in eyes without MT (MNT: $p < 0.01$). Only 50% of eyes with ML had MT, and 55% of eyes without MT had ML. Eyes with MT were likely to have ML (87%) and eyes without ML were unlikely to have MT (89%). Nineteen eyes had only non-central ML (4 with MT, 15 without MT); excluding these slightly improved agreement ($\kappa = 0.42$) and the percentage of eyes with ML that had MT (53%), but slightly decreased the fraction of eyes with MT that had ML (84%).

Conclusions: Macula assessment was accomplished more frequently via OCT than FA. The two methods often disagree in diagnosing ME. To the extent that MT (an anatomic entity) and ML (more of a physiologic entity) actually differ, OCT and FA may offer complementary clinical information in a large minority of cases similar to those studied (particularly cases without MT or with ML).

Program#/Poster#: 6564

Presentation Time: Thursday, May 05, 2:00 PM - 2:15 PM. Session Number: 556, Session Title: Clinical and Translational Studies in Ocular Inflammatory Disease. Location: Room 114

Store-operated Calcium Entry Regulates Intracellular Calcium Homeostasis in Mouse Rod Photoreceptors

Tunde Molnar¹, Peter Barabas¹, Claudio Punzo², David Krizaj¹.

¹Ophthalmology and Visual Science, Moran Eye Ctr, University of Utah, Salt Lake City, UT; ²Ophthalmology, University of Massachusetts Medical School, Worcester, MA.

Purpose: To measure resting $[\text{Ca}^{2+}]_i$ in mouse rods and to determine the properties of store-operated calcium entry (SOCE) within different rod compartments. We also assessed whether SOCE in mouse photoreceptors is mediated by TRPC1 and/or TRPC3 channels which can function as store-operated channels in non-excitable cells.

Methods: Optical imaging was performed in dissociated mouse rods prepared from wild type and *Trpc1/Trpc3* (TRPC1/3^{-/-}) double knockout mouse retinas. Cells were loaded with fura-2 AM, excited at 340/380 nm and visualized using high-resolution 14 bit cooled CCD cameras. Voltage-operated and store-operated signals were evoked with high KCl and prolonged depletion of intracellular Ca^{2+} stores within the endoplasmic reticulum (ER). RT-PCR and in situ hybridization were performed using primers for mouse SOC channel candidates.

Results: Resting $[\text{Ca}^{2+}]_i$ levels in wild type mouse rod somata were 85 ± 15 nM with a median concentration of 55 nM (N=449). Depolarization elevated perikaryal $[\text{Ca}^{2+}]_i > 400$ nM, indicating the maintained excitability of dissociated rods. Depletion of ER stores in Ca^{2+} -free saline supplemented with cyclopiazonic acid induced SOCE (371 ± 30 nM) manifested as sustained $[\text{Ca}^{2+}]_i$ overshoots following the return to control Ca^{2+} -containing saline. Sustained divalent cation entry

was visualized as La^{3+} -, and 1-oleoyl-2-acetyl-glycerol (OAG)-sensitive quenching of Fura-2 by Mn^{2+} . Mouse rods showed prominent *Trpc1* and *Trpc3* mRNA expression that was reduced in *Pde6b^{rd1}* retinas. Genetic ablation of TRPC1 and TRPC3 channels had little effect on baseline $[\text{Ca}^{2+}]_i$ (84 ± 7 nM) or SOCE (452 ± 29 nM) in cells isolated from knockout animals. However, analysis of distribution of $[\text{Ca}^{2+}]_i$ in the TRPC1/3^{-/-} cohort showed a significant decrease in number of rods with elevated (100-250 nM) $[\text{Ca}^{2+}]_i$ levels.

Conclusions: We found that SOCE mediates significant Ca^{2+} influx in mouse rod photoreceptor cell bodies and synaptic terminals. This pathway was activated by low $[\text{Ca}^{2+}]_i$ and depletion of ER stores, indicating that it may play a disproportionately prominent role under light-adapted conditions. TRPC1 and TRPC3 channels do not mediate rod SOCE but may contribute to Ca^{2+} overload in stressed rods.

Program#/Poster#: 6581

Presentation Time: Thursday, May 05, 2:45 PM - 3:00 PM. Session Number: 558, Session Title: Photoreceptors, Phototransduction and Modulation. Location: Room 305

Success of Early Limited Core Vitrectomy in Double Penetrating Globe Injuries

Julia P. Shulman^{1A}, Shameema Sikder^{1B}, Majid Moshirfar^{1B}, Roger Harrie¹, Mary Elizabeth Hartnett^{1A}.

^ARetina, ^BCornea, ¹Moran Eye Center, Salt Lake City, UT.

Purpose: To present a surgical approach for preventing tractional retinal detachment following double penetrating or perforating globe injuries in eyes with extensive corneal trauma without using a keratoprosthesis.

Methods: An IRB approved, retrospective chart review of 3 patients from the Moran Eye Center, all of whom underwent corneal laceration repair by an anterior segment surgeon and were referred to the retina service

for management of posterior segment pathology.

Results: Patients' ages were 9 months, 3 years and 21 years. Two were males and one female. Two patients had perforating knife injuries; the infant suffered trauma from a weed wacker cord hitting and perforating the globe. The lens was involved in all three cases. Because of poor visibility, only limited core vitrectomies without removal of the posterior hyaloid were performed within 6 days of the initial ruptured globe repair. A keratoprosthesis was not done in any of the cases because of the concern of graft rejection, particularly in the pediatric patients. One patient developed retinal traction that was observed with serial ultrasounds for 2 months, prior to repeat vitrectomy, endolaser and gas. All patients remain attached at postoperative follow up of 6 months.

Conclusions: A near complete pars plana vitrectomy, to relieve vitreoretinal traction and remove the posterior hyaloid within 14 days of a double penetrating globe injury has been the standard of care to reduce the risk of tractional retinal detachment. In this series, however, retinal attachment was maintained even though only limited core vitrectomies were performed and the posterior hyaloid was not removed due to poor visualization of the posterior segment. A limited vitrectomy alone, done early, may be useful to stabilize the eye and prevent vitreoretinal traction, in eyes with extensive corneal trauma limiting visibility to the posterior segment. Further study is warranted to assess long-term outcomes with this approach that may provide better corneal recovery particularly in pediatric patients.

Program#/Poster#: 5625/A463
Presentation Time: Thursday, May 05, 8:30 AM -10:15 AM. Session Number: 519, Session Title: Trauma/Endophthalmitis. Location: Hall B/C

Retinal Microcirculation As A Predictor For Retinal And Optic Nerve Structural Changes In Patients With Primary Open Angle Glaucoma

Brent A. Siesky¹, Alon Harris², Kay D. Rittenhouse³, Yochai Z. Shoshani¹, Mohammadali Shoja¹, Yoel Arieli¹, Barbara M. Wirostko⁴, Chris Jonescu⁵, Rita Ehrlich¹, George Eckert⁶.

¹Ophthalmology, Indiana University Sch of Medicine, Indianapolis, IN; ²Ophthalmology, Indiana Univ Sch of Medicine, Indianapolis, IN; ³Translational Medicine Ophthalmology, Pfizer Inc, San Diego, CA; ⁴Ophthalmology, University of Utah Moran Eye Center, Salt Lake City, UT; ⁵Ophthalmology, Saarland University, Homburg / Saar, Germany; ⁶Division of Biostatistics, Indiana University School of Medicine, Indianapolis, IN.

Purpose: To examine the relationship between the retinal microcirculation and retinal nerve fiber layer (RNFL) thickness, and optic nerve head structural changes in patients with primary open angle glaucoma (OAG).

Methods: An analysis of 103 patients with OAG (mean age 67.0; 60 female) participating in the Indianapolis Glaucoma Progression Study was performed after their 18 month follow up visit. An additional analysis of 73 patients with OAG (mean age 68.5; 38 female) who finished their 2 years visit was also performed. Retinal capillary perfusion was examined with confocal scanning laser Doppler flowmetry. RNFL thickness and optic nerve head structure was assessed with optical coherence tomography (OCT). Multivariable linear regression models with log-transformed data were analyzed for the change from baseline for each measurement with the following variables included in all models: sex, race (white vs. non-white), age, baseline intraocular pressure (IOP) and baseline values. Stepwise model selection procedures were then used to evaluate retinal microcirculation for predicting RNFL and optic nerve structure, with only measurements statistically significant at $p < 0.05$ retained in the models.

Results: Multivariable linear regression showed that the percentage of

zero blood flow pixels in the superior retina at the 18 months visit was the only predictor for cup to disk vertical ratio change (adjusted r -squared=0.51, $p < 0.0001$). After 2 years, in a bivariate analysis, there was a negative correlation between the amount of superior zero blood flow pixels and RNFL average thickness ($r = -0.318$, $p = 0.013$) and between superior mean blood flow and cup to disk horizontal ratio. Multivariable linear regression found the number of superior zero pixels was the only predictive value for RNFL average thickness (adjusted r -squared=0.085, $p = 0.017$).

Conclusions: Retinal regional perfusion insufficiency may be a significant predictor of glaucoma progression as assessed by structural changes in the optic nerve and RNFL.

Program#/Poster#: 3475/A21
Presentation Time: Tuesday, May 03, 3:45 PM - 5:30 PM. Session Number: 368, Session Title: Blood Flow and Choroid Studies in Glaucoma. Location: Hall B/C

Decreasing Retrobulbar Blood Flow is Predictive of OCT Structural Changes in Patients with Primary Open Angle Glaucoma

Yochai Z. Shoshani¹, Alon Harris¹, Kay D. Rittenhouse², Brent A. Siesky¹, Mohammadali M. Shoja¹, Yoel Arieli¹, Barbara M. Wirostko³, Christian Jonescu⁴, Rita Ehrlich¹, George Eckert⁵. ¹Ophthalmology, Indiana University Sch of Med, Indianapolis, IN; ²Translational Medicine Ophthalmology, Pfizer Inc, San Diego, CA; ³Ophthalmology, University of Utah, Park City, UT; ⁴Ophthalmology, Saarland University Hospital, Homburg / Saar, Germany; ⁵Division of Biostatistics, Indiana University School of Medicine, Indianapolis, IN.

Purpose: To examine the association between retrobulbar blood flow and retinal nerve fiber layer (RNFL) thickness and optic nerve head (ONH) structure in patients with primary open angle glaucoma (OAG).

Methods: Changes in retrobulbar

blood flow were examined in relation to changes in ONH structure and RNFL thickness after 18 months in 103 patients (age 67.0, 60 females) with OAG participating in the Indianapolis Glaucoma Progression Study (IGPS). Retrobulbar blood flow was assessed by color Doppler imaging (CDI) in the temporal (TPCA) and nasal (NPCA) short posterior ciliary arteries, ophthalmic artery (OA), and central retinal artery (CRA) measuring peak systolic (PSV) and end diastolic (EDV) blood flow velocities and vascular resistance (RI). RNFL thickness and ONH parameters were assessed with optical coherence tomography (OCT). Multivariable linear regression models were analyzed for the change from baseline for each measurement.

Results: When compared to baseline, there was a statistically significant deterioration of horizontal integrated rim width ($p=0.0002$), cup area (0.0038), rim area ($p=0.0037$) and cup/disk vertical ratio (<0.001) after 18 months follow up. The bivariate analysis revealed a negative correlation between the TPCA RI at 18 months and the change in horizontal integrated rim width ($r=-0.32$, $p=0.001$), and a negative correlation between the change from 18 months to baseline in TPCA PSV and cup area ($r=-0.30$, $p=0.0022$). With cup area as a dependent variable, in a multivariable linear regression, a model adjusted for age, race, sex and IOP, showed the change in TPCA PSV was the only significant predictor for the cup area changes (adjusted r -squared=0.20, $P=0.0028$). With horizontal integrated rim width as a dependent variable, TPCA RI at 18 months and OA PSV change from baseline were the two predictors for the change in horizontal integrated rim width adjusted for age, race, sex and IOP (adjusted r -squared=0.29, $p<0.0001$).

Conclusions: Decreasing blood flow in the short posterior ciliary arteries which perfuse the prelaminar and laminar regions of the ONH is associated with deterioration in optic nerve structural parameters in patients with OAG.

Program#/Poster#: 3478/A24
Presentation Time: Tuesday, May 03, 3:45 PM - 5:30 PM. Session Number: 368, Session Title: Blood Flow and Choroid Studies in Glaucoma. Location: Hall B/C

In Vivo and In Vitro MRI of Pseudo-phakic Human Eyes

Susan A. Strenk¹, Bosco Tjan², Liliانا Werner³, Nick Mamalis³, Lawrence M. Strenk¹. ¹MRI Research, Inc, Middleburg Heights, OH; ²Psychology, University of Southern California, Los Angeles, CA; ³Ophthalmology, University of Utah/Moran Eye Center, Salt Lake City, UT.

Purpose: Complications of new intraocular lens (IOL) designs are often not discovered until years after their introduction and often linked to Soemmering's ring (SR), a growth that develops to some extent after most cataract surgeries. SR abundance is directly related to the post operative period and inversely to patient age and care taken in cortical clean-up. IOL design also plays a significant role. MRI is not impeded by the iris or optical distortions and has the unique ability to visualize the entire IOL and surrounding SR.

Methods: Donor eyes (N=100, ages 60-99) were imaged either at 1.5T (General Electric) or 3T (Siemens) using custom rf coils (MRI Research) and T1 weighting. Several donor eyes underwent gross and pathological evaluation in order to characterize SR and validate that the image contrast at 3T was comparable to 1.5T. Cataract patients (N=14, ages 69-87) were imaged at 3T to allow shorter scans, which is an important consideration for geriatric volunteers. The location, size, and nature of SR were measured with MRI, gross and histopathological analysis.

Results: MRI revealed up to three distinct layers of SR: a dark inner-area; a concentric gray layer; and a concentric bright, outer-most layer. Gross analysis confirmed the presence of SR and pathological analysis revealed the dark areas to be calcification; the gray areas to be dense, irregular cortical mate-

rial; and the bright concentric outmost layer to be normal cortical material. SR appears to reach its maximum size within several years post surgery; after which time it may become bi-lamellar, and, ultimately, tri-lamellar as the innermost layer calcifies. In-vivo images were at a lower in plane resolution (156 vs 39 microns) but were otherwise consistent with in-vitro findings.

Conclusions: This study cross-validates MRI of cataract patients with MRI of donor eyes, on which gross and histopathological analysis have been conducted. Accommodating-IOLs may be implanted in younger people with whom SR is likely to develop more abundantly and thus potentially lead to more complications. Additionally, A-IOLs are likely to be in place for longer periods of time, thus allowing multi-lamellar SR to develop; the resulting calcifications may limit haptic movement. Longitudinal in vivo MRI studies of cataract patients provide an opportunity to obtain timely feedback on SR development in newly introduced IOLs.

Program#/Poster#: 4728/D786
Presentation Time: Wednesday, May 04, 1:45 PM - 3:30 PM. Session Number: 460, Session Title: Cataract Surgery I. Location: Hall B/C

Safety and Efficacy of a Novel Topical Rho Kinase Inhibitor ATS907 in Normotensive Cynomolgus Monkeys

Barbara M. Wirostko^{1,3A}, H Umeno², Henry H. Hsu^{1B}, Muralitharan Ken-gatharan^{1C}. ^AOphthalmology, ^BClinical Research, CR & D, ¹Altheos, South San Francisco, CA; ²Research, Asahi Kasei Pharma, Tokyo, Japan; ³Ophthalmology, John Moran Eye Center, Salt Lake City, UT.

Purpose: To determine tolerability and intraocular pressure (IOP) lowering efficacy of a novel topical Rho Kinase (ROCK) inhibitor ATS907 in unanesthetized normotensive (NT) cynomolgus Monkeys. Single dose and repeat 14 day (BID) dose ranging studies were conducted.

Methods: Three to four NT monkeys per dose received a single topical dose OS of AT907. Doses included 0.05% and 0.5% AT907 or 0.005% latanoprost in 50ul. IOP was measured at baseline and 2, 4, 6, 8, and 10 hrs post dose. The repeat dose study utilized 3 NT monkeys per dose given 0.05% and 0.2% AT907 doses, (30 ul BID) OD for 14 days. IOP was measured on the 1st, 4th, 9th and 14th days of administration immediately before the morning dose and 3, 6, 9, 12, and 24 hours thereafter. In both studies the contralateral control eye received saline. In a separate study, tolerability was assessed daily at doses 0.1% to 3.0% given BID for 14 days with gross exams and biomicroscopy, and eventual histopathology. Eyelid closure, corneal opacity, congestion of conjunctiva and iris, and pupil size were evaluated.

Results: A decline in IOP was observed starting 2 hrs post dose. A difference in IOP vs control continued through 10 hrs after instillation of AT907. Maximal IOP reduction following single dose administration of AT907 0.05% and 0.5% were -3.7 mmHg and -4.65 mmHg, respectively compared with 2.43 mmHg seen with latanoprost 0.005%. The mean IOP from 2 hrs to 10 hrs after dosing for the control eyes was 21.43 -21.83 mmHg. With repeat dosing, a drop in IOP occurred on day 1 and was maintained through day 14 with both doses with a mean difference of -2.3 to -3.9 mmHg vs control. No significant ocular abnormalities were observed after either single or repeat dosing across intended therapeutic doses with sufficient safety margins at any observation point.

Conclusions: AT907 is effective in lowering IOP topically after a single dose and after repeat dosing out to 14 days. AT907 has an early onset of action. Repeat dosing maintained the IOP hypotensive efficacy through to 14 days. Tolerability profile was favorable throughout the study. AT907 is a viable therapeutic compound to potentially lower elevated IOP in humans.

Program#/Poster#: 3096/A112

Presentation Time: Tuesday, May 03, 1:45 PM - 3:30 PM. Session Number: 347, Session Title: Injury, Neuroprotection and Drugs in Glaucoma. Location: Hall B/C

Tolerability and IOP Lowering Activity of a Topical Rho Kinase Inhibitor, AT907, in Normotensive Rabbits

Henry H. Hsu^{1,3A}, Muralitharan Kengatharan^{1B}, H Umeno², Barbara M. Wiostko^{1C}. ^AAdministration, ^BResearch, ^CClinical, ¹Altheos, South San Francisco, CA; ²Research, Asahi Kasei Pharma, Tokyo, Japan. ³Ophthalmology, John Moran Eye Center, Salt Lake City, UT

Purpose: To determine the tolerability and efficacy of a topically administered novel rho kinase (ROCK) inhibitor in normotensive (NT) rabbits.

Methods: New Zealand White (NZW) rabbits (5 animals/group) received a single dose OD topically with AT907 (0.02%, 0.05 & 0.2% ophthalmic formulation). OS served as the control. IOP was measured at baseline and 1, 2, 4, 6, 8, 10 and 12 hours post dose. A separate study investigated the effect of formulation pH on IOP following dosing 0.02 % AT907 in saline solution, in which Japanese white rabbits received a single dose OS with the formulation pH adjusted from 4-9. IOP was measured at baseline and 2, 4, and 6 hours post dose. Tolerability was assessed in a separate 7-day dose ranging study in NZW rabbits with 0.1%, 0.3%, 0.5%, 1%, 3%, and 5% (AT907 ophthalmic solution) administered topically BID. Gross exams and biomicroscopy was performed daily, ocular histopathology was performed on day 8.

Results: AT907 dose-dependently lowered IOP in rabbits. The maximum reduction in IOP produced by 0.02%, 0.05%, and 0.2% was -7.2 mmHg, -9.5 mmHg, and -11.0 mmHg, respectively, and occurred 1-2 hours post dose. Mean baseline IOP ranged from 23.3 mmHg to 25.4 mmHg per treatment arm. Increasing the pH enhanced the reduction in IOP. In the tolerability study, AT907 was well tolerated

at all doses up to 1%. Signs of mild-moderate conjunctival hyperemia seen with 3% & 5 % resolved within 2-4 hr of topical instillation. No significant effect was observed in corneal thickness, intraocular hemorrhages, pupillary response, or iris changes. There was no evidence of inflammation.

Conclusions: AT907 ophthalmic solution was effective in rapidly lowering IOP after a single dose in a dose response manner in normotensive rabbits. Increasing the pH of the formulation enhanced IOP lowering. Tolerability profile was acceptable in all dose ranges with a noted increase in transient dose-related conjunctival hyperemia.

Program#/Poster#: 3109/A125
Presentation Time: Tuesday, May 03, 1:45 PM - 3:30 PM. Session Number: 347, Session Title: Injury, Neuroprotection and Drugs in Glaucoma. Location: Hall B/C

Conjugation of Gadolinium Based Contrast Agent to Avastin for Pharmacokinetics with MRI

Randon M. Burr^{1A}, Sarah A. Molokhia^{1B}, Jacquelyn M. Simonis^{1B}, Nathan Gooch^{1A}, Barbara M. Wiostko², Balamurali K. Ambati³. ^ABioengineering, ^BOphthalmology, ¹University of Utah, Salt Lake City, UT; ²Ophthalmology, University of Utah, Park City, UT; ³Ophthalmology, John Moran Eye Center, Salt Lake City, UT.

Purpose: To conjugate Gd-DTPA to the drug Avastin®.

Methods: The use of zero length cross linkers was employed to derivatize Gd-DTPA (Sigma) to Avastin® (Genentech). Gd-DTPA was dissolved in MES of pH 6.0 at 1 mg/ml. EDC and S-NHS (Thermo Scientific) were added to the solution at concentrations of 2 mM and 5 mM respectively. The solution was gently spun for 30 minutes at room temperature. The pH was raised to approximately 7.0 - 7.4 by the addition of 5M NaOH. Immediately following, Avastin® is added to a concentration of 1 mg/ml and the solution is mixed for 24 hours at room

temperature. The solution was diluted to 15 ml and then centrifuged at 4000 g for 20 minutes in a 30 kDa MWCO centrifugal filtrate unit (Millipore) to remove any unconjugated Gd-DTPA and unreacted maleamides. The same centrifugation process was repeated once more. SEC - HPLC was used to confirm the addition of the Gd-DTPA with Superdex 200 10/30 GL column (GE Healthcare) and a mobile phase of PBS pH 7.0 at 0.5 mL/minute. ICP-OES was used to quantify the Gd content in solution and calculate a theoretical binding ratio of Gd-DTPA molecules per Avastin® molecule. Alterations to the binding affinity were identified using ELISA and integrity of the Avastin® was analyzed using IEX-HPLC with a bio MAB column (Agilent).

Results: We were able to detect peak shifts in retention time using SEC of approximately 1 - 2 minutes; the change in time depends upon the reaction conditions. After the use of the spin filter units the presence of Gd was detected. Our group has previously reported the development of a non-degradable drug delivery device for implantation in the capsular bag at the time of cataract surgery. We intend to develop a formulation with the derivatized Avastin® suitable for release from our drug delivery device.

Conclusions: The results suggest the addition of the Gd-DTPA to the Avastin® molecules. We intend to use this formulation to conduct pharmacokinetics analysis of Avastin® using MRI. Further characterization with mass spectrometry can confirm the exact number of Gd-DTPA molecules added per Avastin® molecule. Additional characterization using the combination of IEX and ELISA will be used to confirm the derivatized drug's stability.

Program#/Poster#: 3250/A498
Presentation Time: Tuesday, May 03,
1:45 PM - 3:30 PM. Session Number:
352, Session Title: Drug Delivery.
Location: Hall B/C

Retinal Microcirculation As A Predictor For Retinal And Optic Nerve Structural Changes In Patients With Primary Open Angle Glaucoma

Brent A. Siesky¹, Alon Harris², Kay D. Rittenhouse³, Yochai Z. Shoshani¹, Mohammadali Shoja¹, Yoel Arieli¹, Barbara M. Wirostko⁴, Chris Jones-cu⁵, Rita Ehrlich¹, George Eckert⁶.

¹Ophthalmology, Indiana University Sch of Medicine, Indianapolis, IN; ²Ophthalmology, Indiana Univ Sch of Medicine, Indianapolis, IN; ³Translational Medicine Ophthalmology, Pfizer Inc, San Diego, CA; ⁴Ophthalmology, University of Utah Moran Eye Center, Salt Lake City, UT; ⁵Ophthalmology, Saarland University, Homburg / Saar, Germany; ⁶Division of Biostatistics, Indiana University School of Medicine, Indianapolis, IN.

Purpose: To examine the relationship between the retinal microcirculation and retinal nerve fiber layer (RNFL) thickness, and optic nerve head structural changes in patients with primary open angle glaucoma (OAG).

Methods: An analysis of 103 patients with OAG (mean age 67.0; 60 female) participating in the Indianapolis Glaucoma Progression Study was performed after their 18 month follow up visit. An additional analysis of 73 patients with OAG (mean age 68.5; 38 female) who finished their 2 years visit was also performed. Retinal capillary perfusion was examined with confocal scanning laser Doppler flowmetry. RNFL thickness and optic nerve head structure was assessed with optical coherence tomography (OCT). Multivariable linear regression models with log-transformed data were analyzed for the change from baseline for each measurement with the following variables included in all models: sex, race (white vs. non-white), age, baseline intraocular pressure (IOP) and baseline values. Stepwise model selection procedures were then used to evaluate retinal microcirculation for predicting RNFL and optic nerve structure, with only measurements statistically significant at $p < 0.05$ retained in the models.

Results: Multivariable linear regression showed that the percentage of

zero blood flow pixels in the superior retina at the 18 months visit was the only predictor for cup to disk vertical ratio change (adjusted r-squared=0.51, $p < 0.0001$). After 2 years, in a bivariate analysis, there was a negative correlation between the amount of superior zero blood flow pixels and RNFL average thickness ($r = -0.318$, $p = 0.013$) and between superior mean blood flow and cup to disk horizontal ratio. Multivariable linear regression found the number of superior zero pixels was the only predictive value for RNFL average thickness (adjusted r-squared=0.085, $p = 0.017$).

Conclusions: Retinal regional perfusion insufficiency may be a significant predictor of glaucoma progression as assessed by structural changes in the optic nerve and RNFL.

Program#/Poster#: 3475/A21 Abstract Title:
Presentation Time: Tuesday, May 03,
3:45 PM - 5:30 PM. Session Number:
368, Session Title: Blood Flow and
Choroid Studies in Glaucoma. Location:
Hall B/C

Decreasing Retrobulbar Blood Flow is Predictive of OCT Structural Changes in Patients with Primary Open Angle Glaucoma

Yochai Z. Shoshani¹, Alon Harris², Kay D. Rittenhouse², Brent A. Siesky¹, Mohammadali M. Shoja¹, Yoel Arieli¹, Barbara M. Wirostko³, Christian Jonescu⁴, Rita Ehrlich¹, George Eckert⁵. ¹Ophthalmology, Indiana University Sch of Med, Indianapolis, IN; ²Translational Medicine Ophthalmology, Pfizer Inc, San Diego, CA; ³Ophthalmology, University of Utah, Park City, UT; ⁴Ophthalmology, Saarland University Hospital, Homburg / Saar, Germany; ⁵Division of Biostatistics, Indiana University School of Medicine, Indianapolis, IN.

Purpose: To examine the association between retrobulbar blood flow and retinal nerve fiber layer (RNFL) thickness and optic nerve head (ONH) structure in patients with primary open angle glaucoma (OAG).

Methods: Changes in retrobulbar blood flow were examined in relation to changes in ONH structure and RNFL thickness after 18 months in 103 patients (age 67.0, 60 females) with OAG participating in the Indianapolis Glaucoma Progression Study (IGPS). Retrobulbar blood flow was assessed by color Doppler imaging (CDI) in the temporal (TPCA) and nasal (NPCA) short posterior ciliary arteries, ophthalmic artery (OA), and central retinal artery (CRA) measuring peak systolic (PSV) and end diastolic (EDV) blood flow velocities and vascular resistance (RI). RNFL thickness and ONH parameters were assessed with optical coherence tomography (OCT). Multivariable linear regression models were analyzed for the change from baseline for each measurement.

Results: When compared to baseline, there was a statistically significant deterioration of horizontal integrated rim width ($p=0.0002$), cup area (0.0038), rim area ($p=0.0037$) and cup/disk vertical ratio (<0.001) after 18 months follow up. The bivariate analysis revealed a negative correlation between the TPCA RI at 18 months and the change in horizontal integrated rim width ($r=-0.32$, $p=0.001$), and a negative correlation between the change from 18 months to baseline in TPCA PSV and cup area ($r=-0.30$, $p=0.0022$). With cup area as a dependent

variable, in a multivariable linear regression, a model adjusted for age, race, sex and IOP, showed the change in TPCA PSV was the only significant predictor for the cup area changes (adjusted r -squared=0.20, $P=0.0028$). With horizontal integrated rim width as a dependent variable, TPCA RI at 18 months and OA PSV change from baseline were the two predictors for the change in horizontal integrated rim width adjusted for age, race, sex and IOP (adjusted r -squared=0.29, $p<0.0001$).

Conclusions: Decreasing blood flow in the short posterior ciliary arteries which perfuse the prelaminar and laminar regions of the ONH is associated with deterioration in optic nerve structural parameters in patients with OAG.

Program#/Poster#: 3478/A24
Presentation Time: Tuesday, May 03,
3:45 PM - 5:30 PM Session Number:
368, Session Title: Blood Flow and
Choroid Studies in Glaucoma. Location:
Hall B/C

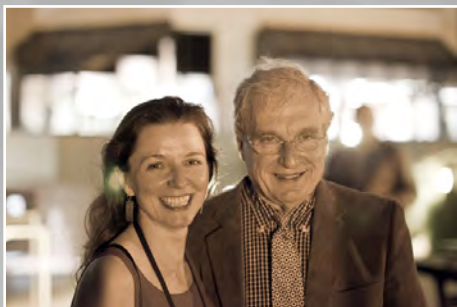
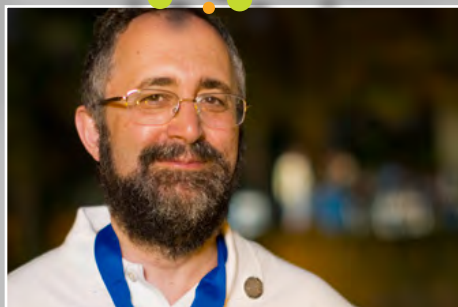
Role Of Vimentin In Corneal Fibrosis And Wound Healing Process

Subrata k. Das, Jr., Ling Luo, Nirbhai Singh, Hironori Uehara, Bonnie Archer, Jacquelyn M. Simonis, Ying Liu, Thomas Olsen, Balamurali K. Am-

bati. University of Utah, Moran Eye Center, Salt Lake City, UT. Salt Lake City VAHCS, Salt Lake City, UT.

Purpose: Vimentin is an intermediate filament protein that contributes to filamentous network between the cell periphery and the nucleus and it has a dynamic link between the nucleus and extracellular matrix. In addition, it is thought to be involved in structural processes such as wound healing. Our main purpose is to examine the role of vimentin for ocular fibrosis at the stage of wound healing.

Methods: C57BL6/j mice corneas were sutured (3 sutures) to induce corneal angiogenesis. Immunohistochemical double staining of α -smooth muscle actin (α -SMA) or vimentin or glial fibrillary acidic protein (GFAP) and CD31 was performed to determine the expression level of vimentin, GFAP and α -SMA in neovascularized and normal corneas 10 days after suture. We designed three distinct plasmids expressing shRNA targeting vimentin mRNA of both mice and humans. Cultured human umbilical vein endothelial cells (HUVEC) were transfected by vimentin shRNA plasmids and the same concentration of the plasmid coding nonspecific shRNA was used as control. The transfection efficiency was examined using GFP-expressing plasmids. Vimentin mRNA expression was evaluated by semi-quantitative



RT-PCR.

Results: Immunostaining indicated that vimentin and GFAP increased in neovascularized (NV) cornea compared to normal cornea 10 days post-suture. Only α -SMA was detected in vessels of neovascularized cornea but not in normal cornea. We found that all the three vimentin shRNA plasmids decrease the expression level of vimentin compared to the control in HUVEC.

Conclusions: Vimentin and GFAP expression are correlated with fibrosis during wound healing. Vimentin shRNA knockdown have potential to be developed as anti-fibrosis treatments.

Program#/Poster#: 6382/D846
Presentation Time: Thursday, May 05, 11:15 AM - 1:00 PM. Session Number: 552, Session Title: Inflammation and Neovascularization Location: Hall B/C

Endostatin Is Increased By Knock-down Of sVEGFR-1 In The Mouse Cornea

Wei Huang^{1,2}, Hiro Uehara^{1,2}, Ling Luo^{1,2}, Nirbhai Singh^{1,2}, Thomas Olsen^{1,2}, Subrata Das^{1,2}, Bala Ambati^{1,2}.
¹Ophthalmology, University of Utah, Salt Lake City, UT; ²Salt Lake VA HCS, Salt Lake City, UT.

Purpose: The cornea is normally avascular to permit visual clarity. However, in disease, neovascularization (NV) can occur and compromise clarity and vision. Vascular endothelial growth factor (VEGF) is a key mediator of angiogenesis in many models, including the cornea. Soluble form of VEGF receptor-1 (sFlt-1) has been shown to be anti-angiogenic in cornea. There are other inhibitors of angiogenesis in the cornea, include endostatin, and pigment epithelium-derived factor (PEDF). Here, we investigate whether these anti-angiogenic factors are affected by sFlt-1 modulation in the cornea.

Methods: sflt-1 was specifically down-regulated by RNA interference (RNAi). We injected into the BALB/C mice's corneas a plasmid expressing a short hairpin RNA (shRNA) targeted against a sequence in the unique carboxyl-terminus region of sflt-1 (pshRNA-sflt-1). The controls were PBS and a plasmid which expressed a nonspecific shRNA (pSEC-negative). RT-PCR, quantitative RT-PCR were performed in corneas from PBS, pSEC-negative and pshRNA.sflt-1 injection groups (n=3) at Day 2, Day 4, and Day 7 three time points.

Results: Corneal neovascularization was induced by pshRNA-sflt within 7 days of injection (n=7), but neither by

pSEC-negative nor PBS. Quantitative RT-PCR data showed that endostatin was upregulated, relative to control (nonspecific plasmid-mediated shRNA) by 250% at Day 2, 400% at Day 4, and 270% at Day 7 (all p's <0.05). However, PEDF was decreased by 51% (P< 0.01) at Day 2 compared to control.

Conclusions: Suppression of sflt-1 is accompanied by increase of mRNA of endostatin after pshRNA-sflt-1 induced corneal neovascularization. The mechanism in which these factors work merits further investigation.

Program#/Poster#: 6390/D854
Presentation Time: Thursday, May 05, 11:15 AM - 1:00 PM. Session Number: 552, Session Title: Inflammation and Neovascularization. Location: Hall B/C





Research at the Moran Eye Center

The John A. Moran Eye Center hosts a collection of collegial and imaginative scientists whose work ranges from the development of the eye and retinal pigmented epithelium to the organization of visual cortex; from basic mechanisms of retinal phototransduction and the visual cycle, to the genetics and plasticity of retinal diseases; from synaptic interactions to immune modulation. Based in the L.S. and Aline Skaggs Research Pavilion, and joined by multiple walkways to the John A. Moran Clinical Pavilion, the Moran Eye Center research effort spans seven floors of laboratories, support resources and expansion space. Community engagement in our research programs is reflected in the es-

tablishment of the William and Pat Child and Ida Smith Vision Research Floors, and the Thomas Dee II & Family Center for Macular Degeneration Research.

The Moran Eye Center currently houses over 38,000 sq. ft. of dedicated, secure research space with primary state-of-the-art research space dedicated to individual research scientists. Each floor also houses core facilities including cold rooms, dark rooms, tissue culture facilities, ultracold freezer storage, office space students and fellows, conference and administrative space. Support include a dishwashing and in-house professional building management.

The Moran Eye Center houses a secure, accredited state-of-the-art vivarium managed and staffed by the University. With capacity of over 3000 mouse cages in a sealed system, the facility has procedure rooms, surgery, cage washing, and staff offices.

Major Moran Eye Center Core equipment includes two electron microscopes including an automated JEOL JEM 1400 with capacity for 5000 images/day; confocal systems; research cryostats, spectrophotometers, gel imagers, sequencing, mass spectrometry, terabyte scale data storage, optical scanning light microscopy, imaging workstations. Computational resources include a high density



of gigabit ports (over 50/floor), secure wireless at all locations, and encrypted communication options.

Our basic and translational science programs include:

- The development and phenotypic maturation of the retinal pigmented epithelium
- Developmental mechanisms of cell proliferation and differentiation in the neural retina
- The genetics and biology of developmental eye defects
- The genetics, molecular and cell biology of macular degenerations
- Macular degeneration therapeutics
- Animal models of macular degeneration
- The molecular biology of phototransduction

- The molecular biology and biochemistry of retinoid metabolism
- The molecular biology and neurobiology of inherited retinal degenerations
- Gene therapy for Usher syndrome and other forms of retinitis pigmentosa
- The molecular and cellular basis of glaucoma
- Calcium signaling and regulation in the neural retina
- Regulation of vessel growth in retina and cornea
- Nanoparticle drug delivery mechanisms
- Synaptic plasticity in the developing and mature retina
- Retinal connectomics
- Retinal metabolomics
- The basis of excitatory signaling in the neural retina
- Parallel processing in visual cortex
- Cortical neuroprosthetics

- Tissue - intraocular lens implant interactions

These programs benefit from a strong collaborative tradition of the University of Utah that includes the Departments of Biology, Biochemistry, Biomedical Engineering, Electrical and Computer Engineering, Human Genetics, Internal Medicine, Mathematics, Medicinal Chemistry, Neurobiology and Anatomy, Neurology, Pediatrics, Physics, and Physiology; the School of Computing; and the Scientific Computing and Imaging Institute. In addition, strong graduate programs in Neuroscience, Biomedical Engineering and Molecular Biology, as well as MD/PhD programs through the University of Utah School of Medicine provide a vibrant collection of students for the John A. Moran Eye Center.



Bala Ambati M.D., Ph.D., has the distinction of being the world's youngest person to graduate from medical school at 17. He received his ophthalmology training at Harvard and Duke Universities. Dr. Ambati is experienced in procedures of the cornea and anterior segment of the eye. He has been an invited speaker at the World Ophthalmology Congress, American Society of Cataract & Refractive Surgery, International Congress of Eye Research, and other national and international conferences. He donates time overseas on missions with ORBIS, a non-profit organization with a Flying Eye Hospital, on which Dr. Ambati has operated and trained local surgeons in Ghana and Malaysia. With respect to clinical research, Dr. Ambati is committed to constant analysis of results of cornea transplants, LASIK, cataract extraction, and other anterior segment procedures.



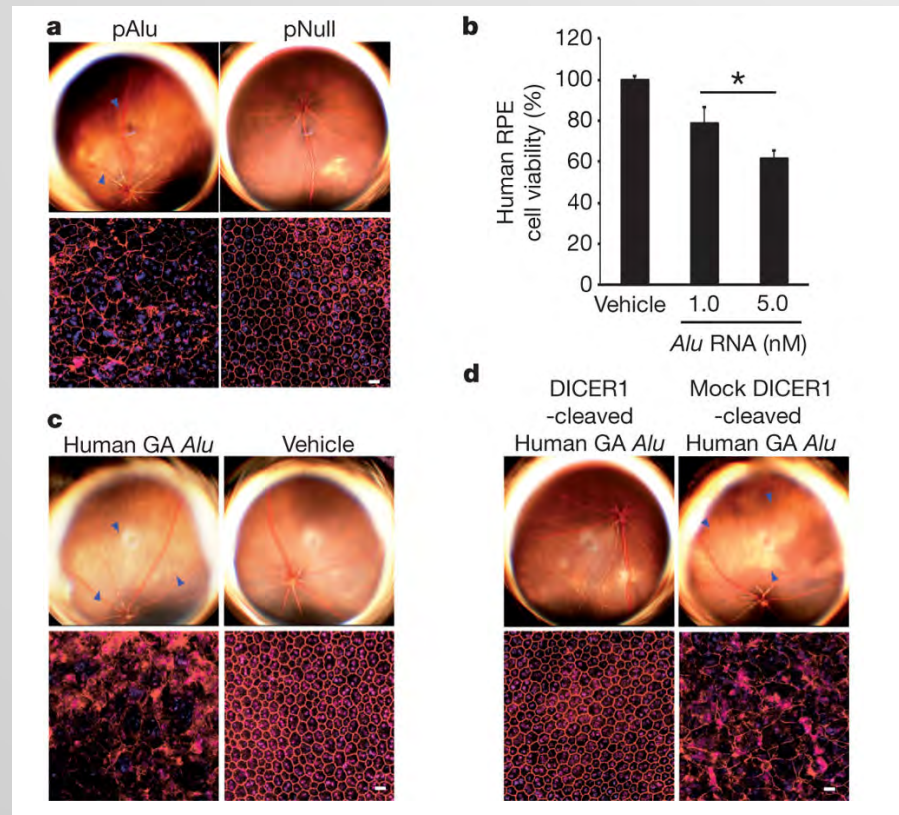
Retinal Research

DICER1 deficit induces Alu RNA toxicity in age-related macular degeneration.

Author: Kaneko H, Dridi S, Tarallo V, Gelfand BD, Fowler BJ, Cho WG, Kleinman ME, Ponicsan SL, Hauswirth WW, Chiodo VA, Karikó K, Yoo JW, Lee DK, Hadziahmetovic M, Song Y, Misra S, Chaudhuri G, Buas FW, Braun RE, Hinton DR, Zhang Q, Grossniklaus HE, Provis JM, Madigan MC, Milam AH, Justice NL, Albuquerque RJ, Blandford AD, Bogdanovich S, Hirano Y, Witte J, Fuchs E, Littman DR, Ambati BK, Rudin CM, Chong MM, Provost P, Kugel JF, Goodrich JA, Dunaief JL, Baffi JZ, Ambati J.

Journal: Nature. 2011 Feb 6.

ABSTRACT: Geographic atrophy (GA), an untreatable advanced form of age-related macular degeneration, results from retinal pigmented epithelium (RPE) cell degeneration. Here we show that the microRNA (miRNA)-processing enzyme DICER1 is reduced in the RPE of humans with GA, and that conditional ablation of *Dicer1*, but not seven other miRNA-processing enzymes, induces RPE degeneration in mice. DICER1 knockdown induces accumulation of Alu RNA in human RPE cells and Alu-like B1 and B2 RNAs in mouse RPE. Alu RNA is increased in the RPE of humans with GA, and this pathogenic RNA



a, Subretinal pAlu, but not pNull, induced wild-type mouse RPE degeneration (fundus photographs, top row; ZO-1 stained (red) flat mounts, bottom row). b, Alu RNA induced human RPE cytotoxicity. Values normalized to pNull or vehicle. * $P < 0.05$ by Student t-test. $n = 4-6$. c, Subretinal Alu RNA isolated and cloned from human GA RPE induced wild-type mouse RPE degeneration. d, Subretinal injection of this Alu RNA, when cleaved by DICER1, did not induce wild-type mouse RPE degeneration (fundus photographs, top row; flat mounts, bottom row) in contrast to mock-cleaved Alu RNA. Degeneration outlined by blue arrowheads (a, c, d). Scale bars, 20 μm . $n = 10-15$.

induces human RPE cytotoxicity and RPE degeneration in mice. Antisense oligonucleotides targeting Alu/B1/B2 RNAs prevent DICER1 depletion-induced RPE degeneration despite global miRNA downregulation. DICER1 degrades Alu RNA, and this digested Alu RNA cannot induce RPE degeneration in mice. These findings reveal a miRNA-independent cell survival function for DICER1 involving retrotransposon transcript degradation, show that Alu RNA can directly cause human pathology, and identify new targets for a major cause of blindness.

Whirlin Replacement Restores the Formation of the USH2 Protein Complex in Whirlin Knockout Photoreceptors.

Author: Zou J, Luo L, Shen Z, Chiodo VA, Ambati BK, Hauswirth WW, Yang J.

Journal: Invest Ophthalmol Vis Sci. 2011.

PURPOSE: Whirlin is the causative gene for Usher syndrome type IID (USH2D), a condition manifested as both retinitis pigmentosa and congenital deafness. Mutations in this gene cause disruption of the USH2 protein complex composed of USH2A and VLGR1 at the periciliary membrane complex (PMC) in photoreceptors. In this study, we evaluated the adeno-associated virus (AAV)-mediated whirlin replacement as a treatment option.

METHODS: Murine whirlin cDNA driven by the human rhodopsin kinase promoter (hRK) was packaged as an AAV2/5 vector and delivered into the whirlin knockout retina through subretinal injection. The efficiency, efficacy and safety of this treatment were examined using immunofluorescent staining, confocal imaging, immunoelectron microscopy, western analysis, histological analysis and electroretinogram.

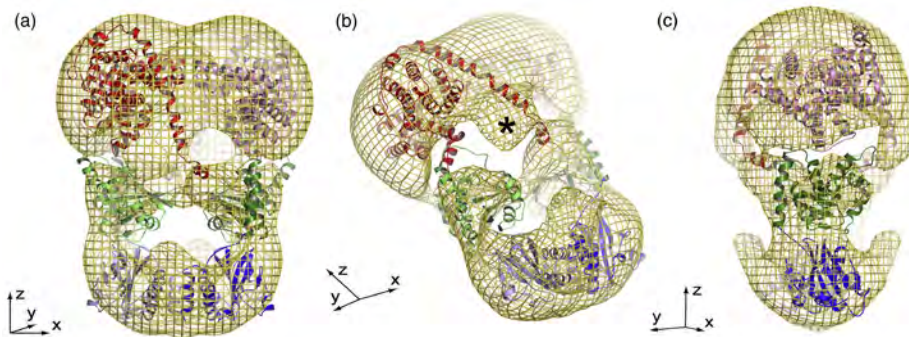
RESULTS: The AAV-mediated whirlin expression started at 2 weeks, reached its maximum level at 10 weeks, and lasted up to 6 months post injection. The transgenic whirlin product had a molecular size and an expression level comparable to the wild-type. It was distributed at the PMC in both rod and cone photoreceptors from the central to peripheral retina. Importantly, the transgenic whirlin restored the cellular localization and expression level of both USH2A and VLGR1 and did not cause defects in the retinal histology and function in the whirlin knockout mouse.

CONCLUSION: Whirlin transgene recruits USH2A and VLGR1 to the PMC and is sufficient for the formation of the USH2 protein complex in photoreceptors. The combined hRK and AAV gene delivery system could be an effective gene therapy approach to treat retinal degeneration in USH2D patients.



Wolfgang Baehr, Ph.D., studied organic chemistry at the University of Heidelberg. His career in retinal research was launched in the Department of Biochemistry, Princeton University, in 1976. He was recruited from the Cullen Eye Institute at Baylor College of Medicine where he was a Jules and Doris Stein Research to Prevent Blindness Professor from 1987 – 1994, and joined the Moran Eye Center as Professor of Ophthalmology and Director of our Foundation Fighting Blindness Center.

Dr. Baehr's career work addresses the biochemistry and molecular biology of the capture of light by photoreceptors in the eye, and the biochemistry of the key elements in the process with a focus on gene defects causative for human retinal disease.



PDE6 exhibits an entangled topology. A homology model for PDE6 was generated by docking the structures of the closest in-sequence of individual subdomains into the 18-Å map. Crystal contacts from subdomain structures were also examined to understand likely interaction surfaces between the individual PDE protamer subdomains (for details, see the text). (a) PDE α and PDE β subunits wrap around one another, exhibiting an entangled topology. Catalytic domains are shown in red/pink, GAF-B domains are shown in green/light green, and GAF-A domains are shown in blue/light blue. (b) The model has been rotated to show unmodeled density (*), which comprises the putative location of the central region of PDE6 γ . (c) View of (a) rotated 90° about the y-axis.

Structural characterization of the rod cGMP phosphodiesterase 6.

Author: Goc A, Chami M, Lodowski DT, Bosshart P, Moiseenkova-Bell V, Baehr W, Engel A, Palczewski K.

Journal: J Mol Biol. 2010 Aug 20;401(3):363-73.

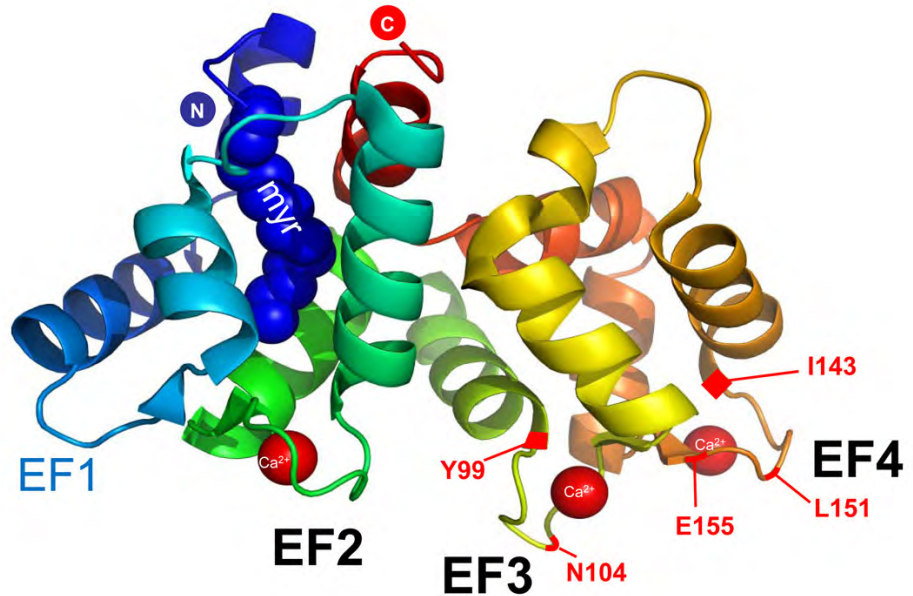
ABSTRACT: Rod cGMP phosphodiesterase 6 (PDE6) is a key enzyme of the phototransduction cascade, consisting of PDE6alpha, PDE6beta, and two regulatory PDE6gamma subunits. PDE6 is membrane associated through isoprenyl membrane anchors attached to the C-termini of PDE6alpha and PDE6beta and can form a complex with prenyl-binding protein delta (PrBP/delta), an isoprenyl-binding protein that is highly expressed in photoreceptors. The stoichiometry of PDE6-PrBP/delta binding and the mechanism by which the PDE6-PrBP/delta complex assembles have not been fully characterized, and the location of regulatory PDE6gamma subunits within the protein assembly has not been elucidated. To clarify these questions, we have developed a rapid purification method for PDE6-PrBP/delta from bovine rod outer segments utilizing recombinant PrBP/delta. Transmission electron microscopy of negatively stained samples revealed the location of PrBP/delta and, thus, where the carboxyl-termini of PDE6alpha and PDE6beta must be located. The three-dimensional structure of the PDE6alphabeta gamma complex was determined up to 18 Å resolution from single-particle projections and was interpreted by model building to identify the probable location of isoprenylation, PDE6gamma subunits, and catalytic sites.

GCAP1 Mutations Associated with Autosomal Dominant Cone Dystrophy.

Author: Jiang L, Baehr W.

Journal: Adv Exp Med Biol. 2010;664:273-82.

ABSTRACT: We discuss the heterogeneity of autosomal dominant cone



Structure of GCAP1 (adapted from (Baehr & Palczewski, 2009). N-terminal (blue) and C-terminal (red) helices bury the myristoyl group attached to Gly-2. The EF hands are solvent exposed and shown with bound Ca^{2+} . The EF1 motif is incompetent for Ca^{2+} binding. Approximate locations of residues associated with cone dystrophy are depicted in red.

and cone-rod dystrophies (adCD, and adCORD, respectively). As one of the best characterized adCD genes, we focus on the GUCA1A gene encoding guanylate cyclase activating protein 1 (GCAP1), a protein carrying three high affinity $\text{Ca}(2+)$ binding motifs (EF hands). GCAP1 senses changes in cytoplasmic free $[\text{Ca}(2+)]$ and communicates these changes to GC1, by either inhibiting it (at high free $[\text{Ca}(2+)]$), or stimulating it (at low free $[\text{Ca}(2+)]$). A number of missense mutations altering the structure and $\text{Ca}(2+)$ affinity of EF hands have been discovered. These mutations are associated with a gain of function, producing dominant cone and cone rod dystrophy phenotypes. In this article we review these mutations and describe the consequences of specific mutations on GCAP1 structure and GC stimulation. We discuss the heterogeneity of autosomal dominant cone and cone-rod dystrophies (adCD, and adCORD, respectively). As one of the best characterized adCD genes, we focus on the GUCA1A gene encoding guanylate cyclase activating protein 1 (GCAP1), a protein carrying three high affinity $\text{Ca}(2+)$ binding motifs (EF hands). GCAP1 senses changes in cytoplasmic free $[\text{Ca}(2+)]$ and communicates these changes to GC1, by either in-

hibiting it (at high free $[\text{Ca}(2+)]$), or stimulating it (at low free $[\text{Ca}(2+)]$). A number of missense mutations altering the structure and $\text{Ca}(2+)$ affinity of EF hands have been discovered. These mutations are associated with a gain of function, producing dominant cone and cone rod dystrophy phenotypes. In this article we review these mutations and describe the consequences of specific mutations on GCAP1 structure and GC stimulation.

PKC α is essential for the proper activation and termination of rod bipolar cell response.

Author: Ruether K, Feigenspan A, Pirngruber J, Leitges M, Baehr W, Strauss O. Charité- Eye-Hospital, Campus Virchow-Klinikum, Universitätsmedizin Berlin, Berlin, Germany. ruether@freenet.de

Journal: Invest Ophthalmol Vis Sci. 2010 Nov;51(11):6051-8.

PURPOSE: Protein kinase (PKC)- α is abundant in retinal bipolar cells. This study was performed to explore its role in visual processing.

METHODS: PKC α -knockout (Prk-

ca(-/-)) mice and control animals were examined by using electroretinography (ERG), light microscopy, and immunocytochemistry.

RESULTS: The Prkca(-/-) mice showed no signs of retinal degeneration up to 12 months of age, but ERG measurements indicated a decelerated increase in the ascending limb of the scotopic (rod-sensitive) b-wave as well as a delayed return to baseline. These results suggest that PKC α is an important modulator that affects bipolar cell signal transduction and termination. Confocal microscopy of retinal sections showed that PKC α co-localized with calbindin, which indicates a PKC α localization in close proximity to the horizontal cell terminals. In addition, the implicit time of the ERG c-wave originating from the retinal pigment epithelium (RPE) and the recovery of photoreceptors from bleaching conditions were substantially faster in the knockout mice than in the wild-type control animals.

CONCLUSIONS: These results suggest that PKC α is a modulator of rod-bipolar cell function by accelerating glutamate-driven signal transduction and termination. This modulation is of importance in the switch between scotopic and photopic vision. Furthermore, PKC α seems to play a role in RPE function.

Human ocular carotenoid-binding proteins.

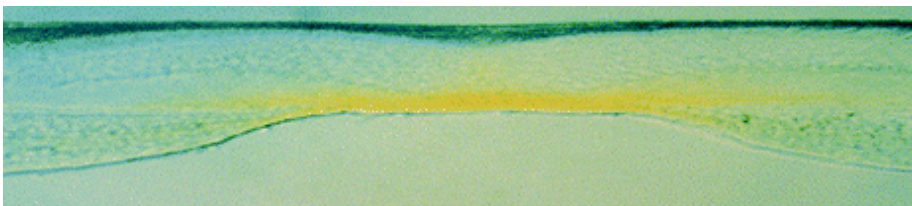
Author: Li B, Vachali P, Bernstein PS.

Journal: Photochem Photobiol Sci. 2010 Nov;9(11):1418-25.

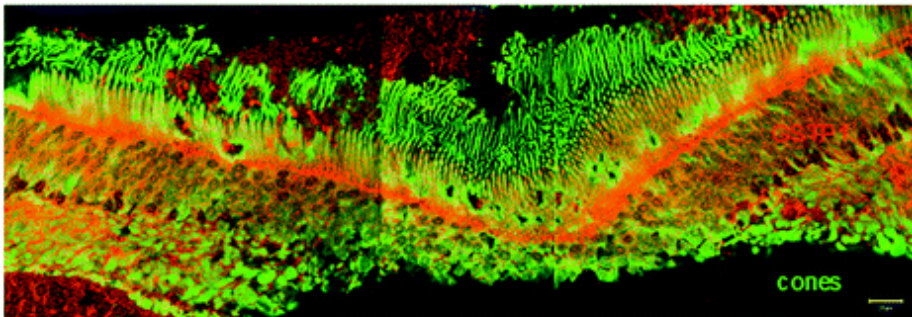
ABSTRACT: Two dietary carotenoids, lutein and zeaxanthin, are specifically delivered to the human macula at the highest concentration anywhere in the body. Whenever a tissue exhibits highly selective uptake of a compound, it is likely that one or more specific binding proteins are involved in the process. Over the past decade, our laboratory has identified and characterized several carotenoid-binding proteins from human retina including a pi isoform of glutathione S-transferase (GSTP1) as a zeaxanthin-binding protein, a member of the steroidogenic acute regulatory domain (StARD) family as a lutein-binding protein, and tubulin as a less specific, but higher capacity site for carotenoid deposition. In this article, we review the purification and characterization of these carotenoid-binding proteins, and we relate these ocular carotenoid-binding proteins to the transport and uptake role of serum lipoproteins and scavenger receptor proteins in a proposed pathway for macular pigment



Paul S. Bernstein, M.D., Ph.D., joined the faculty of the Moran Eye Center in 1995, where he currently divides his time equally between basic science retina research and a clinical practice devoted to medical and surgical treatment of disease of the retina and vitreous, with special emphasis on macular and retinal degenerations. His academic training at Harvard University included a summa cum laude undergraduate degree in chemistry, a PhD with Robert Rando, and an MD from the Division of Health Sciences and Technology, and a joint program between Harvard Medical School and MIT. He did a post-doctoral fellowship with Dr. Dean Bok in retinal cell biology and a residency in ophthalmology at the UCLA Jules Stein Eye Institute.



(a)



(b)

(a) Vertical section (vitreous side down) through a monkey fovea showing the distribution of the yellow macular carotenoids. Image courtesy of D. Max Snodderly, PhD. (b) GSTP1 labeling of foveal cones in the macula of a 3-year-old monkey. The orientation of the section is the same as in (a). This montage shows strongest labeling by antibody against GSTP1 (red) over the myoid and ellipsoid regions of cones identified by monoclonal antibody 7G6 (green).

carotenoid delivery to the human retina.

Long-chain and very long-chain polyunsaturated fatty acids in ocular aging and age-related macular degeneration.

Author: Liu A, Chang J, Lin Y, Shen Z, Bernstein PS.

Journal: J Lipid Res. 2010 Nov;51(11):3217-29.

ABSTRACT: Retinal long-chain PUFAs (LC-PUFAs, C(12)-C(22)) play important roles in normal human retinal function and visual development, and some epidemiological studies of LC-PUFA intake suggest a protective role against the incidence of advanced age-related macular degeneration (AMD). On the other hand, retinal very long-chain PUFAs (VLC-PUFAs, C(n>22)) have received much less attention since their identification decades ago, due to their minor abundance and more difficult assays, but recent discoveries that defects in VLC-PUFA synthetic enzymes are associated with rare forms of inherited macular degenerations have refocused attention on their potential roles in retinal health and disease. We thus developed improved GC-MS methods to detect LC-PUFAs and VLC-PUFAs, and we then applied them to the study of their changes in ocular aging and AMD. With ocular aging, some VLC-PUFAs in retina and retinal pigment epithelium (RPE)/choroid peaked in middle age. Compared with age-matched normal donors, docosahexaenoic acid, adrenic acid, and some VLC-PUFAs in AMD retina and RPE/

choroid were significantly decreased, whereas the ratio of n-6/n-3 PUFAs was significantly increased. All these findings suggest that deficiency of LC-PUFAs and VLC-PUFAs, and/or an imbalance of n-6/n-3 PUFAs, may be involved in AMD pathology.

ARMS2/HTRA1 locus can confer differential susceptibility to the advanced subtypes of age-related macular degeneration.

Author: Sobrin L, Reynolds R, Yu Y, Fagerness J, Leveziel N, Bernstein PS, Souied EH, Daly MJ, Seddon JM.

Journal: Am J Ophthalmol. 2011 Feb;151(2):345-52.e3.

PURPOSE: To determine if genetic variants that have been associated with age-related macular degeneration (AMD) have a differential effect on the risk of choroidal neovascularization (CNV) and geographic atrophy.

DESIGN: Genetic association study.

SETTING: Multicenter study.

STUDY POPULATION: Seven hundred forty-nine participants with geographic atrophy and 3209 participants with CNV were derived from 4 AMD studies with similar procedures from Tufts Medical Center, the Age-Related Eye Disease Study, University of Utah, and Hospital Intercommunal de Creteil.

PROCEDURES: AMD grade was assigned based on fundus photography and examination using the clinical age-related maculopathy staging

system. All samples were genotyped for single nucleotide polymorphisms (SNPs) previously associated with AMD. Allele frequencies were compared between participants with CNV and geographic atrophy using PLINK within each cohort and Mantel-Haenszel meta-analysis was performed to combine odds ratios (OR).

MAIN OUTCOME MEASURES: Differences in allele frequencies between participants with geographic atrophy and CNV.

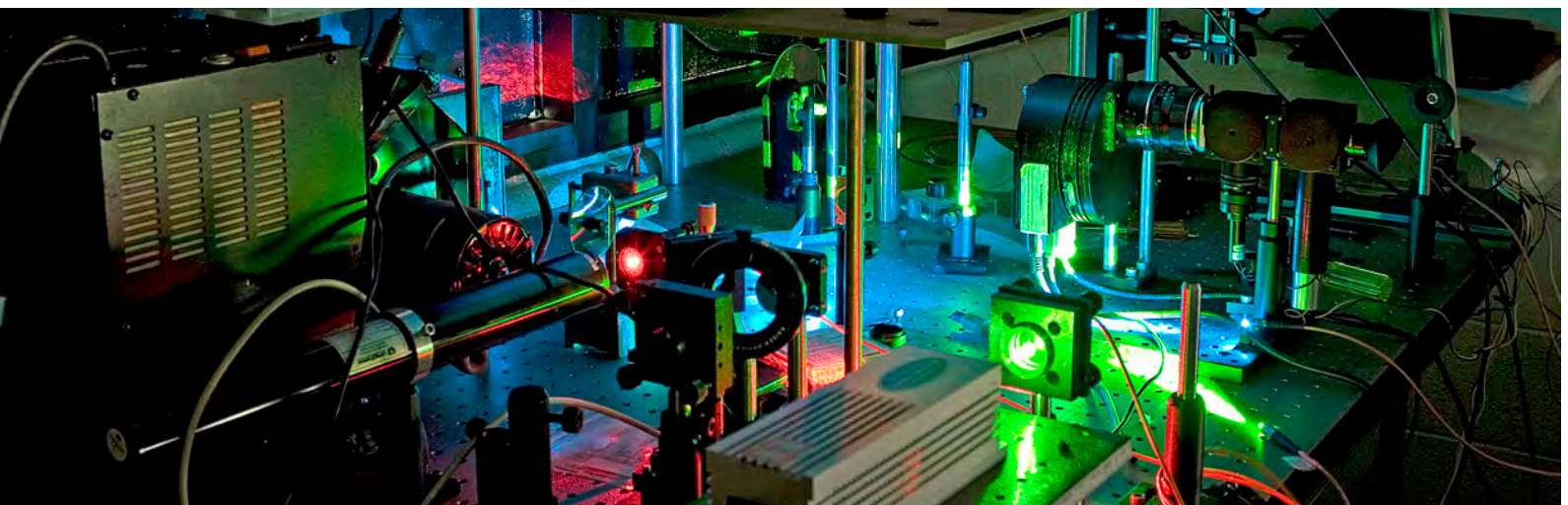
RESULTS: The frequency of the T allele of ARMS2/HTRA1 rs10490924 was significantly higher in participants with CNV than in those with geographic atrophy (OR, 1.37; 95% confidence interval, 1.21-1.54; P value = 4.2×10^{-7}). This result remained statistically significant when excluding individuals who had geographic atrophy in 1 eye and CNV in the contralateral eye (P = 2.2×10^{-4}). None of the other SNPs showed a significant differential effect for CNV vs geographic atrophy, including CFH, C2/CFB, C3, CFI, LIPC, and TIMP3.

CONCLUSIONS: Genetic variation at the ARMS2/HTRA1 locus confers a differential risk for CNV vs geographic atrophy in a well-powered sample.

Studies on the singlet oxygen scavenging mechanism of human macular pigment.

Author: Li B, Ahmed F, Bernstein PS.

Journal: Arch Biochem Biophys. 2010 Dec 1;504(1):56-60.



ABSTRACT: It is thought that direct quenching of singlet oxygen and scavenging free radicals by macular pigment carotenoids is a major mechanism for their beneficial effects against light-induced oxidative stress. Corresponding data from human tissue remains unavailable, however. In the studies reported here, electron paramagnetic resonance (EPR) spectroscopy was used to measure light-induced singlet oxygen generation in post-mortem human macula and retinal pigment epithelium/choroid (RPE/choroid). Under white-light illumination, production of singlet oxygen was detected in RPE/choroid but not in macular tissue, and we show that exogenously added macular carotenoids can quench RPE/choroid singlet oxygen. When the singlet oxygen quenching ability of the macular carotenoids was investigated in solution, it was shown that a mixture of meso-zeaxanthin, zeaxanthin, and lutein in a ratio of 1:1:1 can quench more singlet oxygen than the individual carotenoids at the same total concentration.

Prospective study of common variants in the retinoic acid receptor-related orphan receptor α gene and risk of neovascular age-related macular degeneration.

Author: Schaumberg DA, Chasman D, Morrison MA, Adams SM, Guo Q, Hunter DJ, Hankinson SE, DeAngelis MM.

Journal: Arch Ophthalmol. 2010 Nov;128(11):1462-71.

OBJECTIVES: The retinoic acid receptor (RAR)-related orphan receptor α gene (RORA) is implicated as a candidate for age-related macular degeneration (AMD) through a previous microarray expression study, linkage data, biological plausibility, and 2 clinic-based cross-sectional studies. We aimed to determine if common variants in RORA predict future risk of neovascular AMD.

METHODS: We measured genotypes for 18 variants in intron 1 of the RORA gene among 164 cases who developed neovascular AMD and 485 age- and

sex-matched controls in a prospective, nested, case-control study within the Nurses' Health Study and the Health Professionals Follow-up Study. We determined the incidence rate ratios and 95% confidence intervals (CI) for neovascular AMD for each variant and examined interactions with other AMD-associated variants and modifiable risk factors.

RESULTS: We identified one single-nucleotide polymorphism (rs12900948) that was significantly associated with increased incidence of neovascular AMD. Participants with 1 and 2 copies of the G allele were 1.73 (CI, 1.32-2.27) and 2.99 (CI, 1.74-5.14) times more likely to develop neovascular AMD. Individuals homozygous for both the G allele of rs12900948 and ARMS2 A69S had a 40.8-fold increased risk of neovascular AMD (CI, 10.1-164; $P = .017$). Cigarette smokers who carried 2 copies of the G allele had a 9.89-fold risk of neovascular AMD but the interaction was not significant ($P = .08$). We identified a significant AMD-associated haplotype block containing the single-nucleotide polymorphisms rs730754, rs8034864, and rs12900948, with P values for ACA = 1.16×10^{-9} , ACG = 5.85×10^{-12} , and GAA = .0001 when compared with all other haplotypes.

CONCLUSIONS: Common variants and haplotypes within the RORA gene appear to act synergistically with the ARMS2 A69S polymorphism to increase risk of neovascular AMD. These data add further evidence of a high level of complexity linking genetic and modifiable risk factors to AMD development and should help efforts at risk prediction.

Genome-wide association study of advanced age-related macular degeneration identifies a role of the hepatic lipase gene (LIPC).

Author: Neale BM, Fagerness J, Reynolds R, Sobrin L, Parker M, Raychaudhuri S, Tan PL, Oh EC, Merriam JE, Souied E, Bernstein PS, Li B, Frederick JM, Zhang K, Brantley MA Jr, Lee AY, Zack DJ, Cam-



Margaret DeAngelis, PhD, Dr.

DeAngelis is currently an Associate Professor at the John A. Moran Eye Center, University of Utah School of Medicine. Previously she was an Assistant Professor in the Dept of Ophthalmology at Harvard Medical School/Massachusetts Eye and Ear Infirmary. Dr. DeAngelis focused her career on vision research in 1999 when she received a post-doctoral fellowship training grant on macular degeneration as part of the Molecular Basis of Eye Disease program at Harvard Medical School. Working with retina specialists Drs. Ivana Kim and Joan Miller she recruited and developed a large patient population of families to study the genetic and epidemiologic underpinnings of age-related macular degeneration (AMD). As a result Dr. DeAngelis is a Principal Investigator of a competitive renewal from the National Eye Institute to study the molecular genetics of AMD.

In addition to studying genetic susceptibility to AMD, her group, working in collaboration with Dr. Hageman, who joined the Moran Eye Center in 2009, is utilizing a systems biology based approach to pinpoint the cause for disease by elucidating key regulatory components in pathways or sets of genes which are implicated in AMD. Their aim is to develop appropriate preventive and therapeutic targets to cure this devastating form of blindness.



Jeanne M. Frederick, Ph.D.

Identification of genes involved in inherited human retinal disorders is the goal of research conducted by Jeanne Frederick, PhD and Wolfgang Baehr, PhD. One of the best known heritable retinal diseases is retinitis pigmentosa (RP). Multiple genetic causes, each identified at the molecular level, are responsible for RP. The general approach to this research is two-fold: to understand the molecular mechanism responsible for degeneration, and to design rational strategies to intervene and, eventually, retard or reverse disease onset. One method involves development of an animal strain that mimics a human disease. For example, knowing a specific DNA alteration in human visual pigment that is associated with RP, the same alteration can produce a comparable retinal degeneration in mice which can then be used to study the physiology, biochemistry, and morphology of the retina.

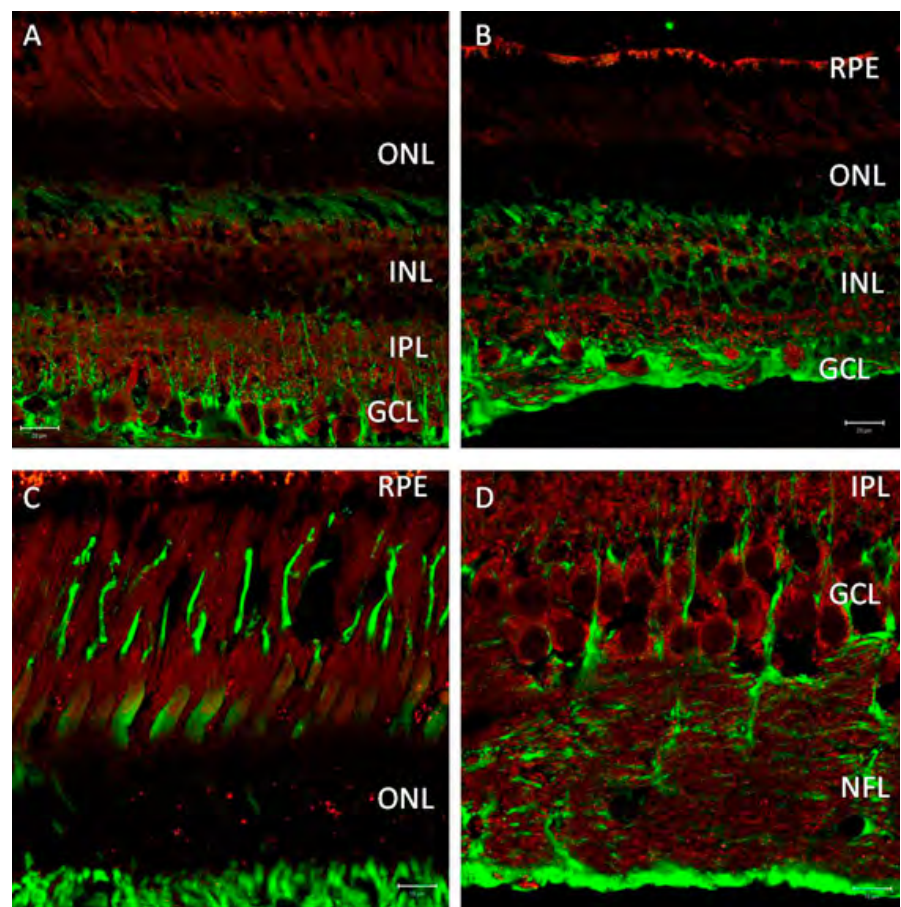


pochiaro B, Campochiaro P, Ripke S, Smith RT, Barile GR, Katsanis N, Allikmets R, Daly MJ, Seddon JM.

Journal: Proc Natl Acad Sci U S A. 2010 Apr 20;107(16):7395-400.

ABSTRACT: Advanced age-related macular degeneration (AMD) is the leading cause of late onset blindness. We present results of a genome-wide association study of 979 advanced AMD cases and 1,709 controls using the Affymetrix 6.0 platform with replication in seven additional cohorts (totaling 5,789 unrelated cases and 4,234 unrelated controls). We also present a comprehensive analysis of copy-number variations and polymorphisms for AMD. Our discovery data implicated the association between AMD and

a variant in the hepatic lipase gene (LIPC) in the high-density lipoprotein cholesterol (HDL) pathway (discovery $P = 4.53 \times 10^{-5}$ for rs493258). Our LIPC association was strongest for a functional promoter variant, rs10468017, ($P = 1.34 \times 10^{-8}$), that influences LIPC expression and serum HDL levels with a protective effect of the minor T allele (HDL increasing) for advanced wet and dry AMD. The association we found with LIPC was corroborated by the Michigan/Penn/Mayo genome-wide association study; the locus near the tissue inhibitor of metalloproteinase 3 was corroborated by our replication cohort for rs9621532 with $P = 3.71 \times 10^{-9}$. We observed weaker associations with other HDL loci (ABCA1, $P = 9.73 \times 10^{-4}$; cholesterylester transfer protein, $P = 1.41 \times 10^{-3}$; FADS1-3, $P =$



(A) Distribution of hepatic lipase C (red) in central monkey retina using a rabbit polyclonal antibody (Cat. #SC-21007) raised against amino acids 91–160 of human origin. This antibody labels all retina neurons, especially ganglion cells of central monkey retina, but does not label Mueller cells (identified by glutamine synthetase; green). (Scale bar, 20 μm .) (B) Distribution of hepatic lipase C (red) in peripheral monkey retina. (Scale bar, 20 μm .) (C) High-magnification images of photoreceptors show immunoreactivity for antihepatic lipase C (red). (Scale bar, 10 μm .) (D) High-magnification images of ganglion cells show immunoreactivity for antihepatic lipase C (red). (Scale bar, 10 μm .) Cones, defined by primate cone arrestin labeling (mAb 7G6; green in C), are positive for hepatic lipase C. However, rods reveal a strong punctate label (red) in the outer nuclear layer as well as over inner and outer segments. In D, strong immunoreactivity for hepatic lipase C (red) observed in ganglion cell somata and axons of the nerve fiber layer (NFL) contrasts with that of a Mueller cell marker (green; glutamine synthetase; BD Transduction).

2.69e-02). Based on a lack of consistent association between HDL increasing alleles and AMD risk, the LIPC association may not be the result of an effect on HDL levels, but it could represent a pleiotropic effect of the same functional component. Results implicate different biologic pathways than previously reported and provide new avenues for prevention and treatment of AMD.

Identification of StARD3 as a Lutein-binding Protein in the Macula of the Primate Retina.

Author: Li B, Vachali P, Frederick JM, Bernstein PS.

Journal: *Biochemistry*. 2011 Feb 15.

ABSTRACT: Lutein, zeaxanthin and their metabolites are the xanthophyll carotenoids that form the macular pigment of the human retina. Epidemiological evidence suggests that high levels of these carotenoids in the diet, serum and macula are associated with decreased risk of age-related macular degeneration (AMD), and the AREDS2 study is prospectively testing this hypothesis. Understanding the biochemical mechanisms underlying the selective uptakes of lutein and zeaxanthin into the human macula may provide important insights into the physiology of the human macula in health and disease. GSTP1 is the macular zeaxanthin-binding protein, but the identity of the human macular lutein-binding protein has remained elusive. Prior identification of the silkworm lutein-binding protein (CBP) as a member of the steroidogenic acute regulatory domain (StARD) protein family, and selective labeling of monkey photoreceptor inner segments by anti-CBP antibody provided an important clue toward identifying the primate retina lutein-binding protein. Homology of CBP to all 15 human StARD proteins was analyzed using database searches, western blotting and immunohistochemistry, and we here provide evidence to identify StARD3 (also known as MLN64) as a human retinal lutein-binding protein. Further, recombinant StARD3 selectively binds lutein with high af-

finity ($KD = 0.45$ micromolar) when assessed by surface plasmon resonance (SPR) binding assays. Our results demonstrate previously unrecognized, specific interactions of StARD3 with lutein and provide novel avenues to explore its roles in human macular physiology and disease.

Heparan sulfate, including that in Bruch's membrane, inhibits the complement alternative pathway: implications for age-related macular degeneration.

Author: Kelly U, Yu L, Kumar P, Ding JD, Jiang H, Hageman GS, Arshavsky VY, Frank MM, Hauser MA, Rickman CB.

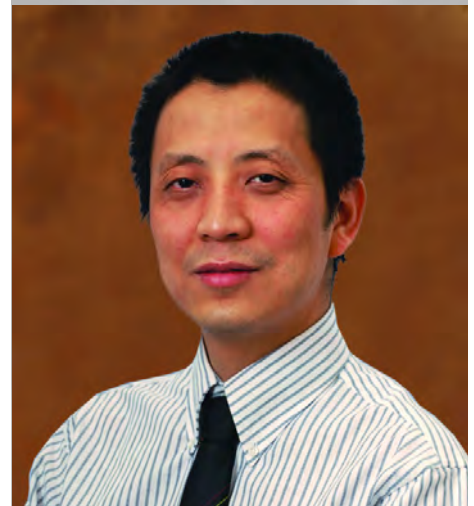
Journal: *J Immunol*. 2010 Nov 1;185(9):5486-94.

ABSTRACT: An imbalance between activation and inhibition of the complement system has been implicated in the etiologies of numerous common diseases. Allotypic variants of a key complement fluid-phase regulatory protein, complement factor H (CFH), are strongly associated with age-related macular degeneration (AMD), a leading cause of worldwide visual dysfunction, although its specific role in AMD pathogenesis is still not clear. CFH was isolated from individuals carrying combinations of two of the nonsynonymous coding variants most strongly associated with AMD risk, V62/H402 (risk haplotype variants), I62/Y402 (nonrisk haplotype variants), and V62/Y402. These proteins

Yingbin Fu, PhD, received his BS in Biochemistry at Peking University, Beijing, China. He received his PhD in Biochemistry at Michigan State University, East Lansing, Michigan, where he was a member of the Honor Society for International Scholars. Prior to coming to the Moran Eye Center, Dr. Fu worked as a postdoc fellow at Dr. King-Wai Yau's lab at The Johns Hopkins University School of Medicine in Baltimore, Maryland.



Gregory Hageman, Ph.D., is the new John A. Moran Presidential Professor of Ophthalmology and Visual Sciences and Director of the Center for Translational Medicine. Prior to his move to the Moran Eye Center, Dr. Hageman served as the Iowa Entrepreneurial Endowed Professor and Professor of Ophthalmology & Visual Sciences at the University of Iowa, Carver College of Medicine. At Iowa he directed the Cell Biology and Functional Genomics Laboratory. He held additional appointments as a Senior Member of the University of Iowa Center for Macular Degeneration, an Associate Faculty Member in the Center of the Study of Macular Degeneration, University of California, Santa Barbara, and Honorary Professorships at Queens University, Belfast, UK and Shandong Eye Institute, Qingdao, China.



were used in two functional assays (cell surface- and fluid-phase-based) measuring cofactor activity of CFH in the factor I-mediated cleavage of C3b. Although no variant-specific differences in the cofactor activity were detected, when heparin sulfate (HS) was added to these assays, it accelerated the rate of C3b cleavage, and this effect could be modulated by degree of HS sulfation. Bruch's membrane/choroid, a site of tissue damage in AMD, contains high concentrations of glycosaminoglycans, including HS. Addition of human Bruch's membrane/choroid to the fluid-phase assay accelerated the C3b cleavage, and this effect was lost post treatment of the tissue with heparinase III. Binding of CFH variants to Bruch's membrane/choroid isolated from elderly, non-AMD donor eyes, was similar, as was the functional activity of bound CFH. These findings refine our understanding of interactions of HS and complement and support the hypothesis that these interactions play a role in the transition between normal aging and AMD in Bruch's membrane/choroid.

Perifoveal müller cell depletion in a case of macular telangiectasia type 2.

Author: Powner MB, Gillies MC, Tretiach M, Scott A, Guymer RH, Hageman GS, Fruttiger M.

Journal: *Ophthalmology*. 2010 Dec;117(12):2407-16.

PURPOSE: To assess the histopathologic changes in a postmortem sample

derived from an eye donor with macular telangiectasia (MacTel) type 2 to gain further insight into the cause of the disease.

DESIGN: Clinicopathological case report.

PARTICIPANTS: Postmortem tissue was collected from 5 different donors: 1 MacTel type 2 patient; 1 healthy control; 2 type 2 diabetic patients, 1 with retinopathy and 1 without retinopathy; and 1 patient with unilateral Coat's disease.

METHODS: Macular pigment distribution in the posterior part of freshly dissected eyes was documented by macro photography. Paraffin sections from both the macular and peripheral regions were assessed using antigen retrieval and immunohistochemistry to study the distribution of cell-specific markers. Blood vessels were visualized with antibodies directed against collagen IV and claudin 5; glial cells with antibodies against glial fibrillary acidic protein (GFAP), vimentin, glutamine synthetase (GS), and retinaldehyde binding protein (RLBP1, also known as CRALBP); microglia with an antibody against allograft inflammatory factor 1 (also known as Iba1); and photoreceptors with antibodies against rhodopsin and opsin. Using anatomic landmarks, the sections then were matched with the macular pigment distribution and a fluorescein angiogram of the patient that was obtained before the patient's death.

MAIN OUTCOME MEASURES: Presence and distribution of macular

pigment and cell-specific markers.

RESULTS: Macular pigment was absent in the macula. Furthermore, abnormally dilated capillaries were identified in a macular region that correlated spatially with regions of fluorescein leakage in an angiogram that was obtained 12 years before death. These telangiectatic vessels displayed a marked reduction of the basement membrane component collagen IV, indicating vascular pathologic features. The presence of GFAP was limited to retinal astrocytes, and no reactive Müller cells were identified. Importantly, reduced immunoreactivity with Müller cell markers (vimentin, GS, and RLBP1) in the macula was observed. The area that lacked Müller cells corresponded with the region of depleted macular pigment.

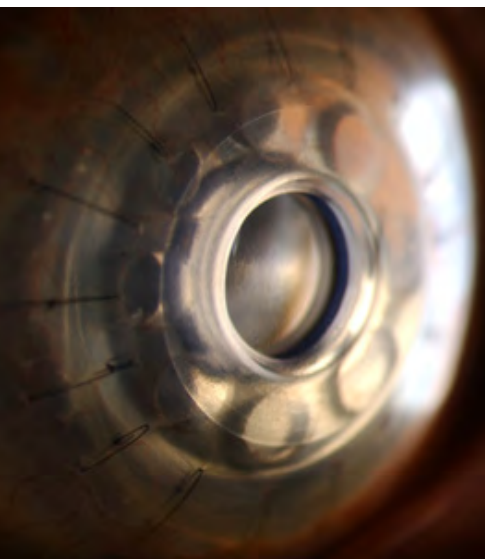
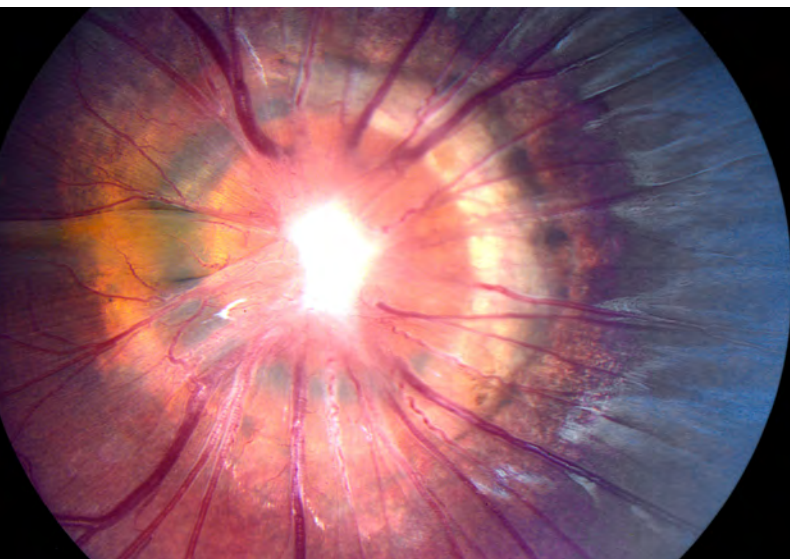
CONCLUSIONS: These findings suggest that macular Müller cell loss or dysfunction is a critical component of MacTel type 2, which may have implications for future treatment strategies.

Vitreoschisis in macular diseases.

Author: Gupta P, Yee KM, Garcia P, Rosen RB, Parikh J, Hageman GS, Sadun AA, Sebag J.

Journal: *Br J Ophthalmol*. 2010 Jun 28.

OBJECTIVES: Vitreoschisis is a possible pathogenic mechanism in macular diseases. Thus, the vitreoretinal interface was evaluated in monkey



eyes and patients with various macular diseases in search of vitreoschisis. It is hypothesized that vitreoschisis is present in macular holes (MH) and macular pucker (MP), but not in other maculopathies.

METHODS: Histopathology was studied in 14 monkey eyes and a vitrectomy specimen of a patient with macular pucker. Optical coherence tomography/scanning laser ophthalmoscopy (OCT/SLO) was performed in 239 eyes: 45 MH, 45 MP, 51 dry age-related macular degeneration (AMD), 53 non-proliferative diabetic retinopathy (NPDR) and 45 controls.

RESULTS: Immunohistochemistry demonstrated lamellae in the posterior vitreous cortex of 12/14 (86%) monkey eyes. With OCT/SLO, vitreoschisis was detected in 24/45 (53%) MH and 19/45 (42%) MP eyes, but in only 7/53 (13%) NPDR, 3/51 (6%) AMD and 3/45 (7%) control eyes ($p < .001$ for all comparisons). Rejoining of the inner and outer walls of the split posterior vitreous cortex was visible in 16/45 (36%) MH eyes and 15/45 (33%) MP eyes. Histopathology of the MP specimen confirmed a split with rejoining in the posterior vitreous cortex.

CONCLUSIONS: Vitreoschisis was detected in half of eyes with MH and MP, but much less frequently in controls, AMD and NPDR patients. These findings suggest that anomalous PVD with vitreoschisis may be pathogenic in MH and MP.

Studies on the pathogenesis of avascular retina and neovascularization into the vitreous in peripheral severe retinopathy of prematurity (an American Ophthalmological Society thesis).

Author: Hartnett ME.

Journal: Trans Am Ophthalmol Soc.
2010 Dec;108:96-119.

PURPOSE: To study vascular endothelial growth factor (VEGF) regulation in the development of intravitre-

ous neovascularization and peripheral avascular retina in peripheral severe retinopathy of prematurity (ROP).

METHODS: The rat 50/10 model of ROP mimics zone II, stage 3 severe ROP and recreates fluctuations in transcutaneous oxygen levels in preterm infants. On postnatal (p) day ages p0, p8, p11-p14, and p18, retinas from the model or room-air (RA) age-matched pups were analyzed for mRNA of VEGF splice variants and receptors using real-time polymerase chain reaction or VEGF protein using enzyme-linked immunosorbent assay.

RESULTS: On p14, when retinas were only 70% vascularized in the model but fully vascularized in RA, VEGF₁₆₄ expression was threefold greater in the model compared to RA. On p18, intravitreal neovascularization was associated with a 5-fold increase in VEGF₁₆₄ mRNA in the model compared to RA. By analysis of variance, VEGF₁₆₄ and VEGFR2 mRNAs were up-regulated in association with increasing developmental age ($P < .0001$ for both comparisons) or exposure to the model compared to RA ($P < .0001$ and $P = .0247$, respectively), whereas increasing developmental age was associated only with up-regulated VEGF₁₂₀ ($P = .0006$), VEGF₁₈₈ ($P = .0256$), and VEGFR1 ($P < .0001$) mRNAs. VEGF protein increased significantly in the model and on p14 and p18 compared to RA ($P < .0001$).

CONCLUSIONS: The model mimics contemporary severe ROP in the United States unlike other models of oxygen-induced retinopathy. Compared to RA retinas, VEGF significantly increased in association with avascular retina and intravitreal neovascularization. A hypothesis is proposed that VEGF up-regulation plays a role in the development of both important features.

The Role of RPE Cell-Associated VEGF189 in Choroidal Endothelial Cell Transmigration across the RPE.

Author: Wang H, Geisen P, Wittchen ES, King B, Burridge K, D'Amore PA, Hartnett ME.



Mary Elizabeth "ME" Hartnett, MD, is a vitreoretinal surgeon and treats and manages adult and pediatric retinal cases. She is now building a pediatric retina center, and pediatric and adult retina clinical practice at the Moran Eye Center. Dr. Hartnett was recently elected into the American Ophthalmological Society.

Dr. Hartnett comes to us from the University of North Carolina at Chapel Hill School of Medicine. She adds an exciting two-fold skill set to our faculty of specialists and experts, as both an accomplished vitreoretinal surgeon and skilled researcher. Dr. Hartnett directs her team in using molecular techniques to study retinal avascularity, or a lack of blood vessel support in areas of the inner retina. Discoveries in her lab have the potential of reducing abnormal damaging blood vessel growth and the diseases associated with this condition.

Journal: Invest Ophthalmol Vis Sci.
2011 Feb 1;52(1):570-8.

PURPOSE: To determine the role of vascular endothelial growth factor 189 (VEGF(189)) in choroidal endothelial cell (CEC) migration across the retinal pigment epithelium (RPE) and to explore the molecular mechanisms involved.

METHODS: Using real-time PCR, the expression of VEGF splice variants VEGF(121,) VEGF(165,) and VEGF(189) was determined in human RPE from donor eyes, cultured human RPE in contact with CECs exposed to hydrogen peroxide (H₂O₂) or hypoxia, and RPE/choroid specimens from mice treated with laser to induce choroidal neovascularization (CNV). Activation of VEGF receptors (VEGFRs), phosphoinositol 3-kinase (PI-3K) or Rac1 was measured in CECs cocultured in contact with RPE exposed to peroxide or silenced for VEGF(189) expression. Migration of CECs across the RPE was determined using fluorescence microscopy.

RESULTS: VEGF(189) expression was increased in human RPE from aged compared with young donor eyes and from mouse RPE/choroids after laser to induce CNV. VEGF(189) was also upregulated in human RPE challenged with peroxide, hypoxia, or cultured in contact with CECs. CEC migration across RPE was greater after RPE exposure to peroxide to induce VEGF(189); VEGFR2 and Rac1 activities were also increased in these CECs. When CECs were cocultured with RPE silenced for VEGF(189), VEGFR2 and Rac1 activities in CECs were significantly reduced, as was CEC migration across the RPE. Inhibition of Rac1 activity significantly inhibited CEC transmigration without affecting PI-3K activity.

CONCLUSIONS: RPE-derived cell-associated VEGF(189) facilitates CEC transmigration by Rac1 activation independently of PI-3K signaling and may have importance in the development of neovascular AMD.

The role of vascular endothelial growth factor-induced activation of NADPH oxidase in choroidal endothelial cells and choroidal neovascularization.

Author: Monaghan-Benson E, Hartmann J, Vendrov AE, Budd S, Byfield G, Parker A, Ahmad F, Huang W, Runge M, Burridge K, Madamanchi N, Hartnett ME.

Journal: Am J Pathol. 2010
Oct;177(4):2091-102.

ABSTRACT: Rac1, a subunit of NADPH oxidase, plays an important role in directed endothelial cell motility. We reported previously that Rac1 activation was necessary for choroidal endothelial cell migration across the retinal pigment epithelium, a critical step in the development of vision-threatening neovascular age-related macular degeneration. Here we explored the roles of Rac1 and NADPH oxidase activation in response to vascular endothelial growth factor treatment in vitro and in a model of laser-induced choroidal neovascularization. We found that vascular endothelial growth factor induced the activation of Rac1 and of NADPH oxidase in cultured human choroidal endothelial cells. Further, vascular endothelial growth factor led to heightened generation of reactive oxygen species from cultured human choroidal endothelial cells, which was prevented by the NADPH oxidase inhibitors, apocynin and diphenyleneiodonium, or the antioxidant, N-acetyl-L-cysteine. In a model of laser-induced injury, inhibition of NADPH oxidase with apocynin significantly reduced reactive oxygen species levels as measured by dihydroethidium fluorescence and the volume of laser-induced choroidal neovascularization. Mice lacking functional p47phox, a subunit of NADPH oxidase, had reduced dihydroethidium fluorescence and choroidal neovascularization compared with wild-type controls. Taken together, these results indicate that vascular endothelial growth factor activates Rac1 upstream from NADPH oxidase in human choroidal endothelial cells and increases generation of reactive oxygen species, contributing to choroidal

neovascularization. These steps may contribute to the pathology of neovascular age-related macular degeneration.

Association of retinal vascular endothelial growth factor with avascular retina in a rat model of retinopathy of prematurity.

Author: Budd SJ, Thompson H, Hartnett ME.

Journal: Arch Ophthalmol. 2010
Aug;128(8):1014-21.

OBJECTIVE: To study the effects of oxygen fluctuations on rat vascular endothelial growth factor (VEGF), VEGF receptor 1(VEGFR1), and VEGFR2 in a model of retinopathy of prematurity (ROP).

METHODS: Retinas at several postnatal days (p) were analyzed for VEGF splice variants, VEGFR1 and VEGFR2 messenger RNAs (mRNAs) using real-time polymerase chain reaction or for VEGF protein using enzyme-linked immunosorbent assay.

RESULTS: Older developmental age was associated with VEGFR1 (P < .001), VEGF(120) (P < .001), and VEGF(188) (P = .03) mRNA overexpression. Expression of VEGFR2 and VEGF(164) mRNAs were associated with older age (P < .001) or exposure to the ROP model (P = .02 and P < .001, respectively). Expression of VEGF protein was greater at p14, when 30% avascular retina existed in the ROP model, compared with room air, when no avascular retina existed, and at p18, when intravitreal neovascularization existed in the model but not in room air (P < .001 for both).

CONCLUSIONS: Unlike models of oxygen-induced retinopathy that describe ROP before implementation of oxygen regulation, the ROP model re-creates oxygen stresses relevant to preterm infants with severe ROP today. Expression of VEGF(164) and VEGFR2 mRNAs and VEGF protein were increased in association with the ROP model and older developmental age and at time points when not

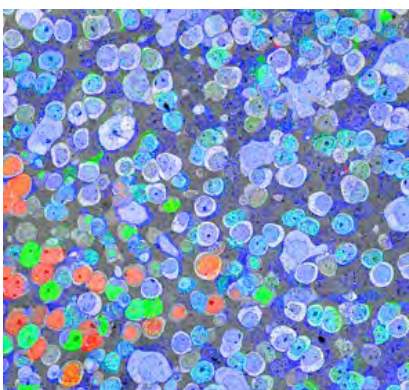
only intravitreal neovascularization but also avascular retina were present in the ROP model and not in room air. Clinical Relevance Regulation of VEGF may have a role in the development of avascular retina and intravitreal neovascularization in some forms of severe ROP.

Retinal Remodeling in the TgP347L Rabbit, a Large-Eye Model of Retinal Degeneration.

Author: Jones BW, Kondo M, Terasaki H, Watt CB, Rapp K, Anderson J, Lin Y, Shaw MV, Yang JH, Marc RE.

Journal: J Comp Neurol, 2011 In Press.

ABSTRACT: Retinitis pigmentosa (RP) is an inherited blinding disease characterized by progressive loss of retinal photoreceptors. There are numerous rodent models of retinal degeneration, but most are poor platforms for interventions that will translate into clinical practice. The rabbit possesses a number of desirable qualities for a model of retinal disease including a large eye and an existing and substantial knowledge base in retinal circuitry, anatomy and ophthalmology. We have analyzed degeneration, remodeling and reprogramming in a rabbit model of retinal degeneration, expressing a rhodopsin proline 347 to leucine transgene in a TgP347L rabbit as a powerful model to study the pathophysiology and treatment of retinal degeneration. We show that disease progression in the TgP347L rabbit closely tracks human cone-sparing RP, including the cone-associated preservation of bipolar cell signaling and triggering of reprogram-



ming. The relatively fast disease progression makes the TgP347L rabbit an excellent model for gene therapy, cell biological intervention, progenitor cell transplantation, surgical interventions and bionic prosthetic studies.

Intracellular pH modulates inner segment calcium homeostasis in vertebrate photoreceptors.

Author: Krizaj D, Mercer AJ, Thoreson WB, Barabas P.

Journal: Am J Physiol Cell Physiol. 2011 Jan;300(1):C187-97.

ABSTRACT: Neuronal metabolic and electrical activity is associated with shifts in intracellular pH (pH(i)) proton activity and state-dependent changes in activation of signaling pathways in the plasma membrane, cytosol, and intracellular compartments. We investigated interactions between two intracellular messenger ions, protons and calcium (Ca^{2+}), in salamander photoreceptor inner segments loaded with Ca^{2+} and pH indicator dyes. Resting cytosolic pH in rods and cones in HEPES-based saline was acidified by $\bullet 0.4$ pH units with respect to pH of the superfusing saline (pH = 7.6), indicating that dissociated inner segments experience continuous acid loading. Cytosolic alkalinization with ammonium chloride (NH_4Cl) depolarized photoreceptors and stimulated Ca^{2+} release from internal stores, yet paradoxically also evoked dose-dependent, reversible decreases in $[\text{Ca}^{2+}]_i$. Alkalinization-evoked $[\text{Ca}^{2+}]_i$ decreases were independent of voltage-operated and store-operated Ca^{2+} entry, plasma membrane Ca^{2+} extrusion, and Ca^{2+} sequestration into internal stores. The $[\text{Ca}^{2+}]_i$ -suppressive effects of alkalinization were antagonized by the fast Ca^{2+} buffer BAPTA, suggesting that pH(i) directly regulates Ca^{2+} binding to internal anionic sites. In summary, this data suggest that endogenously produced protons continually modulate the membrane potential, release from Ca^{2+} stores, and intracellular Ca^{2+} buffering in rod and cone inner segments.



Bryan William Jones, Ph.D., joined the Research Faculty of the Moran Eye Center in 2006. Originally coming to science through the study of epilepsy and sleep medicine, he became fascinated by the beauty of the retina and the complexity of blinding diseases. His work in the laboratory of Dr. Robert E. Marc revealed the nature and extent of pathology seen in retinal degenerative diseases such as retinitis pigmentosa and macular degeneration, now known as retinal remodeling. This work helped to refine approaches to vision rescue through both biomic and biological approaches. Continued work will further define the time lines of retinal remodeling in an effort to determine windows of opportunity for intervention to limit, prevent, or exploit retinal remodeling. Other work in the Marc Laboratory focuses on applying novel molecular and computational approaches to resolving the identities and connectivities of neurons in the retina to discover how the normal retina is wired, how that circuitry is altered in degenerative diseases, and how to potentially engineer artificial biological retinas.



David Krizaj, Ph.D., did graduate training at New York University with Paul Witkovsky focusing on synaptic signaling between retinal cells and postdoctoral work with David Copenhagen at University of California San Francisco School of Medicine, working on intracellular signaling in photoreceptors. He spent six years as faculty at the UCSF Dept of Ophthalmology before joining the Moran Eye Center of the University of Utah in 2007.

He is currently working on intracellular calcium signaling in retinal photoreceptor, ganglion cells and glial cells stimulated by light and in diseases such as retinitis pigmentosa, macular degeneration and glaucoma.



Plasticity of TRPM1 expression and localization in the wild type and degenerating mouse retina.

Author: Krizaj D, Huang W, Furukawa T, Punzo C, Xing W.

Journal: Vision Res. 2010 Nov 23;50(23):2460-5.

ABSTRACT: The light response in retinal ON bipolar cells is associated with disinhibition of current flow through cation channels recently identified as type 1 members of the melastatin transient receptor potential (TRPM) family. We determined the developmental expression of *Trpm1* in the wild type C57BL/6, DBA/2J, DBA2J-Gpnmb mouse retinas and in *Pde6brd1* retinas characterized by degeneration of rod photoreceptors. *Trpm1* mRNA in wild type retinas was low at birth but exhibited progressive increases in abundance up to early adulthood at postnatal day 21 (P21). Retinal *Trpm1* mRNA content did not decrease following loss of photoreceptors. At P21, TRPM1-immunopositive perikarya migrated into the outer nuclear layer. The TRPM1 protein was trafficked to discrete postsynaptic puncta in wild type retinas whereas in adult *Pde6brd1* mouse retinas, TRPM1 translocated to bipolar perikarya and bar-like structures in the distal inner nuclear layer. These findings show that expression and localization of the TRPM1 in the mouse retina is plastic,

Edward Levine, Ph.D., joined the Moran Eye Center in 2000. His laboratory is focused on understanding the molecular and cellular mechanisms of retinal development, as well as determining the contributions of developmental mechanisms to the progression and treatment of retinal degenerative diseases. His research uses the mouse retina because its developmental progression is well understood and several genetic models of retinal degeneration are available, thus facilitating the identifications and characterization of important regulatory molecules. These studies enable direct tests of the roles of these molecules in retinal degenerations.

modulated by use-dependence and availability of sustained excitatory input.

Do Calcium Channel Blockers Rescue Dying Photoreceptors in the *Pde6b* (rd1) Mouse?

Author: Barabas P, Cutler Peck C, Krizaj D.

Journal: Adv Exp Med Biol. 2010;664:491-9.

ABSTRACT: Retinitis pigmentosa (RP) is a genetically heterogeneous set of blinding diseases that affects more than a million people worldwide. In humans, ~5-8% of recessive and dominant RP cases are caused by nonsense mutations in the *Pde6b* gene coding for the ss-subunit of the rod photoreceptor cGMP phosphodiesterase 6 (PDE6-ss). The study of the disease has been greatly aided by the *Pde6b* (rd1) (rd1) mouse model of RP carrying a null PDE6ss allele. Degenerating rd1 rods were found to experience a pathological increase in intracellular calcium concentration ('Ca overload') when they enter the apoptotic process at postnatal day 10. A 1999 study suggested that the Ca(2+) channel antagonist D-cis diltiazem delays the kinetics of rd1 rod degeneration, conferring partial rescue of scotopic vision. Subsequent reports were mixed: whereas several studies failed to replicate the original results, others appeared to confirm the neuroprotective effects of Ca(2+) channel antagonists such as diltiazem, nilvadipine and verapamil. We discuss the discrepancies between the results of different groups and suggest plausible causes for the discordant results. We also discuss potential involvement of recently identified Ca(2+)-dependent mechanisms that include protective calcium ATPase mechanisms, ryanodine and IP3 calcium stores, and store operated channels in *Pde6b* (rd1) neurodegeneration.

Exploring the retinal connectome.

Author: Anderson JR, Jones BW, Watt CB, Shaw MV, Yang JH, Demill

D, Lauritzen JS, Lin Y, Rapp KD, Mastronarde D, Koshevoy P, Grimm B, Tasdizen T, Whitaker R, Marc RE.

Journal: Mol Vis. 2011 Feb 3;17:355-79.

PURPOSE: A connectome is a comprehensive description of synaptic connectivity for a neural domain. Our goal was to produce a connectome data set for the inner plexiform layer of the mammalian retina. This paper describes our first retinal connectome, validates the method, and provides key initial findings.

METHODS: We acquired and assembled a 16.5 terabyte connectome data set RC1 for the rabbit retina at ≈ 2 nm resolution using automated transmission electron microscope imaging, automated mosaicking, and automated volume registration. RC1 represents a column of tissue 0.25 mm in diameter, spanning the inner nuclear, inner plexiform, and ganglion cell layers. To enhance ultrastructural tracing, we included molecular markers for 4-aminobutyrate (GABA), glutamate, glycine, taurine, glutamine, and the *in vivo* activity marker, 1-amino-4-guanidobutane. This enabled us to distinguish GABAergic and glycinergic amacrine cells; to identify ON bipolar cells coupled to glycinergic cells; and to discriminate different kinds of bipolar, amacrine, and ganglion cells based on their molecular signatures and activity. The data set was explored and annotated with Viking, our multiuser navigation tool. Annotations were exported to additional applications to render cells, visualize network graphs, and query the database.

RESULTS: Exploration of RC1 showed that the 2 nm resolution readily recapitulated well known connections and revealed several new features of retinal organization: (1) The well known AII amacrine cell pathway displayed more complexity than previously reported, with no less than 17 distinct signaling modes, including ribbon synapse inputs from OFF bipolar cells, wide-field ON cone bipolar cells and rod bipolar cells, and extensive input from cone-pathway amacrine cells. (2) The axons of most cone

bipolar cells formed a distinct signal integration compartment, with ON cone bipolar cell axonal synapses targeting diverse cell types. Both ON and OFF bipolar cells receive axonal veto synapses. (3) Chains of conventional synapses were very common, with intercalated glycinergic-GABAergic chains and very long chains associated with starburst amacrine cells. Glycinergic amacrine cells clearly play a major role in ON-OFF crossover inhibition. (4) Molecular and excitation mapping clearly segregates ultrastructurally defined bipolar cell groups into different response clusters. (5) Finally, low-resolution electron or optical imaging cannot reliably map synaptic connections by process geometry, as adjacency without synaptic contact is abundant in the retina. Only direct visualization of synapses and gap junctions suffices.

CONCLUSIONS: Connectome assembly and analysis using conventional transmission electron microscopy is now practical for network discovery. Our surveys of volume RC1 demonstrate that previously studied systems such as the AII amacrine cell network involve more network motifs than previously known. The AII network, primarily considered a scotopic pathway, clearly derives ribbon synapse input from photopic ON and OFF cone bipolar cell networks and extensive photopic GABAergic amacrine cell inputs. Further, bipolar cells show extensive inputs and outputs along their axons, similar to multistratified nonmammalian bipolar cells. Physiologic evidence of significant ON-OFF channel crossover is strongly supported by our anatomic data, showing alternating glycine-to-GABA paths. Long chains of amacrine cell networks likely arise from homocellular GABAergic synapses between starburst amacrine cells. Deeper analysis of RC1 offers the opportunity for more complete descriptions of specific networks.

$\alpha\beta\gamma$ -Synuclein triple knockout mice reveal age-dependent neuronal dysfunction.

Greten-Harrison B, Polydoro M, Morimoto-Tomita M, Diao L, Wil-



Robert Marc, Ph.D., joined the Research Faculty of the Moran Eye Center in 1993 after 15 years at the university of Texas at Houston, where he was the Robert Greg Professor of Biomedical science. Dr. Marc's early research provided the first maps of the different color varieties of photoreceptors in the retina. It is now clear that it is this unique pattern of color sensitive cones which dictates many features of our perception of color and form. And as a retinal disease inexorably disassembles the retina, these exquisite sensors are often among the first to fail.

After more than 30 years of continuous NIH funding, Dr. Marc's laboratory now exploits advanced molecular detection, imaging, and computational technologies to produce new, richer visualizations of neurons and how they are connected. These new approaches allow the Marc Laboratory to track disruptions in these connections triggered by retinal diseases such as retinitis pigmentosa and macular degeneration. The ultimate goal of this research is to learn enough about the assembly, function and disassembly of these networks to guide the development of strategies to repair defects triggered by retinal diseases.



Ning Tian, Ph.D., did graduate training at SUNY at Buffalo with Malcolm Slaughter focusing on synaptic transmission of retinal neurons and postdoctoral work with David Copenhagen at University of California San Francisco School of Medicine, working on developmental regulation of retinal synaptic circuitry. He was a faculty member at the UCSF Dept of Ophthalmology for one year and a faculty member at Yale University, Department of Ophthalmology for nine years before joining the Moran Eye Center in 2009. Research in Dr. Tian's lab is focused on the synaptic pathways of the body's visual nervous system.



liams AM, Nie EH, Makani S, Tian N, Castillo PE, Buchman VL, Chandra SS. Proc Natl Acad Sci USA, 2010; 107:19573-19578.

ABSTRACT: Synucleins are a vertebrate-specific family of abundant neuronal proteins. They comprise three closely related members, α -, β -, and γ -synuclein. α -Synuclein has been the focus of intense attention since mutations in it were identified as a cause for familial Parkinson's disease. Despite their disease relevance, the normal physiological function of synucleins has remained elusive. To address this, we generated and characterized $\alpha\beta\gamma$ -synuclein knockout mice, which lack all members of this protein family. Deletion of synucleins causes alterations in synaptic structure and transmission, age-dependent neuronal dysfunction, as well as diminished survival. Abrogation of synuclein expression decreased excitatory synapse size by ~30% both in vivo and in vitro, revealing that synucleins are important determinants of presynaptic terminal size. Young synuclein null mice show improved basic transmission, whereas older mice show a pronounced decrement. The late onset phenotypes in synuclein null mice were not due to a loss of synapses or neurons but rather reflect specific changes in synaptic protein composition and axonal structure. Our results demonstrate that synucleins contribute importantly to the long-term operation of the nervous system and that alterations in their physiological function could contribute to the development of Parkinson's disease.

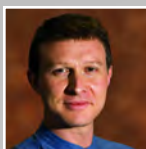
Monica Vetter, PhD, is an Adjunct Professor at the Moran Eye Center, Dept of Ophthalmology and Visual Sciences, as well as Professor and Acting Chair Neurobiology and Anatomy Dept at the University of Utah. Her research specializes in the retinal signaling pathways.

Early microglia activation in a mouse model of chronic glaucoma.

Author: Bosco A, Steele MR, Vetter ML.

Journal: J Comp Neurol. 2011 Mar 1;519(4):599-620.

ABSTRACT: Changes in microglial cell activation and distribution are associated with neuronal decline in the central nervous system (CNS), particularly under pathological conditions. Activated microglia converge on the initial site of axonal degeneration in human glaucoma, yet their part in its pathophysiology remains unresolved. To begin with, it is unknown whether microglia activation precedes or is a late consequence of retinal ganglion cell (RGC) neurodegeneration. Here we address this critical element in DBA/2J (D2) mice, an established model of chronic inherited glaucoma, using as a control the congenic substrain DBA/2J Gpnmb(+/-SjJ) (D2G), which is not affected by glaucoma. We analyzed the spatial distribution and timecourse of microglial changes in the retina, as well as within the proximal optic nerve prior to and throughout ages when neurodegeneration has been reported. Exclusively in D2 mice, we detected early microglia clustering in the inner central retina and unmyelinated optic nerve regions, with microglia activation peaking by 3 months of age. Between 5 and 8 months of age, activated microglia persisted and concentrated in the optic disc, but also localized to the retinal periphery. Collectively, our findings suggest microglia activation is an early alteration in the retina and optic nerve in D2 glaucoma, potentially contributing to disease onset or progression. Ultimately, detection of microglial activation may have value in early disease diagnosis, while modulation of microglial responses may alter disease progression.



Bryan William Jones, Ph.D

Detection of neuron membranes in electron microscopy images using a serial neural network architecture.

Author: Jurrus E, Paiva AR, Watanabe S, Anderson JR, Jones BW, Whitaker RT, Jorgensen EM, Marc RE, Tasdizen T.

Journal: Med Image Anal. 2010 Dec;14(6):770-83.

ABSTRACT: Study of nervous systems via the connectome, the map of connectivities of all neurons in that system, is a challenging problem in neuroscience. Towards this goal, neurobiologists are acquiring large electron microscopy datasets. However, the sheer volume of these datasets renders manual analysis infeasible. Hence, automated image analysis methods are required for reconstructing the connectome from these very large image collections. Segmentation of neurons in these images, an essential step of the reconstruction pipeline, is challenging because of noise, anisotropic shapes and brightness, and the presence of confounding structures. The method described in this paper uses a series of artificial neural networks (ANNs) in a framework combined with a feature vector that is composed of image intensities sampled over a stencil neighborhood. Several ANNs are applied in series allowing each ANN to use the classification context provided by the previous network to improve detection accuracy. We develop the method of serial ANNs and show that the learned context does improve detection over traditional ANNs. We also demonstrate advantages over previous membrane detection methods. The results are a significant step towards an automated system for the reconstruction of the connectome.



Robert Marc, Ph.D

The Viking viewer for connectomics: scalable multi-user annotation and summarization of large volume data sets.

Author: Anderson JR, Mohammed S, Grimm B, Jones BW, Koshevoy P, Tasdizen T, Whitaker R, Marc RE.

Journal: J Microsc. 2011 Jan;241(1):13-28.

ABSTRACT: Modern microscope automation permits the collection of vast amounts of continuous anatomical imagery in both two and three dimensions. These large data sets present significant challenges for data storage, access, viewing, annotation and analysis. The cost and overhead of collecting and storing the data can be extremely high. Large data sets quickly exceed an individual's capability for timely analysis and present challenges in efficiently applying transforms, if needed. Finally annotated anatomical data sets can represent a significant investment of resources and should be easily accessible to the scientific community. The Viking application was our solution created to view and annotate a 16.5 TB ultrastructural



retinal connectome volume and we demonstrate its utility in reconstructing neural networks for a distinctive retinal amacrine cell class. Viking has several key features. (1) It works over the internet using HTTP and supports many concurrent users limited only by hardware. (2) It supports a multi-user, collaborative annotation strategy. (3) It cleanly demarcates viewing and analysis from data collection and hosting. (4) It is capable of applying transformations in real-time. (5) It has an easily extensible user interface, allowing addition of specialized modules without rewriting the viewer.

Automatic mosaicking and volume assembly for high-throughput serial-section transmission electron microscopy.

Author: Tasdizen T, Koshevoy P, Grimm BC, Anderson JR, Jones BW, Watt CB, Whitaker RT, Marc RE.

Journal: J Neurosci Methods. 2010 Oct 30;193(1):132-44.

ABSTRACT: We describe a computationally efficient and robust, fully-automatic method for large-scale electron microscopy image registration. The proposed method is able to construct large image mosaics from thousands of smaller, overlapping tiles with unknown or uncertain positions, and to align sections from a serial section capture into a common coordinate system. The method also accounts for nonlinear deformations both in constructing sections and in aligning sections to each other. The underlying algorithms are based on the Fourier shift property which allows for a computationally efficient and robust method. We demonstrate results on two electron microscopy datasets. We also quantify the accuracy of the algorithm through a simulated image capture experiment. The publicly available software tools include the algorithms and a Graphical User Interface for easy access to the algorithms.

The Hartnett Laboratory



When they say, “she wrote the book on it” if they are talking about pediatric retina, the “she” is Mary Elizabeth Hartnett (or ME Hartnett as she is better known) and the book is “Pediatric Retina: Medical and Surgical Approaches”, a book that ME put together with co-authors Michael Trese and Antonio Capone.

Dr. Hartnett came to the Moran Vision Institute in 2010 from the University of North Carolina and, in addition to having authored the definitive work in pediatric retina, ME is the Director of the Moran Pediatric Retina Center and a highly sought after clinician and vitreoretinal surgeon. On top of all of this ME’s most significant contribution to her patients may be her work as a physician/scientist directing her NIH-funded research laboratory.

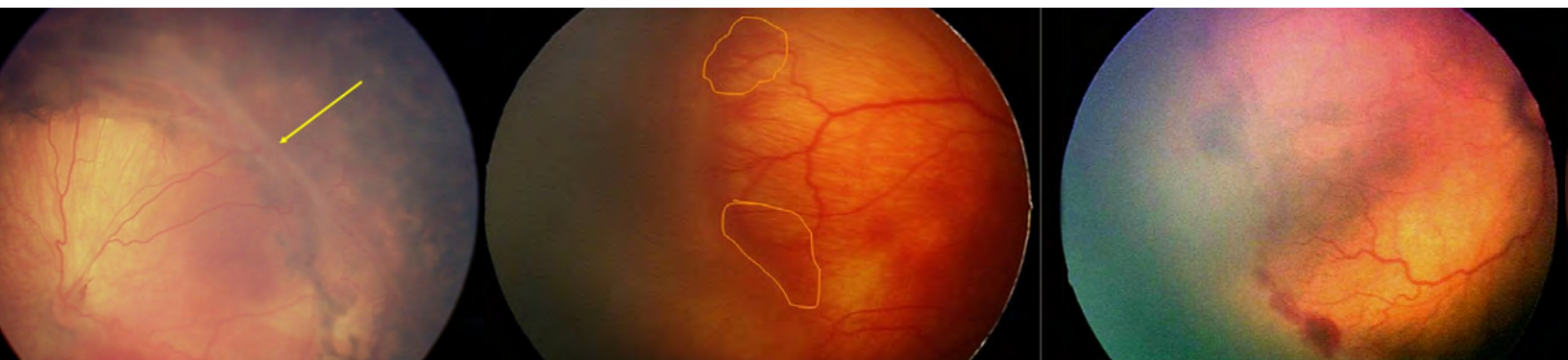
M.E. Hartnett’s research uses molecular techniques to study growth factor mechanisms involved in cell-to-cell interactions. She also studies models of retinal diseases associated with abnormal or unwanted angiogenesis, the growth of new blood vessels from pre-existing vessels. Dr. Hartnett’s team is

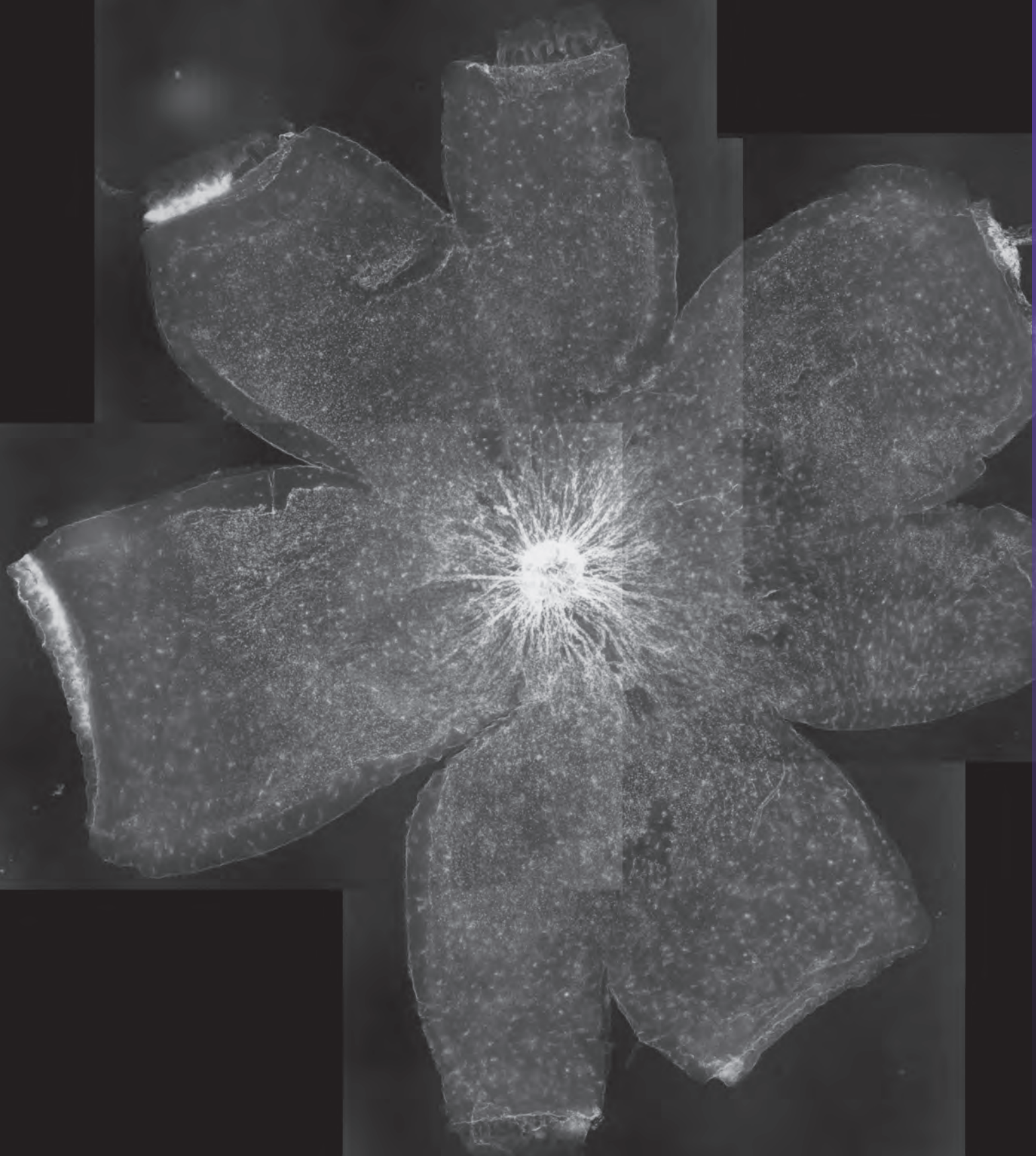
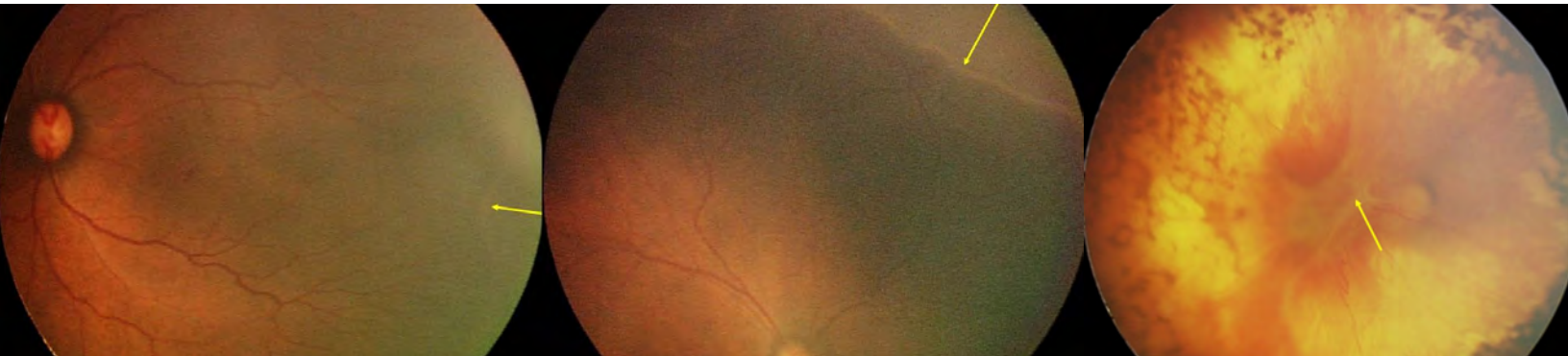
investigating causes of retinal avascularity, or a lack of blood vessel support in areas of the inner retina that leads to retinal hypoxia. Retinal avascularity is a common finding prior to the formation of damaging, abnormal blood vessel growth (abnormal angiogenesis) in the eye. This growth causes retinal detachment and vitreous hemorrhage, which have blinding consequences. Understanding why blood vessels do not grow into the avascular and hypoxic retinal areas may allow doctors to find methods to promote helpful blood vessel support of the inner retina and reduce abnormal damaging blood vessel growth.

Dr. Hartnett and her team are also studying mechanisms of choroidal neovascularization in age-related macular degenera-

tion. Specifically, the Hartnett team is investigating the molecular events causing choroidal endothelial cells to become activated and migrate across the retinal pigment epithelial layer to develop into vision-threatening scars, such as what occurs in age-related macular degeneration.

What does all this mean to her patients? Discoveries in Dr. Hartnett’s laboratory have the potential of reducing abnormal damaging blood vessel growth and the diseases associated with this condition. These are vital links to eventual treatments and cures for several eye diseases, including retinopathy of prematurity, age-related macular degeneration and diabetic retinopathy.







Alessandra Angelucci, MD, PhD. Dr Angelucci's research goal is to understand the computational function of neural circuits in the visual cortex. The laboratory uses optical imaging to map the activity of neuronal populations combined with electrophysiological recordings of neuronal populations using multielectrode arrays, and with high resolution tract tracing techniques to label neuronal circuits. These methods allow us to map the anatomical structure onto the underlying functional architecture of the visual cortex and, to relate both to the real-time responses of neuronal populations. In collaboration with the group of Prof. Paul Bressloff (Dept. Mathematics, University of Utah) and Dr Lars Schwabe (University of Rostock- Germany) we also generate anatomically and physiologically-constrained neural network models of visual cortex.

Research in the lab is currently directed towards understanding: 1) the circuits & mechanisms underlying contextual influences in visual information processing and perception; 2) the role of context in the processing of natural images; 3) the degree of segregation and/or cross-talk between parallel channels in the visual cortex specialized in processing specific visual attributes (e.g. color, form, motion, etc); 4) the anatomical and functional characterization of primate area V3. 5) the functional organization and role of top-down feedback pathways in the visual cortex of primates.

Visual Cortex Research

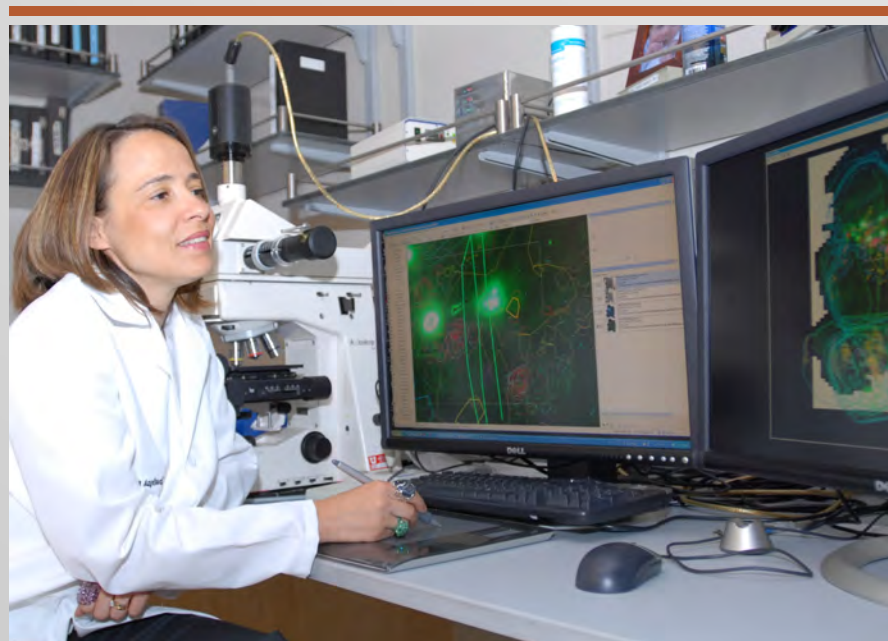
Contrast-dependence of surround suppression in Macaque V1: experimental testing of a recurrent network model.

Author: Schwabe L, Ichida JM, Shushruth S, Mangapathy P, Angelucci A.

Journal: Neuroimage. 2010 Sep;52(3):777-92.

ABSTRACT: Neuronal responses in primary visual cortex (V1) to optimally oriented high-contrast stimuli in the receptive field (RF) center are suppressed by stimuli in the RF surround, but can be facilitated when the RF center is stimulated at low contrast. The neural circuits and mechanisms for surround modulation are still unknown. We previously proposed that topdown feedback connections mediate suppression from the "far" surround, while "near" surround suppression is mediated primarily by horizontal connections. We implemented this idea in a recurrent network model of V1. A model assumption needed to account for the contrast-dependent sign of surround modulation is a re-

sponse asymmetry between excitation and inhibition; accordingly, inhibition, but not excitation, is silent for weak visual inputs to the RF center, and surround stimulation can evoke facilitation. A prediction stemming from this same assumption is that surround suppression is weaker for low than for high contrast stimuli in the RF center. Previous studies are inconsistent with this prediction. Using single unit recordings in macaque V1, we confirm this model's prediction. Model simulations demonstrate that our results can be reconciled with those from previous studies. We also performed a systematic comparison of the experimentally measured surround suppression strength with predictions of the model operated in different parameter regimes. We find that the original model, with strong horizontal and no feedback excitation of local inhibitory neurons, can only partially account quantitatively for the experimentally measured suppression. Strong direct feedback excitation of V1 inhibitory neurons is necessary to account for the experimentally measured surround suppression strength.



Developmental Research



Wolfgang Baehr, PhD

Vitamin A deficiency results in meiotic failure and accumulation of undifferentiated spermatogonia in prepubertal mouse testis.

Author: Li H, Palczewski K, Baehr W, Clagett-Dame M.

Journal: Biol Reprod. 2011 Feb;84(2):336-41.

ABSTRACT: Vitamin A (retinol) is required for maintenance of adult mammalian spermatogenesis. In adult rodents, vitamin A withdrawal is followed by a loss of differentiated germ cells within the seminiferous epithelium and disrupted spermatogenesis that can be restored by vitamin A replacement. However, whether vitamin A plays a role in the differentiation and meiotic initiation of germ cells during the first round of mouse spermatogenesis is unknown. In the present study, we found that vitamin A depletion markedly decreased testicular expression of the all-trans retinoic acid-responsive gene, *Stra8*, and caused meiotic failure in prepubertal male mice lacking lecithin:retinol acyltransferase (*Lrat*), encoding for the major enzyme in liver responsible for the formation of retinyl esters. Rather than undergoing normal differentiation, germ cells accumulated in the testes of *Lrat*(-/-) mice maintained on a vitamin A-deficient diet. These results, together with our previous observations that germ cells fail to enter meiosis and remain undifferentiated in embryonic vitamin A-deficient ovaries, support the hypothesis that vitamin A regulates the initiation of meiosis I of both oogenesis and spermatogenesis in mammals.

Ectopic Mitf in the embryonic chick retina by co-transfection of β -catenin and Otx2.

Author: Westenskow PD, McKean JB, Kubo F, Nakagawa S, Fuhrmann S.

Journal: Invest Ophthalmol Vis Sci. 2010 Oct;51(10):5328-35.

PURPOSE: Development of the retinal pigment epithelium (RPE) is controlled by intrinsic and extrinsic regulators including orthodenticle homeobox 2 (*Otx2*) and the Wnt/ β -catenin pathway, respectively. *Otx2* and β -catenin are necessary for the expression of the RPE key regulator microphthalmia-associated transcription factor (*Mitf*); however, neither factor is sufficient to promote *Mitf* expression in vivo. The study was conducted to determine whether *Otx2* and β -catenin act in a combinatorial manner and tested whether co-expression in the presumptive chick retina induces ectopic *Mitf* expression.

METHODS: The sufficiency of Wnt/ β -catenin activation and/or *Otx2* expression to induce RPE-specific gene expression was examined in chick optic vesicle explant cultures or in the presumptive neural retina using in ovo-electroporation. Luciferase assays were used to examine the transactivation potentials of *Otx2* and β -catenin on the *Mitf*-D enhancer and autoregulation of the *Mitf*-D and *Otx2*T0 enhancers.

RESULTS: In optic vesicles explant cultures, RPE-specific gene expression was activated by lithium chloride, a Wnt/ β -catenin agonist. However, in vivo, *Mitf* was induced only in the presumptive retina if both β -catenin and *Otx2* are co-expressed. Furthermore, both *Mitf* and *Otx2* can autoregulate their own enhancers in vitro.



Sabine Fuhrmann, PhD, received her PhD from the University of Freiburg in Germany and postdoctoral training at the University of Washington/Seattle, investigating the role of tissue-tissue interactions during early eye development. In 2000, she joined the faculty at the Moran Eye Center. Her laboratory studies the role of extra cellular signaling pathways in regulating patterning and differentiation of ocular tissues such as the neural retina and pigmented epithelium. The molecular signals that mediate these patterning events are largely unknown. Multiple congenital eye disorders, including anophthalmia, microphthalmia, aniridia, coloboma, and retinal dysplasia, stem from disruptions in early eye development. It is thus critical to define the signals that regulate normal patterning and development of the optic vesicle. The goal of Dr. Fuhrmann's research is to elucidate the cellular and molecular mechanisms that regulate the patterning and differentiation of ocular tissues using chick and mouse as model organisms.

CONCLUSIONS: The present study provides evidence that β -catenin and Otx2 are sufficient, at least in part, to convert retinal progenitor cells into presumptive RPE cells expressing Mitf. Otx2 may act as a competence factor that allows RPE specification in concert with additional RPE-promoting factors such as β -catenin.

Eye morphogenesis and patterning of the optic vesicle.

Author: Fuhrmann S.

Journal: *Curr Top Dev Biol.* 2010;93:61-84.

ABSTRACT: Organogenesis of the eye is a multistep process that starts with the formation of optic vesicles followed by evagination of the distal domain of the vesicles and the overlying lens placode resulting in morphogenesis of the optic cup. The late optic vesicle becomes patterned into distinct ocular tissues: the neural retina, retinal pigment epithelium (RPE), and optic stalk. Multiple congenital eye disorders, including anophthalmia or microphthalmia, aniridia, coloboma, and retinal dysplasia, stem from disruptions in embryonic eye development. Thus, it is critical to understand the mechanisms that lead to initial specification and differentiation of ocular tissues. An accumulating number of studies demonstrate that a complex interplay between inductive signals and cell-intrinsic factors is critical to ensuring proper specification of ocular tissues as well as maintenance of RPE cell fate. While several of the extrinsic and intrinsic determinants have been identified, we are just at the beginning in understanding how these signals are integrated. In addition, we know very little about the actual output of these interactions. In this chapter, we provide an update of the mechanisms controlling the early steps of eye development in vertebrates, with emphasis on optic vesicle evagination, specification of neural retina and RPE at the optic vesicle stage, the process of invagination during morphogenesis of the optic cup, and maintenance of the RPE cell fate.



Ning Tian, PhD

The immune protein CD3zeta is required for normal development of neural circuits in the retina.

Author: Xu HP, Chen H, Ding Q, Xie ZH, Chen L, Diao L, Wang P, Gan L, Crair MC, Tian N.

Journal: *Neuron.* 2010 Feb 25;65(4):503-15.

ABSTRACT: Emerging evidence suggests that immune proteins regulate activity-dependent synapse formation in the central nervous system (CNS). Mice with mutations in class I major histocompatibility complex (MHC I) genes have incomplete eye-specific segregation of retinal ganglion cell (RGC) axon projections to the CNS. This effect has been attributed to causes that are nonretinal in origin. We show that a key component of MHC I receptor, CD3zeta, is expressed in RGCs. CD3zeta-deficient mice have reduced RGC dendritic motility, an increase in RGC dendritic density, and a selective defect of glutamate-receptor-mediated synaptic activity in the retina. Disrupted RGC synaptic activity and dendritic motility is associated with a failure of eye-specific segregation of RGC axon projections to the CNS. These results provide direct evidence of an unrecognized requirement for immune proteins in the developmental regulation of RGC synaptic wiring and indicate a possible retinal origin for the disruption of eye-specific segregation found in immune-deficient mice.

Light-evoked synaptic activity of retinal ganglion and amacrine cells is regulated in developing mouse retina.

Author: He Q, Wang P, Tian N.

Journal: *Eur J Neurosci.* 2011 Jan;33(1):36-48.

ABSTRACT: Recent studies have shown a continued maturation of visual responsiveness and synaptic activity of retina after eye opening, including the size of receptive fields of retinal ganglion cells (RGCs), light-evoked synaptic output of RGCs, bipolar cell spontaneous synaptic inputs to RGCs, and the synaptic connections between RGCs and ON and OFF bipolar cells. Light deprivation retarded some of these age-dependent changes. However, many other functional and morphological features of RGCs are not sensitive to visual experience. To determine whether light-evoked synaptic responses of RGCs undergo developmental change, we directly examined the light-evoked synaptic inputs from ON and OFF synaptic pathways to RGCs in developing retinas, and found that both light-evoked excitatory and inhibitory synaptic currents decreased, but not increased, with age. We also examined the light-evoked synaptic inputs from ON and OFF synaptic pathways to amacrine cells in developing retinas and found that the light-evoked synaptic input of amacrine cells is also downregulated in developing mouse retina. Different from the developmental changes of RGC spontaneous synaptic activity, dark rearing has little effect on the developmental changes of light-evoked synaptic activity of both RGCs and amacrine cells. Therefore, we concluded that the synaptic mechanisms mediating spontaneous and light-evoked synaptic activity of RGCs and amacrine cells are likely to be different.

Ablation of whirlin long isoform disrupts the USH2 protein complex and causes vision and hearing loss.

Author: Yang J, Liu X, Zhao Y, Adamian M, Pawlyk B, Sun X, McMillan DR, Liberman MC, Li T.

Journal: *PLoS Genet.* 2010 May 20;6(5):e1000955.

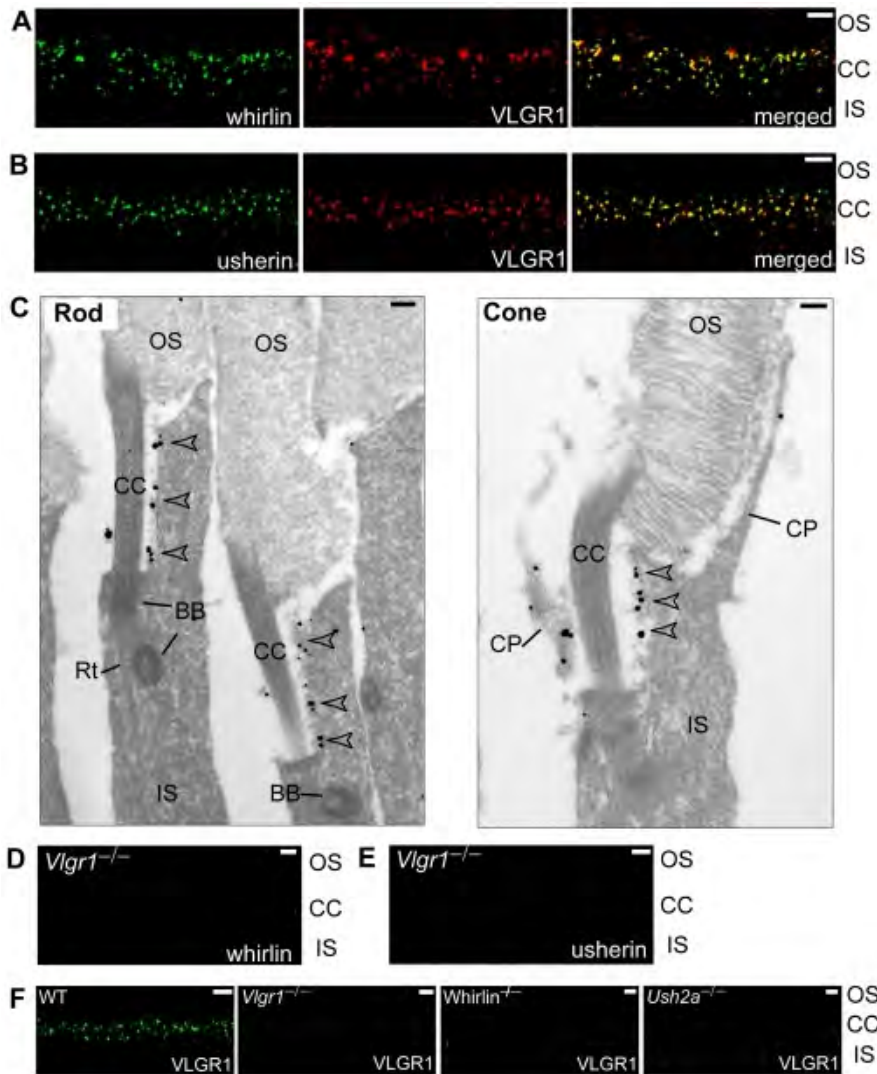
ABSTRACT: Mutations in whirlin cause either Usher syndrome type II (USH2), a deafness-blindness disorder, or nonsyndromic deafness. The molecular basis for the variable dis-

ease expression is unknown. We show here that only the whirlin long isoform, distinct from a short isoform by virtue of having two N-terminal PDZ domains, is expressed in the retina. Both long and short isoforms are expressed in the inner ear. The N-terminal PDZ domains of the long whirlin isoform mediates the formation of a multi-protein complex that includes usherin and VLGR1, both of which are also implicated in USH2. We localized this USH2 protein complex to the periciliary membrane complex (PMC) in mouse photoreceptors that appears analogous to the frog periciliary ridge complex. The latter is proposed to play a role in photoreceptor protein trafficking through the connecting cilium. Mice carrying a targeted disruption near the N-terminus of whirlin manifest retinal and inner ear defects, reproducing the clinical

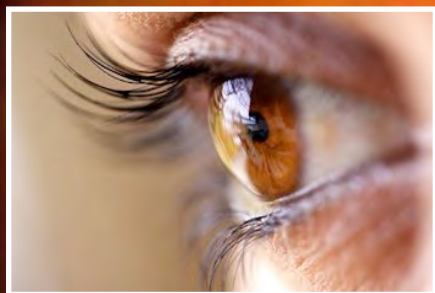
features of human USH2 disease. This is in contrast to mice with mutations affecting the C-terminal portion of whirlin in which the phenotype is restricted to the inner ear. In mice lacking any one of the USH2 proteins, the normal localization of all USH2 proteins is disrupted, and there is evidence of protein destabilization. Taken together, our findings provide new insights into the pathogenic mechanism of Usher syndrome. First, the three USH2 proteins exist as an obligatory functional complex in vivo, and loss of one USH2 protein is functionally close to loss of all three. Second, defects in the three USH2 proteins share a common pathogenic process, i.e., disruption of the PMC. Third, whirlin mutations that ablate the N-terminal PDZ domains lead to Usher syndrome, but non-syndromic hearing loss will result if they are spared.



Jun Yang, PhD. Dr. Yang's laboratory is focused on the disease mechanisms and therapeutic treatments for retinal degenerative diseases using mouse models. Her research group investigates the biological functions of genes whose mutations are known to cause human retinal disease. Using mouse models for these diseases, the group also studies treatment of these diseases by means of gene therapy. Dr. Yang's team is also interested in the cell biology of photoreceptors, especially the cellular processes of intracellular trafficking, structural maintenance, and calcium regulation.



VLGR1 (red) was colocalized with whirlin (green, A) and usherin (green, B) at the PMC in mouse photoreceptors. Immunoelectron microscopy (C) demonstrated that the gold labels of VLGR1 were present at the plasma membrane of the apical inner segment facing the connecting cilium, the PMC, in both mouse rod and cone photoreceptors (arrowheads). The signals of whirlin (D) and usherin (E) disappeared at the PMC in *Vlgr1* knockout photoreceptors. The signals of VLGR1 diminished in whirlin and *Ush2a* knockout mice (F). The staining of VLGR1 in wild-type (WT) and *Vlgr1* knockout mice serves as a positive and negative control, respectively. OS, outer segments; CC, connecting cilia; BB, basal bodies; Rt, the rootlet; IS, inner segments; CP, calycal processes. Scale bars, 5 μ m (A,B,D-F) and 200 nm (C).



AMD at the Center for Translational Medicine: The Hageman Laboratory

Gregory Hageman, PhD came to the Moran Eye Center in the Fall of 2009 as the John A. Moran Presidential Professor of Ophthalmology and Visual Sciences and the founding director of the Center for Translational Medicine. His laboratory's move to Utah was the largest known research laboratory transfer in the university's history: seven semi-trucks carrying several tons of the laboratory equipment, and 18 full-size freezers holding over 8,000 human eyes and an astounding number of clinical and laboratory images. His laboratory is focused on extending and refining his previous observations related to the etiology of age-related macular degeneration (AMD), including the identification of identifying new genetic markers for AMD and co-segregating disease with AMD. Among other approaches, Greg and his colleagues are mining the state's extensive genealogical records in hopes of identifying

new treatments and cures for AMD and related conditions.

Dr. Hageman's primary research interest over the past 20 years has been directed toward assessment of pathways involved in the etiology of age-related macular degeneration (AMD), the leading cause of irreversible worldwide blindness. He and his colleagues have generated a definitive body of evidence that implicates a role for immune-mediated processes, specifically that of the complement system, in AMD pathogenesis and progression. Early pathobiologic investigations of eyes from human donors led to the identification of numerous complement proteins, complement activators, and complement regulatory proteins in drusen, the hallmark pathological biomarkers of the disease. More recent genetic studies, including those conducted by Hageman and colleagues, led to the discovery that common variants in several

complement genes - including Complement Factor H (CFH), Complement Factor H Related 1 and 3 (CFHR1 and CFHR3), Complement Factor B (CFB), Complement Factor I (CFI) and Complement Components 2 and 3 (C2 and C3) -- confer significant risk for, or protection from, the development of AMD late in life. A former director of the Human Genome Project called this breakthrough, "The first major translational research discovery to come from the Human Genome Project."

The work of Dr. Hageman is driven from his group's observations in the clinic and their employment of a large and well characterized work with the Hageman laboratory's extensive collection of donor tissue. His work is divining His The identification of new AMD specific phenotypes is driving that in turn drives current genetic research activities, as well as and the development of increas-

ingly meaningful more specific biomarkers. These phenotypes and the increased understanding of the disease pathways specific to them will It is hoped that these activities, when combined with previous discoveries, will lead to the next generation of therapeutics for disease like AMD. As the Moran Eye Center strives to make a difference in the lives of its patients and patients around the world, Greg Hageman is playing a leadership role in defining a new model of translational research - using employing a multidisciplinary approach combination of clinical data and observations to move and basic research discoveries results back into the clinic to expedite the pace at which basic scientific discoveries are translated into clinically effective diagnostics and therapies for the treatment of devastating eye disorders.



Translational Research



Paul Bernstein, PhD

Noninvasive assessment of dermal carotenoids as a biomarker of fruit and vegetable intake.

Author: Mayne ST, Cartmel B, Scarmo S, Lin H, Leffell DJ, Welch E, Ermakov I, Bhosale P, Bernstein PS, Gellermann W.

Journal: Am J Clin Nutr. 2010 Oct;92(4):794-800.

BACKGROUND: Resonance Raman spectroscopy (RRS) has been suggested as a feasible method for noninvasive carotenoid measurement of human skin. However, before RRS measures of dermal carotenoids can be used as a biomarker, data on intra- and intersubject variability and validity are needed.

OBJECTIVE: The purpose of this study was to evaluate the reproducibility and validity of RRS measures of dermal total carotenoids and lycopene in humans.

DESIGN: In study 1, 74 men and women with diverse skin pigmentation were recruited. RRS measures of the palm, inner arm, and outer arm were obtained at baseline, 1 wk, 2 wk, 1 mo, 3 mo, and 6 mo (to maximize seasonal variation). The RRS device used visible light at 488 nm to estimate total carotenoids and at 514 nm to estimate lycopene. Reproducibility was assessed by intraclass correlation coefficients (ICCs). In study 2, we recruited 28 subjects and assessed dietary carotenoid intake, obtained blood for HPLC analyses, performed RRS measures of dermal carotenoid status, and performed dermal biopsies (3-mm punch biopsy) with dermal carotenoids assessed by HPLC.

RESULTS: ICCs for total carotenoids across time were 0.97 (palm), 0.95 (inner arm), and 0.93 (outer arm). Total dermal carotenoids assessed by RRS were significantly correlated with total dermal carotenoids assessed by HPLC of dermal biopsies ($r = 0.66$, $P = 0.0001$). Similarly, lycopene assessed by RRS was significantly correlated with lycopene assessed by HPLC of dermal biopsies ($r = 0.74$, $P < 0.0001$).

CONCLUSION: RRS is a feasible and valid method for noninvasively assessing dermal carotenoids as a biomarker for studies of nutrition and health.

Significant correlations of dermal total carotenoids and dermal lycopene with their respective plasma levels in healthy adults.

Author: Scarmo S, Cartmel B, Lin H, Leffell DJ, Welch E, Bhosale P, Bernstein PS, Mayne ST.

Journal: Arch Biochem Biophys. 2010 Dec 1;504(1):34-9.

ABSTRACT: Carotenoids in skin have been known to play a role in photoprotection against UV radiation. We performed dermal biopsies of healthy humans ($N=27$) and collected blood samples for pair-wise correlation analyses of total and individual carotenoid content by high performance liquid chromatography (HPLC). The hydrocarbon carotenoids (lycopene and beta-carotene) made up the majority of carotenoids in both skin and plasma, and skin was somewhat enriched in these carotenoids relative to plasma. Beta-cryptoxanthin, a monohydroxycarotenoid, was found in similar proportions in skin as in plasma. In contrast, the dihydroxycarotenoids, lutein and zeaxanthin, were relatively lacking in human skin in absolute and

relative levels as compared to plasma. Total carotenoids were significantly correlated in skin and plasma ($r=0.53$, $p<0.01$). Our findings suggest that human skin is relatively enriched in lycopene and beta-carotene, compared to lutein and zeaxanthin, possibly reflecting a specific function of hydrocarbon carotenoids in human skin photoprotection.



Greg Hageman, PhD

Fundus Autofluorescence and Spectral Domain Optical Coherence Tomography Characteristics in a Rapidly Progressing Form of Geographic Atrophy.

Author: Fleckenstein M, Schmitz-Valckenberg S, Martens C, Kosanetzky S, Brinkmann CK, Hageman GS, Holz FG.

Journal: Invest Ophthalmol Vis Sci. 2011 Feb 10.

PURPOSE: To further characterize a previously described phenotypic variant of geographic atrophy (GA) associated with rapid progression and a “diffuse-trickling” appearance on fundus autofluorescence (FAF).

METHODS: Thirty-six patients (60 eyes) (72.2% female, mean age 69.4 ± 10.7 years) with this distinct phenotype were examined by simultaneous confocal scanning-laser-ophthalmoscopy (cSLO) and spectral-domain optical coherence tomography (SD-OCT) imaging (Spectralis HRA+OCT, Heidelberg Engineering). Images were qualitatively and quantitatively analyzed and compared to 60 eyes (38 patients) with “non-diffuse-trickling” GA.

RESULTS: The atrophic area in the “diffuse-trickling” phenotype showed a grayish FAF signal and characteristic coalescent lobular configuration at the lesion boundaries. SD-OCT imaging revealed a marked splitting of band

4 (the presumptive retinal pigment epithelium (RPE)/Bruch's membrane (BM) complex) in all 240 analysed border sections of "diffuse-trickling" GA eyes (four borders/eye) with a mean distance between in inner- and outer part of band 4 of $23.2 \pm 7.5 \mu\text{m}$. This finding was only present in 13.8% (33/240) of analysed border sections in "non-diffuse-trickling" GA.

CONCLUSIONS: Patients with the rapid progressing "diffuse-trickling" GA phenotype exhibit a characteristic marked separation within the RPE/BM complex on SD-OCT-imaging. The presumed histopathological correlates are basal laminar deposits. Such deposits may promote RPE cell death and, thus, contribute to rapid GA-progression. The persistence of these deposits within the atrophic lesion may account for the distinct grayish FAF appearance which differs from the markedly reduced signal in other forms of GA. Identification of such alterations based on FAF- and SD-OCT imaging may be helpful in future interventional trials directed towards slowing GA progression.

Variants in the APOE Gene are Associated with Improved Treatment Outcome Following Anti-VEGF Therapy for Neovascular AMD.

Author: Wickremasinghe SS, Xie J, Lim J, Chauhan DS, Robman L, Richardson AJ, Hageman G, Baird PN, Guymer R.

Journal: Invest Ophthalmol Vis Sci. 2011 Jan 18.

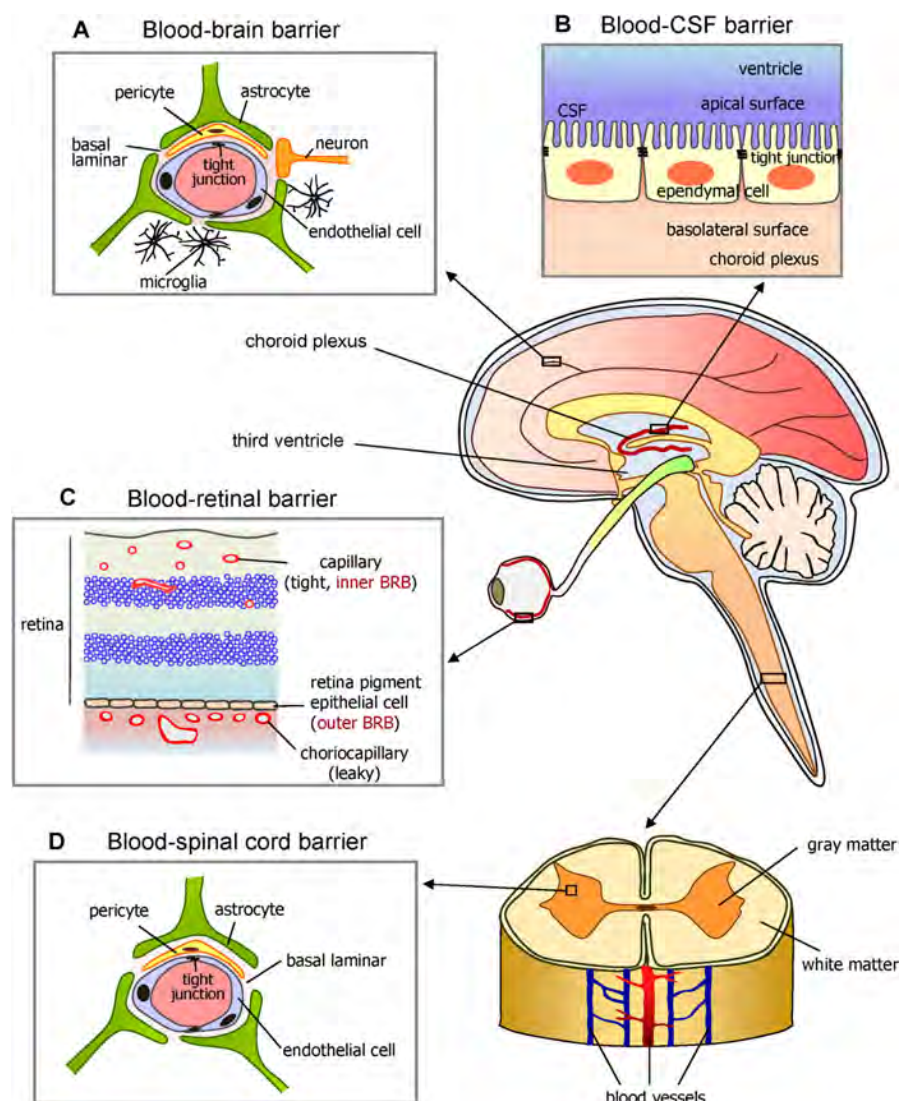
OBJECTIVE: Anti-vascular endothelial growth factor (anti-VEGF) drugs have dramatically improved the treatment of neovascular AMD. In pivotal studies, almost 90% of patients maintain vision, with around 30% showing significant improvement. Despite this, 10-15% of patients continue to lose vision even with treatment. It has been reported that variants in some AMD-associated genes are associated with treatment outcome. Herein, we report an association with variants in the Apolipoprotein E (APOE) gene.

METHODS: 172 patients receiving anti-VEGF treatment for subfoveal choroidal neovascularization secondary to AMD were enrolled. Information relating to demographics, lesion characteristics, delay to treatment, visual acuity and number of treatments was collected and variants of APOE were assessed in all patients at baseline. Best-corrected logarithm of the minimum angle of resolution (logMAR) VA was recorded for all patients.

RESULTS: The presence of the APOE $\epsilon 4$ allele was associated with improved treatment outcome at three ($p=0.02$) and 12 months ($p = 0.06$) compared to those with an $\epsilon 2$ allele, after controlling for baseline acuity,

treatment delay from first symptoms, as well as age and gender. Patients with an APOE $\epsilon 4$ allele had an odds ratio (OR) of 4.04 (confidence interval 95% CI 1.11, 14.70) for a two-line gain in vision from baseline at three months ($p=0.03$) and OR of 2.54 ($p=0.20$) at 12 months after treatment, based on multivariate analysis.

CONCLUSIONS: In patients with neovascular AMD, presence of the APOE $\epsilon 4$ allele confers significantly better visual outcomes following anti-VEGF treatment compared to those with the $\epsilon 2$ allele. These findings suggest a possible future role for a personalized approach to anti-VEGF treatments.





Nick Mamalis, MD, presented at the 2010 American Academy of Ophthalmology, Cataract Spotlight of Anterior Segment Surgery/Research. He is Director of the Intermountain Ocular Research Center, a nonprofit, independent laboratory that performs basic, in depth scientific research on intra-ocular lenses. In addition, the Center provides services and education to surgeons, clinical ophthalmologists, their patients, and intra-ocular lens manufacturers worldwide. Dr. Mamalis is also Academic Appointments: Professor of Ophthalmology & Visual Sciences – University of Utah School of Medicine and Director of Ocular Pathology. His research focuses on intra-ocular lenses, cataract surgical techniques and instruments, as well as post operative inflammation.



Serum VEGF and CFH in Exudative Age-Related Macular Degeneration.

Author: Haas P, Steindl K, Aggermann T, Schmid-Kubista K, Krugluger W, Hageman GS, Binder S.

Journal: *Curr Eye Res.* 2011 Feb;36(2):143-8.

PURPOSE: To determine serum vascular endothelial growth factor 165 (VEGF165) levels and the association of the complement factor H gene (CFH) Y402H polymorphism in patients with exudative age-related macular degeneration (AMD) in comparison to unaffected control subjects.

METHODS: Sixty-six AMD patients and 66 healthy age- and gender-matched controls were included in this case-control study. The serum VEGF165 was assayed by ELISA (R&D). Genotypes were determined by polymerase chain reaction-restriction fragment length polymorphism analysis. Chi-squared tests were used regarding the polymorphism, a t-test regarding the VEGF-levels.

RESULTS: Levels of serum VEGF165 were similar in both groups (p -value=0.2112). Genotype frequency differed significantly between patients with exudative AMD and the healthy control group ($p = 0.003136$). The serum VEGF165 levels were similar irrespective of the presence of the CFH Y402H polymorphism ($p = 0.4113$) and independent of the specific genotype ($p = 0.9634$).

CONCLUSION: In the present study, exudative AMD is not associated to serum VEGF165 levels; furthermore, our data does not establish a statistical link between VEGF165 and the CFH Y402H polymorphism.

Ophthalmic drug delivery systems for the treatment of retinal diseases: basic research to clinical applications.

Author: Edelhauser HF, Rowe-Rendleman CL, Robinson MR, Dawson DG, Chader GJ, Grossniklaus HE, Rittenhouse KD, Wilson

CG, Weber DA, Kuppermann BD, Csaky KG, Olsen TW, Kompella UB, Holers VM, Hageman GS, Gilger BC, Campochiaro PA, Whitcup SM, Wong WT.

Journal: *Invest Ophthalmol Vis Sci.* 2010 Nov;51(11):5403-20.

The ARVO 2009 Summer Eye Research Conference (SERC 2009) on Ophthalmic Drug Delivery Systems was held July 31 and August 1, 2009, at the National Institutes of Health (NIH) in Bethesda, Maryland. The conference provided an opportunity to gather a diverse group of more than 200 experts from both academic ophthalmology and the ophthalmic pharmaceutical industry, including laboratory researchers and

clinicians, to discuss recent advances in delivery systems that convey ocular drugs to the posterior segment and how these systems might be successfully used in commercial products.

The two-day meeting comprised the following nine sessions: (1) eye anatomy and ocular barriers to drug transport, (2) the vitreous humor in drug delivery, (3) intravitreal drug delivery, (4) transscleral drug delivery for retinal diseases, (5) preclinical benchmarks for retinal drug therapy, (6) animal models for evaluating drug delivery systems, (7) topical therapy for retinal diseases, (8) clinical trials, and (9) new data from abstracts.

This meeting was co-sponsored by the Association in Research in Vision and Ophthalmology (ARVO) and the NIH to expand and continue ongoing collaborative interchange and synergic endeavors that were addressed at an earlier conference, held May 4 and 5, 2007, and sponsored by the Pfizer Ophthalmics Research Institute Conference.1 SERC 2009 was organized by Cheryl L. Rowe-Rendleman, PhD (Omar Consulting Group, LLC), Michael R. Robinson, MD (Allergan Inc.), and Henry F. Edelhauser, PhD (Emory University). Edelhauser and Paul A. Sieving, MD, PhD, started off the meeting with introductory comments.

Edelhauser began by briefly discussing the history of basic science research involving ophthalmic drug delivery. He touched on the difficulty in finding a flawless technique to deliver drugs targeting diseases that directly affect the retina and vitreous humor, owing to the anatomic barriers and physiologic clearance mechanisms of the blood–neural barriers (BNBs). The BNBs comprise the blood–retinal barrier (BRB) posteriorly and the blood–aqueous barrier (BAB) anteriorly (Fig. 1). He also mentioned the importance of the transcellular and paracellular transport pathways across or between epithelial or endothelial BRBs (Fig. 2). Edelhauser described the purpose of SERC 2009, designed as a forum in which researchers and clinicians could have an open dialog about their work, during and between meeting sessions, all in the service of advancing the field of ophthalmology.

Sieving, director of the National Eye Institute (NEI), outlined the major ophthalmic blinding diseases in the United States and their pathophysiology, pointing out their economic costs to society. In conclusion, he noted that, many times, the most crucial step in successfully translating

promising drugs from the bench to the bedside is identifying the best drug delivery route.

Given the emphasis on translational science and the non-synchronized arrangement of lectures and posters, this summary of SERC 2009 presents the major topics of the meeting by theme, not necessarily in the order of their original presentation. Each lecture has been included in the material for the pertinent area of study. The basic science part of this article focuses on the anatomic barriers to the five major modes of ocular drug delivery: intraocular, periocular, hybrid, topical, and systemic. The second half is a review of the clinical and regulatory components of translational science.



Bryan William Jones, Ph.D

Retinal Remodeling and Visual Prosthetics.

Author: Jones BW, Watt CB, Marc RE.

Chapter: Visual Prosthetics, Elsevier Press, 2011 In Press.

ABSTRACT: Retinal degenerative disease induces a cascade of events that ultimately result in phased revision of neuronal populations and circuitry of the retina. These changes reveal plasticity in the retina that mimics that seen during development and in instances of neural deafferentation in other Central Nervous System (CNS) systems, involving neuronal as well as glial cell populations. These retinal remodeling changes occur across the spectrum of retinal degenerative disease and are observed in defects of the retinal pigment epithelium (RPE), rhodopsin packaging and transport defects as well as other non-retinitis pigmentosa (RP) related diseases with the final result being fundamental revision of neuronal populations and circuitry. These revisions impact potential biological and bionic rescues of visual function and must be overcome before vision restoration strategies can be viable.

A cross-linked hyaluronan gel accelerates healing of corneal epithelial abrasion and alkali burn injuries in rabbits.

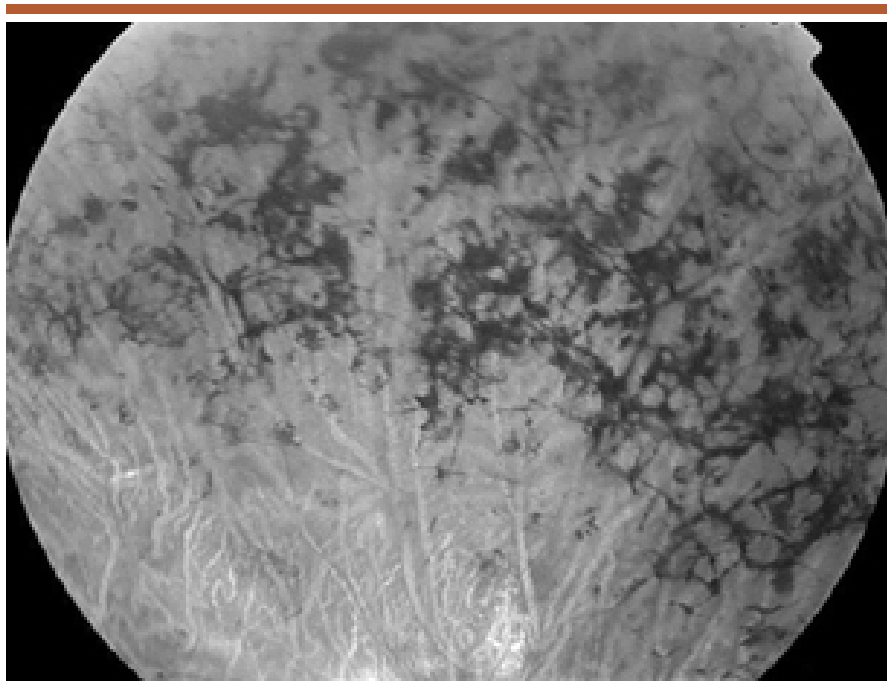
Author: Yang G, Espandar L, Mamlis N, Prestwich GD.

Journal: Vet Ophthalmol. 2010 May;13(3):144-50.

OBJECTIVE: To evaluate the efficacy of a chemically modified and cross-linked derivative of hyaluronan (CMHA-SX) for treatment of corneal epithelial abrasion and standardized alkali burn injuries.

ANIMALS: Twelve female New Zealand white rabbits in two groups were used.

PROCEDURES: Bilateral 6-mm diameter corneal epithelial abrasions were made in each of six rabbits in one group and 6-mm standardized alkali burn injuries were made in the second group. A 1% CMHA-SX formulation was applied topically four times per day in right eye of each rabbit for 1



Fundoscopic image from 46 year old male with a diagnosis of X-linked retinitis pigmentosa, showing 'pigmented bone spicules', accumulations of pigment epithelium that are formed by migration of the pigment epithelium into the neural retina along glial columns. These clinically pathologic findings are often seen in the peripheral retina in patients with RP.



Randall J. Olson, MD, is the CEO of the John A. Moran Eye Center. He is the author of more than 300 professional publications and a worldwide lecturer. Dr. Olson specializes in research dealing with intra-ocular lens complications, teleophthalmology and corneal transplantation techniques. He was selected as one of the 15 best cataract surgeons in the United States in a peer survey conducted by Ophthalmology Times. Cataract and Refractive Surgery Today named Dr. Olson as one of 50 international opinion leaders. In 2010 Dr. Olson received the Utah Governor's Medal for Science and Technology. These medals are a symbol of recognition to individuals who have provided distinguished service to Utah in the fields of science and technology.

week, and phosphate buffered saline (PBS) was placed in left (control) eye of each rabbit. The wound size was determined by staining with 1% fluorescein and photographed at the slit lamp with a digital camera at 0, 1, 2, 3 days postoperatively in the first group and 0, 1, 2, 3, 7, 12 days in the second group. Rabbit corneas were collected for histological examination on day 7 in the first group and day 12 in the second group.

RESULTS: Closure of corneal wound in the abrasion model was complete in the CMHA-SX treated eye by 48 h. The wound closure rate and thickness of the central corneal epithelium in the CMHA-SX treated group was greater than in control eyes for both the abrasion and alkali burn injuries. Moreover, the CMHA-SX treated cornea exhibited better epithelial and stromal organization than the untreated control cornea.

CONCLUSIONS: Chemically modified and cross-linked derivative of hyaluronan improved corneal wound healing and could be useful for treating noninfectious corneal injuries.

Comparison of wound strength with and without a hydrogel liquid ocular bandage in human cadaver eyes.

Author: Maddula S, Davis DK, Ness PJ, Burrow MK, Olson RJ.

Journal: J Cataract Refract Surg. 2010 Oct;36(10):1775-8.

PURPOSE: To determine whether a hydrogel liquid ocular bandage improves wound strength.

SETTING: John A. Moran Eye Center, University of Utah, Salt Lake City, Utah, USA.

DESIGN: Laboratory investigation.

METHODS: The wound strength of 2.8 mm clear corneal incisions and 23-gauge scleral incisions was tested in cadaver eyes by raising the intraocular pressure (IOP) until leakage occurred. The pressure at the first sign of incision leakage with the liquid bandage and without the liquid bandage was determined.

dage and without the liquid bandage was determined.

RESULTS: Four corneal incisions and 4 scleral incisions were made in 5 cadaver eyes. The mean pressure at the first sign of corneal incision leakage was 59.5 mm Hg \pm 21.0 (SD) without the liquid bandage and 198.1 \pm 57.6 mm Hg with the liquid bandage ($P < .0001$). The mean pressure at the first sign of scleral incision leakage was 47.9 \pm 21.4 mm Hg and 209.0 \pm 42.9 mm Hg, respectively ($P < .0001$). Eight corneal incisions and 8 scleral incisions did not leak at the maximum pressure of 246 mm Hg. With both incision types, the difference in leakage with a liquid bandage in place and with no liquid bandage was statistically significant ($P = .002$).

CONCLUSION: With application of a hydrogel liquid ocular bandage, incisions withstood significantly higher IOP before leakage occurred than when no liquid bandage was used.

The risk of capsular breakage from phacoemulsification needle contact with the lens capsule: a laboratory study.

Author: Meyer JJ, Kuo AF, Olson RJ.

Journal: Am J Ophthalmol. 2010 Jun;149(6):882-886.e1.

PURPOSE: To determine capsular breakage risk from contact by phacoemulsification needles by machine and tip type.

DESIGN: Experimental laboratory investigation.

METHODS: Infiniti (Alcon, Inc.) with Intrepid cartridges and Signature (Abbott Medical Optics, Inc.) phacoemulsification machines were tested using 19- and 20-gauge sharp and rounded tips. Actual and unoccluded flow vacuum were determined at 550 mm Hg, bottle height of 75 cm, and machine-indicated flow rate of 60 mL/minute. Breakage from brief tip contact with a capsular surrogate and human cadaveric lenses was calculated.

RESULTS: Nineteen-gauge tips had more flow and less unoccluded flow vacuum than 20-gauge tips for both machines, with highest unoccluded flow vacuum in the Infiniti. The 19-gauge sharp tip was more likely than the 20-gauge sharp tip to cause surrogate breakage for Signature with micropulse and Ellips (Abbott Medical Optics, Inc.) ultrasound at 100% power. For Infiniti using OZil (Alcon, Inc.) ultrasound, 20-gauge sharp tips were more likely than 19-gauge sharp tips to break the membrane. For cadaveric lenses, using rounded 20-gauge tips at 100% power, breakage rates were micropulse (2.3%), Ellips (2.3%), OZil (5.3%). Breakage rates for sharp 20-gauge Ellips tips were higher than for rounded tips.

CONCLUSIONS: Factors influencing capsular breakage may include active vacuum at the tip, flow rate, needle gauge, and sharpness. Nineteen-gauge sharp tips were more likely than 20-gauge tips to cause breakage in lower vacuum methods. For higher-vacuum methods, breakage is more likely with 20-gauge than with 19-gauge tips. Rounded-edge tips are less likely than sharp-edged tips to cause breakage.

Pathology of 157 human cadaver eyes implanted with round-edge or modern square-edge silicone IOLs: Analyses of capsular bag opacification.

Author: Maddula S, Werner L, Ness PJ, Davis D, Zaugg B, Stringham J, Burrow M, Yeh O.

Journal: J Cataract Refract Surg 2011;37 in press.

PURPOSE: To assess the degree of capsule bag opacification in human cadaver eyes with silicone intraocular lenses (IOLs), specifically comparing the differences between round-edged IOLs and modern square-edged IOLs.

SETTING: John A. Moran Eye Center, University of Utah, USA.

DESIGN: Experimental Study.

METHODS: The eyes were immersed in 10% formalin on enucleation. They had anterior segment scanning with a very-high-frequency ultrasound (Artemis). After sectioning at the equator, gross examination of the anterior segment was performed from the posterior aspect to assess the degree of capsular bag opacification, coverage of the IOL edge by the anterior capsule, and IOL fixation. Selected eyes also had histopathologic examination.

RESULTS: Eighty-seven eyes with a 3-piece round-edged IOL, 43 with a 3-piece square-edged IOL, 26 with a 1-piece plate IOLs, and 1 with an accommodating IOL design were included in the analyses of capsular bag opacification. Comparison between 3-piece round-edged IOLs and square-edged IOLs showed statistically significant differences in central posterior capsule opacification (PCO) ($P = .0001687$) and peripheral PCO ($P < .0001$). In eyes with square-edged IOLs, PCO had a tendency to start in areas without capsulorhexis coverage of the optic. Twenty-one of 26 eyes with a silicone plate IOL had a neodymium:YAG posterior capsulotomy for dense PCO.

CONCLUSIONS: This first study using pseudophakic human cadaver eyes that includes a significant number of modern 3-piece silicone IOLs with square optic edges confirmed the role of this design in the prevention of PCO.

Pathology of 219 human cadaver eyes with single-piece or three-piece hydrophobic acrylic IOLs: Capsular bag opacification and sites of square edge barrier breach.

Author: Ness PJ, Werner L, Maddula S, Davis D, Zaugg B, Stringham J, Burrow M, Yeh.

Journal: J Cataract Refract Surg 2011;37 in press.

PURPOSE: To assess capsular bag opacification and sites of initial posterior capsule opacification (PCO) in human cadaver eyes with square-edged 1-piece or 3-piece hydrophobic



Liliana Werner, MD, PhD, presented at the 2010 American Academy of Ophthalmology, Cataract Spotlight of Anterior Segment Surgery/Research. She joined the Moran Eye Center in September 2002 and co-directs the Intermountain Ocular Research Center. Dr. Werner's research is centered on the interaction between ocular tissues and different intraocular lens designs, materials and surface modifications. These include intraocular lenses implanted after cataract surgery, and also phakic lenses for refractive surgery and ophthalmic implantable devices in general.





Majid Moshirfar, MD, FACS, is the Director of Cornea and Refractive Surgery Services at the Moran Eye Center. Dr. Moshirfar specializes in refractive surgery, medical and surgical management of corneal disorders, cataract removal and inflammatory eye diseases. Dr. Moshirfar lectures extensively around the country on a variety of vision correction procedures and has become a community spokesperson on the benefits and risks of vision correction surgery. Dr. Moshirfar is the first surgeon to use the Intralase iFS laser and the Boston Keratoprosthesis together to restore vision.



acrylic intraocular lenses (IOLs).

SETTING: John A. Moran Eye Center, University of Utah, Salt Lake City, Utah, USA.

DESIGN: Experimental Study.

METHODS: Eyes were immersed in 10% formalin after enucleation and had anterior segment scanning with very-high-frequency ultrasound (Artemis). After sectioning at the equator, gross examination of the anterior segment was performed from the posterior aspect to assess capsular bag opacification, anterior capsule coverage of the IOL edge, and IOL fixation. Selected eyes had histopathologic examination.

RESULTS: One hundred nineteen eyes with 1-piece IOLs and 100 with 3-piece IOLs were included in the analyses of capsular bag opacification. There was no difference in central ($P = .29$) or peripheral ($P = .76$) PCO. In 63 of 84 eyes with a 1-piece IOL and peripheral PCO, the optic-haptic junction was the site of initiation. In eyes with a 3-piece IOL, initial peripheral PCO was observed at nearly the same rate whether there was full 360-degree anterior capsulorhexis overlap over the optic or no overlap ($P = .13$). In these later, the site of PCO initiation was in areas lacking capsulorhexis coverage in 46% of eyes.

CONCLUSIONS: There was no difference in central or peripheral PCO between 1-piece and 3-piece hydrophobic acrylic IOLs. With 1-piece IOLs, PCO tended to start at the optic-haptic junctions. With 3-piece IOLs, full anterior capsule coverage did not produce a statistically significant benefit with respect to PCO prevention.

Accelerated 20-year sunlight exposure simulation of a photochromic foldable intraocular lens in a rabbit model.

Author: Werner L, Abdel-Aziz S, Cutler Peck C, Monson B, Espandar L, Zaugg B, Stringham J, Wilcox C, Mamalis N.

Journal: J Cataract Refract Surg. 2011 Feb;37(2):378-85.

PURPOSE: To assess the long-term biocompatibility and photochromic stability of a new photochromic hydrophobic acrylic intraocular lens (IOL) under extended ultraviolet (UV) light exposure.

SETTING: John A. Moran Eye Center, University of Utah, Salt Lake City, Utah, USA.

DESIGN: Experimental study.

METHODS: A Matrix Aurium photochromic IOL was implanted in right eyes and a Matrix Acrylic IOL without photochromic properties ($n = 6$) or a single-piece AcrySof Natural SN60AT IOL ($n = 5$) in left eyes of 11 New Zealand rabbits. The rabbits were exposed to a UV light source of 5 mW/cm² for 3 hours during every 8-hour period, equivalent to 9 hours a day, and followed for up to 12 months. The photochromic changes were evaluated during slitlamp examination by shining a penlight UV source in the right eye. After the rabbits were humanely killed and the eyes enucleated, study and control IOLs were explanted and evaluated in vitro on UV exposure and studied histopathologically.

RESULTS: The photochromic IOL was as biocompatible as the control IOLs after 12 months under conditions simulating at least 20 years of UV exposure. In vitro evaluation confirmed the retained optical properties, with photochromic changes observed within 7 seconds of UV exposure. The rabbit eyes had clinical and histopathological changes expected in this model with a 12-month follow-up.

CONCLUSIONS: The new photochromic IOL turned yellow only on exposure to UV light. The photochromic changes were reversible, reproducible, and stable over time. The IOL was biocompatible with up to 12 months of accelerated UV exposure simulation.

Mechanized model to assess capsulorhexis resistance to tearing.

Author: Werner L, Jia G, Sussman G, Maddula S, Ness P, Davis D, Burrow M, Mamalis N.

Journal: J Cataract Refract Surg. 2010 Nov;36(11):1954-9.

PURPOSE: To evaluate a model of mechanically measuring resistance to tearing of a continuous curvilinear capsulorhexis (CCC) using the entire capsular bag of fresh human cadaver eyes isolated from the eyes after complete evacuation.

SETTING: John A. Moran Eye Center, University of Utah, Salt Lake City, Utah, USA.

DESIGN: Experimental study.

METHODS: After the cornea and iris were removed, a 5.0 to 5.5 mm anterior CCC was created. The nucleus was hydroexpressed and the capsular bag evacuated by irrigation/aspiration. A pair of metal shoetree-shaped fixtures, designed based on human lens geometric dimensions, were implanted separately in the capsular bag and assembled together with a screw nut. After complete zonullectomy, the fixture-capsular bag assembly was removed from the eye and loaded onto a mechanical tester. The fixtures were separated at a velocity of 7.0 mm/min in 0.15 μ m intervals to stretch the CCC to its rupture point. Rupture load (N) and extension were measured and graphed.

RESULTS: Testing of 23 donor eyes a mean of 69.04 hours \pm 22.72 (SD) after death showed the following mean values: CCC diameter, 5.3 \pm 0.12 mm; load, 0.39 \pm 0.16 N; extension at CCC tearing, 5.85 \pm 1.17 mm. There was a moderately strong negative correlation between donor age and load ($P = .0018$).

CONCLUSIONS: Previous mechanized methods of assessing CCC strength used excised anterior capsules or partially phacoemulsified crystalline lenses, yielding lower tension strength values. This force-dis-

placement method may facilitate assessment of small differences between anterior capsulotomy techniques.

Cataract development associated with collagen copolymer posterior chamber phakic intraocular lenses: clinicopathological correlation.

Author: Khalifa YM, Moshirfar M, Mifflin MD, Kamae K, Mamalis N, Werner L.

Journal: J Cataract Refract Surg. 2010 Oct;36(10):1768-74.

PURPOSE: To assess the histopathology of anterior subcapsular cataract associated with a collagen copolymer posterior chamber phakic intraocular lens (pIOL) (Visian Implantable Collamer Lens) using light microscopy after pIOL explantation and cataract surgery.

SETTING: John A. Moran Eye Center, University of Utah, Salt Lake City, Utah, USA.

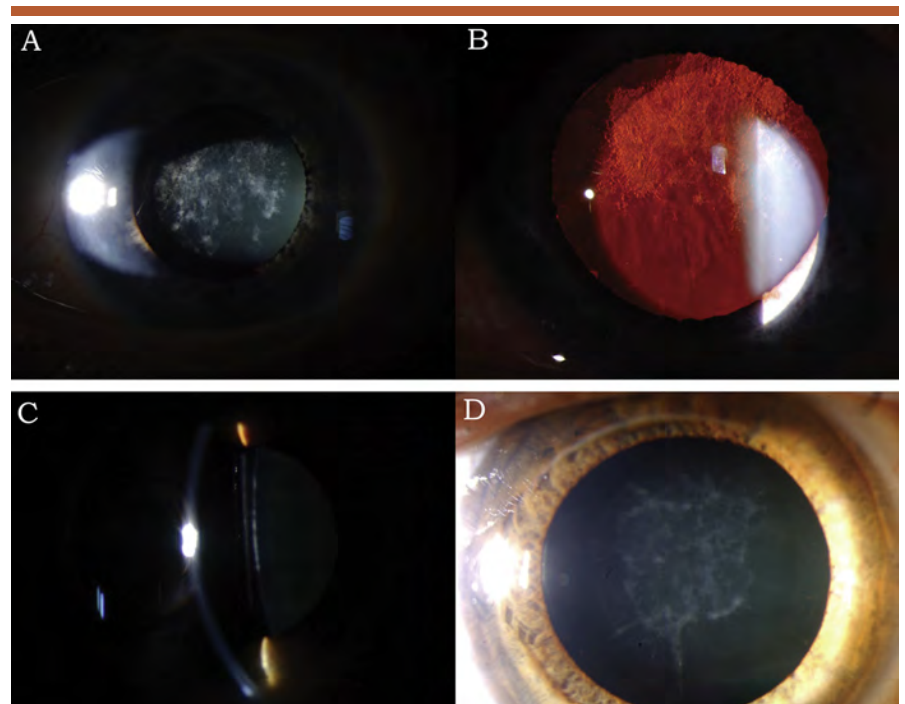
DESIGN: Laboratory investigation.

METHODS: Pathology specimens related to explanted pIOLs were reviewed and preoperative and post-

operative patient data collected. The anterior lens capsules and explanted pIOLs were examined.

RESULTS: Four eyes (3 patients) had pIOL explantation for low vault and anterior subcapsular cataract. The explanted pIOLs were the shorter length models (3, 12.1 mm; 1, 12.6 mm). Anterior segment optical coherence tomography (AS-OCT) confirmed the low pIOL vault before explantation in 2 eyes. Histopathology of the anterior subcapsular cataract showed fibrous metaplasia with a variable number of lens epithelial cell (LEC) layers attached to the inner surface of the anterior capsulorhexis specimens. Light microscopy of the explanted pIOLs showed no pigment on 1 lens, mild pigment deposition on 1 haptic, and pigment deposition throughout the anterior surface of 2 pIOLs.

CONCLUSIONS: Anterior subcapsular cataract associated with the pIOLs was caused by low vaulting (confirmed on AS-OCT) and consequent fibrous metaplasia of the anterior LECs. Surgeons should consider the possibility of anterior subcapsular cataract associated with shorter platforms when selecting a pIOL length for appropriate vault.



Slitlamp photography of case 1 (A), case 2 (B), case 3 (C), and case 4 (D) shows anterior subcapsular cataract and low pIOL vault.

The DeAngelis Laboratory: A New Look at Eye Disease

Focus stacked image from the diseased retina of a patient with AMD who donated his eyes to research. What you are seeing is a complex presentation with a number of pathologies including drusen, pigmented bone spicules and geographic atrophy. This retina will be one of the first examined for some of these diseases.

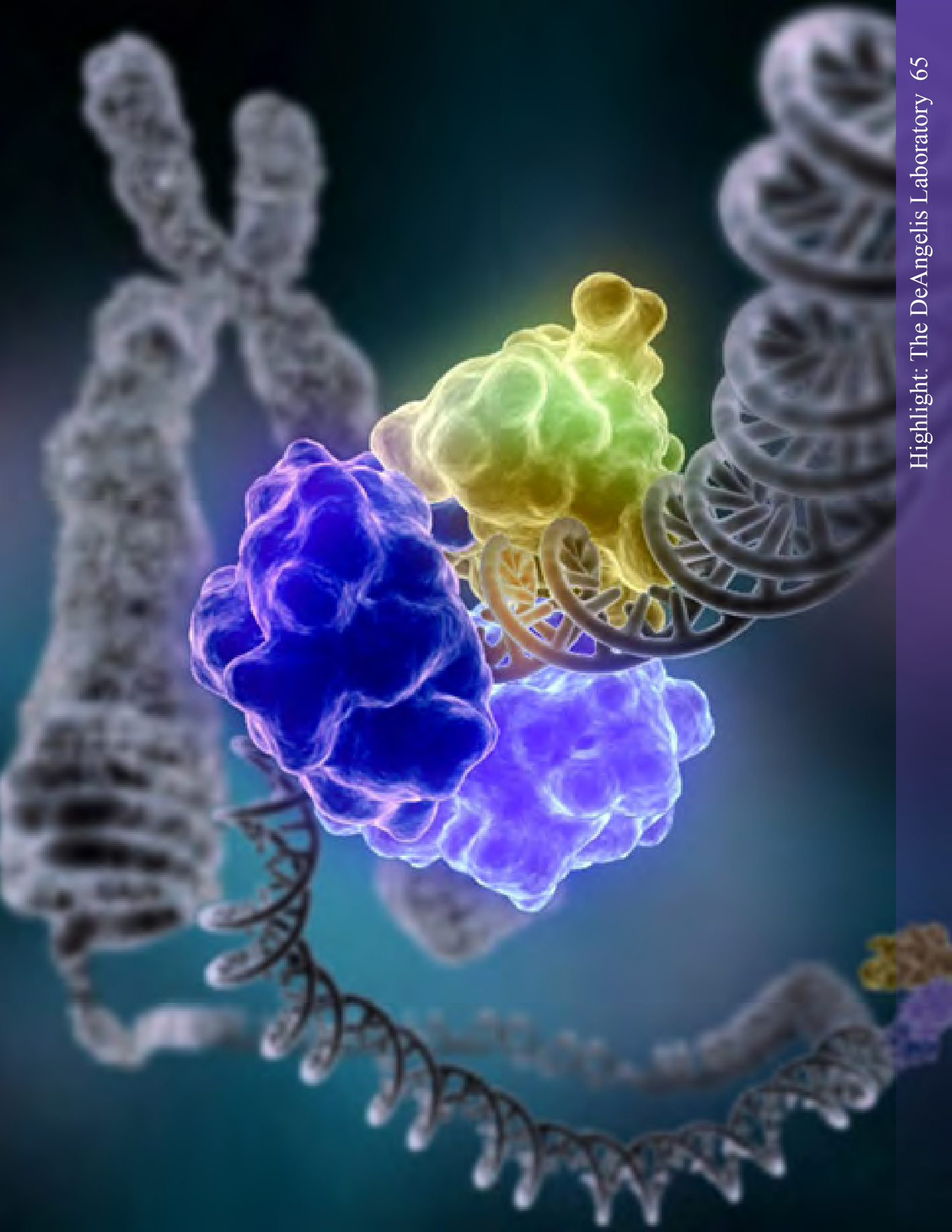
The pun is intended.

Meg DeAngelis, as a new member of the Moran Vision Institute, looks at the genetics of eye disease with a very different vision when compared to other geneticists. Like many others in the field Dr. DeAngelis laboratory's main research focus is applying a genomic convergent/systems biology based approach to uncover factors that may underlie eye diseases of complex inheritance such as age-related macular degeneration (AMD). AMD is a multifactorial disease and the using both family based and unrelated case control methods is a powerful approaches for revealing factors that individually may have only modest effects on disease

risk. Additionally the recruitment, ascertainment and evaluation of populations throughout the world should help to better pinpoint disease causality and ensure that a therapeutic target has global applicability. To complement ongoing genetic and epidemiological work, the DeAngelis laboratory is also conducting gene expression microarray and proteomic studies in order to examine the functional significance of disease-associated genetic variation. In addition to AMD DeAngelis and crew have expanded their efforts to include other retinal diseases such as retinopathy of prematurity and diabetic retinopathy with the ultimate goal

of correlating genotype with phenotype so that appropriate therapeutic targets can be developed with the hope of curing and preventing disease.

The DeAngelis laboratory was recently recruited from Harvard Medical School and is joining the fight against AMD alongside the Greg Hageman laboratory. The combination of the Hageman laboratory's clinical data, tissue repository and proteomic expertise—coupled with the DeAngelis laboratory's genetics/molecular expertise is sure to achieve great strides in teasing out the etiology of AMD and other vision disorders.





Bradley J. Katz, MD, PhD, specializes in neuro-ophthalmology, cataract, and comprehensive ophthalmology. He also evaluates patients with diseases that affect the optic nerve, diseases of the brain that affect vision and eye movements. Dr. Katz also conducts research in these areas.



Alan S. Crandall, MD, focuses on the medical and surgical management of glaucoma and cataracts. He presented at the 2010 American Academy of Ophthalmology, Cataract Spotlight of anterior segment surgery/research. Dr. Crandall has experience with trabeculectomy and laser cyclophotocoagulation. He is involved in numerous clinical research studies at the Moran Eye Center. Dr. Crandall is also the Director of the Medical Education Program. Dr. Crandall lectures all over the world and was selected by Cataract and Refractive Surgery Today as one of the 50 international opinion leaders.

Clinical Research: Anterior Segment

Randomized comparison of postoperative use of hydrogel ocular bandage and collagen corneal shield for wound protection and patient tolerability after cataract surgery.

Author: Dell SJ, Hovanesian JA, Raizman MB, Crandall AS, Doane J, Snyder M, Masket S, Lane S, Fram N; Ocular Bandage Study Group.

Journal: J Cataract Refract Surg. 2011 Jan;37(1):113-21.

PURPOSE: To compare the safety and efficacy of a hydrogel bandage and a collagen corneal shield in providing wound protection and relief of pain/discomfort in the acute period after uneventful unilateral clear corneal phacoemulsification cataract surgery with foldable intraocular lens (IOL) implantation.

SETTING: Seventeen investigational sites in the United States.

DESIGN: Prospective randomized single-masked parallel study.

METHODS: The study comprised patients scheduled to have unilateral clear corneal cataract surgery with posterior chamber intraocular lens implantation. The patients were examined preoperatively and frequently for 30 days postoperatively. The design was a noninferiority study of the 2 primary endpoints, device performance and maximum reported postoperative pain.

RESULTS: The device performance success was 78.6% (228/290) for the hydrogel bandage and 26.5% (26/98) for the corneal shield ($P < .0001$ for

noninferiority). Analyses indicated that the hydrogel bandage was superior to the corneal shield in device performance ($P < .001$; difference = 52.1%; 95% confidence interval, 41.6%-61.4%). The maximum postoperative pain/discomfort score of the hydrogel bandage (mean 1.3 ± 1.8 [SD]; scale 0 to 10) was noninferior to that of the corneal shield (1.1 ± 1.6) in the first 4 hours after surgery ($P < .001$). Adverse events in the cataract surgeries were reported in 22.2% (70/316) and 36.5% (38/104) of hydrogel bandage patients and corneal shield patients, respectively ($P = .0045$).

CONCLUSION: The hydrogel bandage was safe and effective for ocular surface protection and relief of pain/discomfort when applied topically to clear corneal incisions used in cataract or IOL implantation surgery.

Ab externo iris fixation of posterior chamber intraocular lens through small incision.

Author: Zandian M, Moghimi S, Fallah M, Crandall A.

Journal: J Cataract Refract Surg. 2010 Dec;36(12):2032-4.

ABSTRACT: During secondary posterior chamber intraocular lens (PC IOL) implantation with iris fixation in the absence of capsule support, we implanted an acrylic 3-piece PC IOL through a small clear corneal incision with haptics secured in knots; there was no need for IOL capture. Sutures were placed appropriately in the iris tissue before the IOL was inserted, ensuring safety of the procedure and centration of the IOL.



Nick Mamalis, MD

Toxic anterior segment syndrome: common causes.

Author: Cutler Peck CM, Brubaker J, Clouser S, Danford C, Edelhauser HE, Mamalis N.

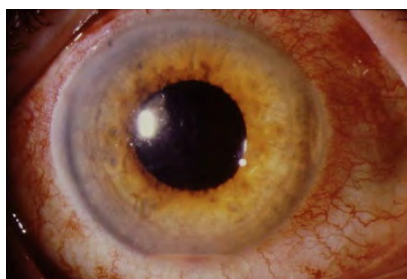
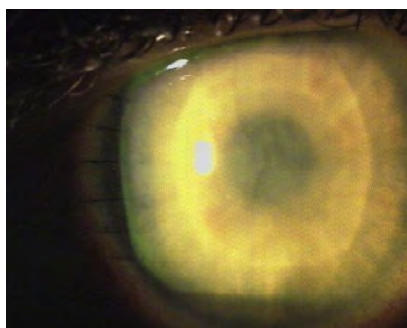
Journal: J Cataract Refract Surg. 2010 Jul;36(7):1073-80.

PURPOSE: To identify the most common risk factors associated with toxic anterior segment syndrome (TASS).

SETTING: Ophthalmic surgical centers in the United States, Argentina, Brazil, Italy, Mexico, Spain, and Romania.

METHODS: A TASS questionnaire on instrument cleaning and reprocessing and extraocular and intraocular products used during cataract surgery was placed on the American Society of Cataract and Refractive Surgery web site. A retrospective analysis of questionnaires submitted by surgical centers reporting cases of TASS was performed between June 1, 2007, and May 31, 2009, to identify commonly held practices that could cause TASS. Members of the TASS Task Force made site visits between October 1, 2005, and May 31, 2009, and the findings were evaluated.

RESULTS: Data from 77 questionnaires and 54 site visits were analyzed. The reporting centers performed 50 114 cataract surgeries and reported 909 cases of TASS. From January 1, 2006, to date, the 54 centers reported 367 cases in 143 919 procedures; 61% occurred in early 2006. Common practices associated with TASS included inadequate flushing of phaco and irrigation/aspiration handpieces, use of enzymatic cleansers, detergents at the wrong concentration, ultrasonic bath, antibiotic agents in balanced salt solution, preserved epinephrine, inappropriate agents for skin prep, and powdered gloves. Reuse of single-use



Top: Toxic anterior segment syndrome after phakic IOL surgery. Note the limbus-to-limbus corneal edema. Bottom: Hypopyon is seen in the anterior chamber of this patient with TASS.

products and poor instrument maintenance and processing were other risk factors.

CONCLUSIONS: The survey identified commonly held practices associated with TASS. Understanding these findings and the safe alternatives will allow surgical center personnel to change their practices as needed to prevent TASS.

Prevention of lens capsule opacification with ARC neodymium: YAG laser photolysis after phacoemulsification.

Author: Wehner W, Waring GO 3rd, Mamalis N, Walker R, Thyzel R.

Journal: J Cataract Refract Surg. 2010 Jun;36(6):881-4.

ABSTRACT: We describe a technique that uses a neodymium: YAG (Nd: YAG) laser photolysis system to prevent lens capsule opacification. The photolysis instrument consists of a 1064 nm Nd: YAG laser transmitted along a fiber-optic cable into a handpiece containing an angulated titanium plate that the laser beam strikes, creating plasma and a shockwave that ex-

its the handpiece through an aperture. Under direct visualization, the shockwave is aimed at the inner surface of the anterior capsule, where it removes LECs and proteoglycan attachment molecules; the shockwave probably extends to the capsule fornix, destroying germinal epithelial cells. We report preliminary results in 12 eyes followed for approximately 2.5 years in which the treated nasal anterior capsule remained clear or with only slight opacity and the untreated temporal capsule developed moderate to severe opacification.



Majid Moshirfar, MD, FACS

Laser in situ keratomileusis flap complications using mechanical microkeratome versus femtosecond laser: retrospective comparison.

Author: Moshirfar M, Gardiner JP, Schliesser JA, Espandar L, Feiz V, Mifflin MD, Chang JC.

Journal: J Cataract Refract Surg. 2010 Nov;36(11):1925-33.

PURPOSE: To compare the incidence of flap complications after creation of laser in situ keratomileusis (LASIK) flaps using a zero-compression microkeratome or a femtosecond laser.

SETTING: John A. Moran Eye Center, Department of Ophthalmology, University of Utah, Salt Lake City, Utah, USA.

DESIGN: Evidence-based manuscript.

METHODS: The flap complication rate was evaluated during the initial 18 months of experience using a zero-compression microkeratome (Hansatome) or a femtosecond laser (IntraLase FS60) for flap creation.

RESULTS: The flap complication rate was 14.2% in the microkeratome group and 15.2% in the femtosecond

laser group ($P = .5437$). The intraoperative flap complication rate was 5.3% and 2.9%, respectively ($P = .0111$), and the postoperative flap complication rate, 8.9% and 12.3%, respectively ($P = .0201$). The most common intraoperative complication in the microkeratome group was major epithelial defect/sloughing; the rate (2.6%) was statistically significantly higher than in the femtosecond laser group ($P = .0006$). The most common postoperative complication in both groups was diffuse lamellar keratitis (DLK) (6.0%, microkeratome; 10.6%, femtosecond laser) ($P = .0002$).

CONCLUSION: Although the total complication rates between the 2 groups were similar, the microkeratome group had significantly more epithelial defects intraoperatively and the femtosecond laser group had significantly more DLK cases postoperatively.

Simultaneous and sequential implantation of intacs and verisyse phakic intraocular lens for refractive improvement in keratectasia.

Author: Moshirfar M, Fenzl CR, Meyer JJ, Neuffer MC, Espandar L, Mifflin MD.

Journal: *Cornea*. 2011 Feb;30(2):158-63.

PURPOSE: To evaluate the safety, efficacy, and visual outcomes of simultaneous and sequential implantation of Intacs (Addition Technology, Inc, Sunnyvale, CA) and Verisyse phakic intraocular lens (AMO, Santa Ana, CA) in selected cases of ectatic corneal disease.

SETTING: John A. Moran Eye Center, University of Utah, UT.

METHODS: Prospective data were collected from 19 eyes of 12 patients (5 eyes, post-laser in situ keratomileusis ectasia and 14 eyes, keratoconus). Intacs segments were implanted followed by insertion of a phakic Verisyse lens at the same session (12 eyes) in the simultaneous group or several months later (7 eyes) in the sequential

group. The uncorrected visual acuity, best spectacle-corrected visual acuity (BSCVA), and manifest refraction were recorded at each visit.

RESULTS: No intraoperative or postoperative complications were observed. At the last follow-up (19 ± 6 months), in the simultaneous group, mean spherical error was -0.79 ± 1.0 diopter (D) (range, -2.0 to $+1.50$ D) and cylindrical error $+2.06 \pm 1.21$ D (range, $+0.5$ to $+3.75$ D). In the sequential group, at the last follow-up, at 36 ± 21 months, the mean spherical error was -1.64 ± 1.31 D (range, -3.25 to $+1.0$ D) and cylindrical error $+2.07 \pm 1.03$ D (range, $+0.75$ to $+3.25$ D). There were no significant differences in mean uncorrected visual acuity or BSCVA between the 2 groups preoperatively or postoperatively. No eye lost lines of preoperative BSCVA.

CONCLUSIONS: Combined insertion of Intacs and Verisyse was safe and effective in all cases. The outcomes of the simultaneous implantation of the Intacs and Verisyse lens in 1 surgery were similar to the results achieved with sequential implantation using 2 surgeries.

Improved centration of the type 1 Boston Keratoprosthesis in donor carrier tissue.

Author: Khalifa YM, Moshirfar M.

Journal: *Clin Ophthalmol*. 2010 Aug 19;4:931-3.

ABSTRACT: The type 1 Boston Keratoprosthesis preparation requires a 3-mm central punch and an 8.5 mm or larger punch in the carrier tissue. These punches are ideally concentric,

but we have found difficulty in achieving concentric punches when the larger punch is performed first. We present a modification in the preparation procedure to help minimize centration error.

Comparison of simulated keratometric changes induced by custom and conventional laser in situ keratomileusis after myopic ablation: retrospective chart review.

Author: Leng C, Feiz V, Modjtahedi B, Moshirfar M.

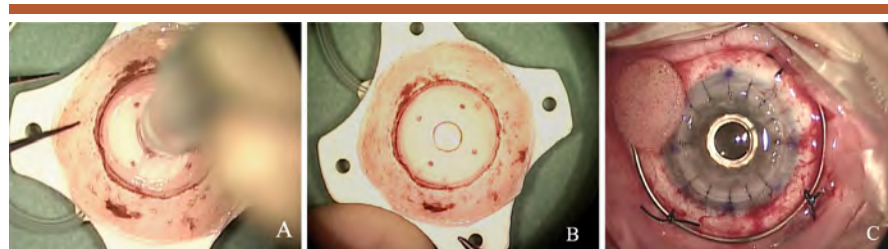
Journal: *J Cataract Refract Surg*. 2010 Sep;36(9):1550-5.

PURPOSE: To determine the relationship between the achieved refractive change and the change in simulated keratometry (K) after myopic laser in situ keratomileusis (LASIK) and compare this relationship between custom and conventional treatments.

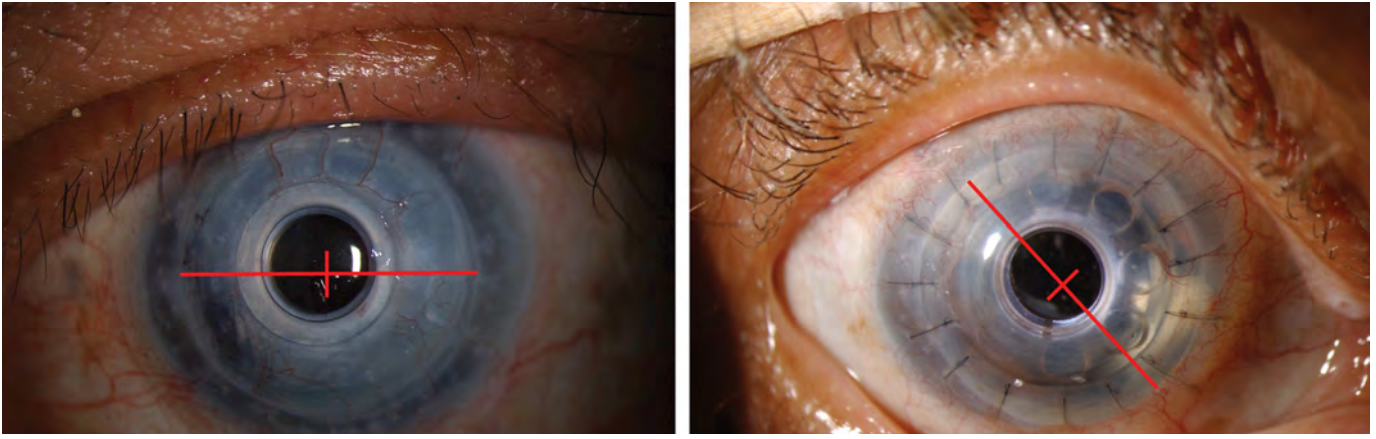
SETTING: Department of Ophthalmology, University of California, Davis, Sacramento, California, and John A. Moran Eye Center, Salt Lake City, Utah, USA.

METHODS: The change in simulated K and the refractive change induced by custom myopic LASIK and conventional LASIK were determined. The relationship between the variables was analyzed by regression methods.

RESULTS: Custom treatment was performed in 106 eyes and conventional treatment in 224 eyes. Simple linear regression analysis did not fit the clinical observation when the refractive change was less than 2.00 diopters (D) of myopic correction



Preparation of the carrier tissue with a 3-mm dermatologic punch first (A). The 3-mm hole is then centered between the vacuum ports of the punch block to create 2 concentric punches (B). The keratoprosthesis optic is perfectly centered in the carrier tissue, minimizing scatter and other optical phenomena and allowing for easier suturing and better tension distribution (C).



Examples of type 1 Boston Keratoprosthesis when prepared with the outer punch first and then the 3-mm central punch. Centration measurements show that the keratoprosthesis optic is poorly centered in the donor tissue.

with both treatments. Under the linear model and nonlinear model, each unit of refractive change yielded a greater change in corneal topographic power with custom treatment than with conventional treatment. With both treatments, the rate of change in simulated K was not constant and was much more variable with lower amounts of correction. The relationship was more constant and linear with larger amounts of refractive correction.

CONCLUSIONS: The relationship between the measured change in simulated K and the induced refractive change better fit a nonlinear relationship with smaller amounts of refractive correction in custom LASIK and conventional LASIK. Under all forms of analysis, custom treatments yielded a greater per-unit change in corneal curvature than conventional treatments, especially for refractive corrections of 4.00 D and higher.

Prospective, Contralateral Comparison of 120-mum and 90-mum LASIK Flaps Using the IntraLase FS60 Femtosecond Laser.

Author: Moshirfar M, Hatch BB, Chang JC, Kurz CJ, Eugarrrios MF, Mifflin MD.

Journal: J Refract Surg. 2010 Jul 13:1-9.

PURPOSE: To compare differences in visual acuity, contrast sensitivity, higher order ocular aberrations, quality

of life, and patient-reported outcomes at 3 and 6 months postoperatively in eyes with stable myopia undergoing thin-flap (intended flap thicknesses of 120 or 90 mum) LASIK using the VISX Star S4 CustomVue excimer laser (VISX Inc), with flaps created by the IntraLase FS60 femtosecond laser (Abbott Medical Optics).

METHODS: In this prospective study, thin-flap LASIK was performed contralaterally on 94 eyes: 47 eyes with 120-mum intended flap thickness and 47 eyes with 90-mum intended flap thickness. Primary outcome measures were uncorrected distance visual acuity (UDVA), corrected distance visual acuity (CDVA), contrast sensitivity, and higher order aberrations.

RESULTS: At 6 months, mean values for UDVA (logMAR) were -0.064 ± 0.077 and -0.051 ± 0.070 in the 120-mum and 90-mum groups, respectively ($n=40$, $P=.431$). Visual acuity of 20/20 was achieved in 98% of eyes with 120-mum flaps and 95% of eyes with 90-mum flaps, whereas 20/15 vision was achieved in 50% of eyes with 120-mum flaps and 45% of eyes with 90-mum flaps ($P \geq .454$). Both groups had significant increases in total higher order aberrations ($P \leq .003$). Significant differences were not found between groups in contrast sensitivity ($P \geq .258$), CDVA ($P \geq .726$), total higher order aberrations ($P \geq .477$), or patient-reported outcomes ($P \geq .132$). Patients in both groups reported increased quality of life postoperatively ($P \leq .002$).

CONCLUSIONS: Under well-controlled surgical conditions, thin-flap LASIK achieved similar results in visual acuity, contrast sensitivity, and low induction of higher order aberrations in eyes with intended flap thicknesses of either 120 or 90 mum.

Visual outcomes after wavefront-guided photorefractive keratectomy and wavefront-guided laser in situ keratomileusis: Prospective comparison.

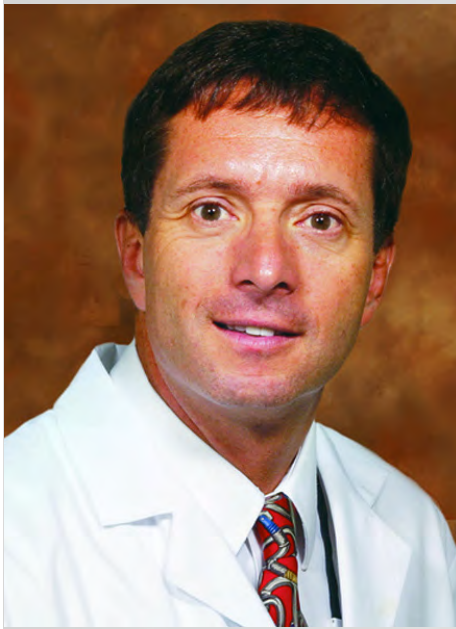
Author: Moshirfar M, Schliesser JA, Chang JC, Oberg TJ, Mifflin MD, Townley R, Livingston MK, Kurz CJ.

Journal: J Cataract Refract Surg. 2010 Aug;36(8):1336-43.

PURPOSE: To compare visual outcomes between wavefront-guided photorefractive keratectomy (PRK) and wavefront-guided laser in situ keratomileusis (LASIK).

SETTING: Academic center, Salt Lake City, Utah, USA.

METHODS: In this randomized prospective study, myopic eyes were treated with wavefront-guided PRK and or wavefront-guided LASIK using a Visx Star S4 CustomVue platform with iris registration. Primary outcome measures were uncorrected (UDVA) and corrected (CDVA) distance visual acuities and manifest refraction. Secondary outcome measures were higher-order aberrations (HOAs) and contrast sensitivity.



Geoffrey C. Tabin, MD, is a corneal specialist and Director of the International Ophthalmology Division at the Moran Eye Center. In addition to his work in Utah providing corneal and refractive care, Dr. Tabin is working to develop eye care delivery in developing countries. Part of his research includes improving cataract and corneal surgery.



RESULTS: The PRK group comprised 101 eyes and the LASIK group, 102 eyes. At 6 months, the mean UDVA was $-0.03 \log\text{MAR} \pm 0.10$ [SD] (20/19) and $0.07 \pm 0.09 \log\text{MAR}$ (20/24), respectively ($P = .544$). In both groups, 75% eyes achieved a UDVA of 20/20 or better ($P = .923$); 77% of eyes in the PRK group and 88% in the LASIK group were within ± 0.50 diopter of emmetropia ($P = .760$). There was no statistically significant difference between groups in contrast sensitivity at 3, 6, 12, or 18 cycles per degree. The mean postoperative HOA root mean square was $0.45 \pm 0.13 \mu\text{m}$ in the PRK group and $0.59 \pm 0.22 \mu\text{m}$ in the LASIK group ($P = .012$), representing an increase factor of 1.22 and 1.74, respectively.

CONCLUSIONS: Wavefront-guided PRK and wavefront-guided LASIK had similar efficacy, predictability, safety, and contrast sensitivity; however, wavefront-guided PRK induced statistically fewer HOAs than wavefront-guided LASIK at 6 months.

Central toxic keratopathy.

Author: Moshirfar M, Hazin R, Khalifa YM.

Journal: *Curr Opin Ophthalmol*. 2010 Jul;21(4):274-9.

PURPOSE OF REVIEW: To describe recent evidence from the literature regarding central toxic keratopathy syndrome (CTK).

RECENT FINDINGS: CTK describes a rare, self-limited, noninflammatory postsurgical condition that presents with central corneal opacity and a significant hyperopic shift. Although its cause remains uncertain, CTK bears a striking clinical resemblance to other more serious conditions and is, therefore, often misdiagnosed and mismanaged. Despite its noninflammatory nature, the overlapping clinical features CTK shares with other inflammatory and infectious processes have led some to treat CTK with steroids. Recent studies discourage the use of steroids in CTK and recommend al-

lowing the condition to resolve on its own.

SUMMARY: Although CTK resembles other inflammatory conditions that are responsive to steroids, current studies suggest that steroid administration is contraindicated in CTK and can exacerbate preexisting refractive alterations in patients with the condition.

Etiologic diagnosis of corneal ulceration at a tertiary eye center in Kathmandu, Nepal.

Author: Feilmeier MR, Sivaraman KR, Oliva M, Tabin GC, Gurung R.

Journal: *Cornea*. 2010 Dec;29(12):1380-5.

PURPOSE: To determine the etiologic diagnosis of infectious corneal ulcers at Tilganga Institute of Ophthalmology, a tertiary teaching hospital in Kathmandu Nepal, from 2006-2009.

METHODS: This study involved a review of all microbiology records at Tilganga Institute of Ophthalmology from August 2006 through July 2009. Microbiologic records from the corneal scrapings of all patients suspected of having infectious corneal ulcers were included.

RESULTS: Corneal scrapings were obtained from 468 patients. The average patient age was 52 years, and 55% of the affected cases were males. Microorganisms were grown from 185 of the corneal scrapings (40%). Pure bacterial cultures were obtained from 72 patients (39%), and pure fungal cultures were obtained from 113 patients (61%). Gram stain was 75% sensitive (95% confidence interval, 0.632-0.841) in identifying bacterial infection, whereas KOH prep was 80.5% sensitive (95% confidence interval, 0.718-0.871) in identifying fungal organisms. Of 72 bacterial isolates, 50 isolates (69%) were *Streptococcus pneumoniae*, the most common organism isolated in this study. Of 113 fungal isolates, 40 of isolates (35%) were identified as *Aspergillus* sp.

CONCLUSIONS: Fungal organisms

(61%) are the most common cause of infectious keratitis in this patient population. Of all organisms, *S. pneumoniae* was the most common organism identified. Smear microscopy is reliable in rapidly determining the etiology of the corneal infection and can be used to help guide initial therapy in this setting.



**Liliana Werner,
MD, PhD**

Long-term pathological follow-up of 2-loop iridocapsular intraocular lens.

Author: Burrow MK, Werner L, Maddula S, Ness PJ, Davis D, Mamalis N.

Journal: J Cataract Refract Surg. 2011 Feb;37(2):409-12.

ABSTRACT: We analyzed an enucleated postmortem eye from an 86-year-old donor who had a 2-loop iridocapsular intraocular lens (IOL) that had been implanted at least 30 years earlier. High-frequency ultrasound showed a relatively well-centered iris-supported optic in front of the pupil. Gross and light microscopic analyses of the eye and the IOL showed loop fixation outside the capsular bag remnants, a thickened cornea, mild attenuation of the corneal endothelium, multiple areas of iris trauma secondary to haptic abrasion, fragments of iris tissue attached to the haptics, as well as pigment dispersion within the eye with pigmented epithelial cells attached to the IOL haptics. Histopathological examination of the posterior segment was unremarkable.

Clinicopathologic correlation of capsulorhexis phimosis with anterior flexing of single-piece hydrophilic acrylic intraocular lens haptics.

Author: Zaugg B, Werner L, Neuhann T, Burrow M, Davis D, Mamalis N, Tetz M.

Journal: J Cataract Refract Surg. 2010 Sep;36(9):1605-9.

ABSTRACT: We describe 2 cases in which patients with 4-looped single-piece hydrophilic acrylic intraocular lenses (IOLs) exhibited postoperative complications including capsulorhexis phimosis, decentration, tilt, hyperopic shift, and luxation leading to explantation of the IOL-capsular bag complex. The excessive capsule fibrosis led to anterior flexing of the IOL haptics in both cases, even in the presence of a capsular tension ring (CTR). Histopathological analyses revealed a thick fibrocellular tissue attached to the inner surface of the anterior capsules, corresponding to the anterior capsule opacification and folds. An amorphous substance was observed on the outer surface of the anterior capsule in the case with a CTR, suggesting pseudo-exfoliation material. These and similar cases raise concerns about the postoperative behavior of highly flexible IOLs in the presence of excessive capsular bag fibrosis.

Glistenings and surface light scattering in intraocular lenses.

Author: Werner L.

Journal: J Cataract Refract Surg. 2010 Aug;36(8):1398-420.

ABSTRACT: Glistenings are fluid-filled microvacuoles that form within the intraocular lens (IOL) optic when the IOL is in an aqueous environment.

They are observed in all types of IOLs but have been mainly associated with hydrophobic acrylic IOLs. Experimental and clinical studies suggest the various hydrophobic acrylic IOLs on the market exhibit different tendencies toward glistenings. Factors influencing glistening formation include IOL material composition, manufacturing technique, packaging, associated conditions such as glaucoma or those leading to breakdown of the blood-aqueous barrier, as well as concurrent use of ocular medications. Although the impact of glistenings on postoperative visual function and the evolution of glistenings in the late postoperative period remain controversial, IOL explantation has rarely been reported. The phenomenon of surface light scattering has also been described in association with hydrophobic acrylic IOLs. Its mechanism of formation is controversial but may be related to long-term phase separation water near the IOL surface, although not seen as microvacuoles.

Calcification of different designs of silicone intraocular lenses in eyes with asteroid hyalosis.

Author: Stringham J, Werner L, Monson B, Theodosis R, Mamalis N.

Journal: Ophthalmology. 2010 Aug;117(8):1486-92.



Gross photographs of the anterior segment of the eye implanted with the 2-loop iridocapsular IOL. A: Posterior view showing the residual capsular bag containing dense Soemmering ring formation, an iridectomy, and areas lacking iris pigment. Two closed loops extending from the optic can be seen coursing behind the iris. The left loop mostly makes direct contact with the capsular bag, while the right loop is mostly in direct contact with the posterior surface of the iris. B: Anterior view after removal of the cornea showing the IOL optic sitting in front of the iris.

PURPOSE: To describe the association between calcification of older and newer designs of silicone intraocular lenses (IOLs) and asteroid hyalosis.

DESIGN: Case series with clinicopathologic correlation.

PARTICIPANTS: Sixteen silicone IOLs explanted because of decreased visual acuity associated with opacifying deposits on the posterior optic surface.

METHODS: All 16 lenses underwent gross and light microscopic analyses. Selected lenses underwent alizarin red staining or scanning electron microscopy coupled with energy dispersive x-ray spectroscopy for elemental composition. Clinical data in each case were obtained by a questionnaire sent to the explanting surgeons. Clinical data in relation to 111 hydrophilic acrylic lenses explanted because of calcification also were assessed for comparison.

MAIN OUTCOME MEASURES: Deposit morphologic features and location were evaluated under gross and light microscopy. The calcified nature of the deposits was assessed by histochemical staining and surface analyses. Clinical data obtained included age at IOL implantation, gender, implantation and explantation dates, as well as history of neodymium:yttrium-aluminum-garnet laser treatment. The presence of asteroid hyalosis in the affected eye was investigated for the explanted silicone and hydrophilic acrylic lenses.

RESULTS: The 16 lenses were of 8 designs manufactured from different silicone materials, which were explanted 9.21+/-3.66 years after implantation. Neodymium:yttrium-aluminum-garnet laser applications performed in 12 cases partially removed deposits from the lens, followed by a gradual increase in their density after the procedures. The presence of asteroid hyalosis was confirmed in 13 cases; no notes regarding this condition were found in patient charts in the other 3 cases. The deposits were only on the posterior optic surface of the silicone lenses and were composed

of calcium and phosphate. A history of asteroid hyalosis was not found in relation to any of the 111 cases of postoperative calcification of hydrophilic acrylic lenses.

CONCLUSIONS: Including this current series, there are 22 cases of calcification of silicone lenses involving 8 designs manufactured from different silicone materials described in the literature. The presence of asteroid hyalosis was confirmed in 86.4% of cases. These findings may be added to the list of pros and cons surgeons consider when selecting or recommending an IOL.

Clinical Comparison of Latanoprost and Timolol in Pediatric Glaucoma: A Phase 3, 12-Week, Randomized, Double-Masked Multicenter Study

Author: Tomoko Maeda-Chubachi, MD, PhD, Katherine Chi-Burris, MPH, Brad D. Simons, MD, PhD, Sharon F. Freedman, MD, Peng T. Khaw, MD, PhD, Barbara Wirostko, MD, Eric Yan, PhD, for the A611137 Study Group

Journal: Ophthalmology., 2011, In Press

OBJECTIVE: To compare the efficacy and safety of latanoprost versus

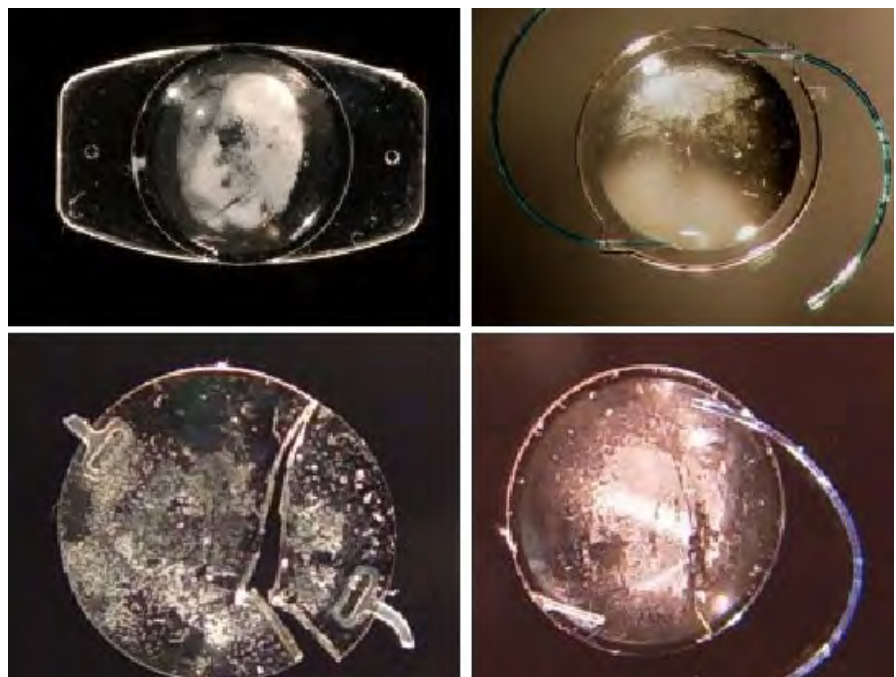
timolol in pediatric patients with glaucoma.

DESIGN: Prospective, randomized, double-masked, 12-week, multicenter study.

PARTICIPANTS: Individuals ≤ 18 years of age with glaucoma.

METHODS: Stratified by age, diagnosis, and IOP level, subjects were randomized (1:1) to latanoprost vehicle at 8 AM and latanoprost 0.005% at 8 PM or timolol 0.5% (0.25% for those < 3 years old) twice daily (8 AM, 8 PM). At baseline and weeks 1, 4, and 12, IOP and ocular safety were assessed and adverse events were recorded. Therapy was switched to open-label latanoprost PM and timolol AM and PM for uncontrolled IOP.

MAIN OUTCOME MEASURES: Mean IOP reduction from baseline to week 12. Latanoprost was considered noninferior to timolol if the lower limit of the 95% confidence interval (CI) of the difference was > -3 mmHg. Proportion of responders (subjects with $\geq 15\%$ IOP reduction at weeks 4 and 12) were evaluated. Analyses were performed in diagnosis subgroups: primary congenital glaucoma (PCG) and non-PCG.



Gross photographs of different silicone lens models explanted because of surface deposits.

RESULTS: In total, 137 subjects were treated (safety population; 12-18 years, n=48; 3-<12 years, n=55; 0-<3 years, n=34). Mean age was 8.8±5.5 years, and mean baseline IOP was 27.7±6.17 mmHg; 125 subjects completed the study, and 107 were in the per protocol population. Mean IOP reductions for latanoprost and timolol at week 12 were 7.2 and 5.7 mmHg, respectively, with a difference of 1.5 mmHg (95% CI: -0.8, 3.7; P=0.21). Responder rates were 60% for latanoprost and 52% for timolol (P=0.33). Between-treatment differences in mean IOP reduction for PCG and non-PCG subgroups were 0.6 mmHg (95% CI: -2.3, 3.4) and 2.6 mmHg (95% CI: -0.8, 6.1), respectively. Responder rates for latanoprost vs. timolol were: PCG, 50% vs. 46%; non-PCG, 72% vs. 57%. Both therapies were well tolerated.

CONCLUSIONS: Latanoprost 0.005% is not inferior (i.e., is either more or similarly effective) to timolol and produces clinically relevant IOP reductions across pediatric PCG and non-PCG patients. Both latanoprost and timolol had favorable safety profiles over the duration of this three month trial.

Latanoprost Systemic Pharmacokinetics in Pediatric and Adult Glaucoma Patients: A Phase 1, Open-label Study

Author: Susan Raber, PharmD, Rachel Courtney, PhD, Tomoko Maeda-Chubachi, MD, PhD, Brad Simons, MD, Sharon Freedman, MD, Barbara Wirostko, MD

Journal: Ophthalmology, 2011

OBJECTIVE: To evaluate the safety and steady-state systemic pharmacokinetics (PK) of latanoprost acid in pediatric subjects with glaucoma or ocular hypertension administered the adult latanoprost dose.

DESIGN: Phase 1, open-label, multicenter study.

PARTICIPANTS: Pediatric patients of three age groups (<3; 3 to <12; 12 to <18 years) and adults (≥18 years

of age) receiving stable treatment with latanoprost ophthalmic solution 0.005% once daily in one or both eyes for ≥2 weeks.

INTERVENTION: Latanoprost was administered in both eyes each morning following the screening visit. Subjects returned 3 to 28 days later for PK evaluation, withholding the latanoprost morning dose. At the clinic, a single drop of latanoprost ophthalmic solution was instilled into both eyes. Blood samples for plasma latanoprost acid concentrations were collected predose, and at 5, 15, 30, and 60 minutes after topical latanoprost administration.

MAIN OUTCOME MEASURE: Latanoprost acid plasma exposure.

RESULTS: The evaluable PK analysis set included data from 39 of 47 enrolled subjects. The median C_{max} values were higher in the <3 year age group (166 pg/ml) versus the other groups (49, 16 and 26 pg/mL for the 3 to <12, 12 to <18 and ≥18 year age groups, respectively). The median AUC_{last} values were also higher in the <3 year age group (2716 pg•min/mL) versus the other groups (588, 106, and 380 pg•min/mL for the 3 to <12, 12 to <18 and ≥18 year groups, respectively). Latanoprost acid was rapidly eliminated from the blood with plasma concentrations undetectable within 10 to 30 minutes postdose in all but the <3-year age group. There were no discontinuations or dose reductions due to adverse events or treatment-emergent adverse events.

CONCLUSIONS: Latanoprost acid systemic exposure was higher in younger children compared to adolescents and adults, attributed primarily to lower body weight and a smaller blood volume. Latanoprost acid was rapidly eliminated in all age groups and resulted in only a brief period of systemic exposure following once-daily dosing. Higher systemic exposure was not accompanied by adverse events, and based on historical data, a sufficient safety margin for systemic adverse effects was demonstrated in pediatric patients administered the adult dose.



Barbara Wirostko, MD, works in Dr. Bala Ambati's lab assisting the iVeena research team on a novel ocular drug delivery device with pre IND enabling studies and clinical strategy. She is the Chief Medical Officer of Altheos, a biotech company based in South San Francisco, California, developing a novel NCE for glaucoma treatment. She is responsible for the medical messaging, clinical development plan and the glaucoma strategy. She is a board certified Ophthalmologist with glaucoma fellowship training. She serves on the Grant Review Working Group for CIRM, California Institute for Regenerative Medicine, and is on the editorial board of *Acta Ophthalmologica*.

Prior to joining Pfizer, Barbara was Chief Ophthalmologist practicing as a clinician and specializing in glaucoma at the Huntington Medical Group PC, in Huntington, NY. During her 10 years in practice, she served as Principle Investigator for various pivotal glaucoma clinical trials for major Pharmaceutical companies specialized in eye care.

Clinical Research: Posterior Segment



Paul Bernstein, PhD

Demographic characteristics, patterns and risk factors for retinal vein occlusion in Nepal: a hospital-based case-control study.

Author: Thapa R, Paudyal G, Bernstein PS.

Journal: Clin Experiment Ophthalmol. 2010 Aug;38(6):583-90.

PURPOSE: Retinal vein occlusion (RVO) is an increasing problem leading to visual impairment in Nepal. Our study investigates the demographic characteristics, patterns and risk factors for RVO in this developing Asian country.

METHODS: This is a hospital-based case-control study conducted at the Tilganga Institute of Ophthalmology of Nepal during the period of January 2007 to January 2008. All consecutive new cases of RVO diagnosed at the Institute were included. Cases with intraocular inflammation or a prior history of intraocular injections, laser therapy or vitrectomy for RVO were excluded from the study. Age, sex and geographically matched subjects were recruited as a control group from patients who presented for regular eye examinations at the same hospital during the study period.

RESULTS: A total of 218 patients with RVO presented during the study period. The mean age of the patients was 61.1 + or - 12.3 years with more men (58.3%) than women. The mean age for control groups was 61.3 + or - 13.0 years. Seventy per cent of subjects had branch retinal vein occlusion, whereas central retinal vein oc-

clusion was present in 26.6%. 63.9% of branch retinal vein occlusion was found in the superotemporal branch. Hypermetropia, primary open angle glaucoma, hypertension, mixed diabetes and hypertension, and heart disease were significantly higher in RVO cases as compared with the control group.

CONCLUSION: The demographic characteristics, patterns and risk factors of RVO in Nepal can help guide interventions against these blinding diseases in similar developing countries.



ME Hartnett, PhD

Association between assisted reproductive technology and advanced retinopathy of prematurity.

Author: Chan RP, Yonekawa Y, Morrison MA, Sun G, Wong RK, Perlman JM, Chiang MF, Lee TC, Hartnett ME, DeAngelis MM.

Journal: Clin Ophthalmol. 2010 Nov 26;4:1385-90.

PURPOSE: To investigate the associations between assisted reproductive technology (ART) and severe retinopathy of prematurity (ROP) requiring treatment.

METHODS: Retrospective analyses of inborn preterm infants screened for severe ROP at the Weill Cornell Medical Center Neonatal Intensive Care Unit at the New York-Presbyterian Hospital by single factor logistic regression and multifactor models.

RESULTS: Of 399 ethnically diverse infants, 253 were conceived naturally and 146 by ART. Eight (3.16%) patients conceived naturally, and 11 (7.53%) with ART required laser treatment. In multifactor analyses, significant risks for severe ROP requiring treatment included both gestational age (odds ratio [OR] 0.34; 95% confidence interval [CI] 0.23-0.52; $P < 0.001$) and ART ([OR] 4.70; [CI], 1.52-4.57; $P = 0.007$).

CONCLUSIONS: ART is associated with severe ROP requiring treatment in this cohort. This is the first report that demonstrates a statistically significant association between ART and severe ROP requiring treatment in infants in the US.

Baseline Predictors of Visual Acuity and Retinal Thickness Outcomes in Patients with Retinal Vein Occlusion: Standard Care versus Corticosteroid for RETinal Vein Occlusion Study Report 10.

Author: Scott IU, Vanveldhuisen PC, Oden NL, Ip MS, Blodi BA, Hartnett ME, Cohen G; Standard Care versus Corticosteroid for RETinal Vein Occlusion Study Investigator Group.

Journal: Ophthalmology. 2011 Feb;118(2):345-52.

OBJECTIVE: To investigate baseline factors associated with visual acuity and central retinal thickness outcomes in patients with macular edema secondary to retinal vein occlusion in the Standard Care versus Corticosteroid for RETinal Vein Occlusion (SCORE) Study.

DESIGN: Two multicenter, randomized clinical trials: one evaluating participants with central retinal vein occlusion (CRVO) and one evaluating participants with branch retinal vein occlusion (BRVO).

PARTICIPANTS: Participants with follow-up data of 1 year or more, including 238 with CRVO and 367 with BRVO.

METHODS: Visual acuity was mea-

sured by the electronic Early Treatment Diabetic Retinopathy Study (E-ETDRS) method, and central retinal thickness was measured by optical coherence tomography (OCT). Regression analysis related these outcomes to 20 baseline measures. Multiple P values were adjusted to control the false discovery rate.

MAIN OUTCOME MEASURES:

Outcome measures of visual acuity letter score included absolute change from baseline, a gain of ≥ 15 from baseline, and a loss of ≥ 15 from baseline. Outcome measures of center point thickness included absolute change from baseline, a measurement of ≤ 250 μm , and a measurement of ≥ 500 μm . Outcomes were assessed at 1 and 2 years.

RESULTS: For CRVO and BRVO, younger age was associated with improved visual acuity and central retinal thickness outcomes. For CRVO, triamcinolone treatment and less severe anatomic abnormalities of the retina (center point thickness and areas of retinal hemorrhage, thickening, and fluorescein leakage) were predictive of better visual acuity outcomes. For BRVO, no history of coronary artery disease was predictive of improved visual acuity outcomes. For center point thickness outcomes, shorter duration of macular edema was associated with improvement in both disease entities. For CRVO, higher baseline visual acuity letter score was predictive of favorable OCT outcomes. For BRVO, lower baseline visual acuity letter score, presence of dense macular hemorrhage, and no prior grid photocoagulation were predictive of favorable OCT outcomes.

CONCLUSIONS: Several factors were predictive of better visual acuity outcomes and more favorable OCT outcomes, including younger age and shorter duration of macular edema, respectively. These factors may assist clinicians in predicting disease course for patients with CRVO and BRVO.

Randomized trial evaluating ranibizumab plus prompt or deferred laser or triamcinolone plus prompt laser for diabetic macular edema.

Author: Diabetic Retinopathy Clinical Research Network, Elman MJ, Aiello LP, Beck RW, Bressler NM, Bressler SB, Edwards AR, Ferris FL 3rd, Friedman SM, Glassman AR, Miller KM, Scott IU, Stockdale CR, Sun JK. Collaborators (583)

Journal: Ophthalmology. 2010 Jun;117(6):1064-1077

OBJECTIVE: Evaluate intravitreal 0.5 mg ranibizumab or 4 mg triamcinolone combined with focal/grid laser compared with focal/grid laser alone for treatment of diabetic macular edema (DME).

DESIGN: Multicenter, randomized clinical trial.

PARTICIPANTS: A total of 854 study eyes of 691 participants with visual acuity (approximate Snellen equivalent) of 20/32 to 20/320 and DME involving the fovea.

METHODS: Eyes were randomized to sham injection + prompt laser (n=293), 0.5 mg ranibizumab +

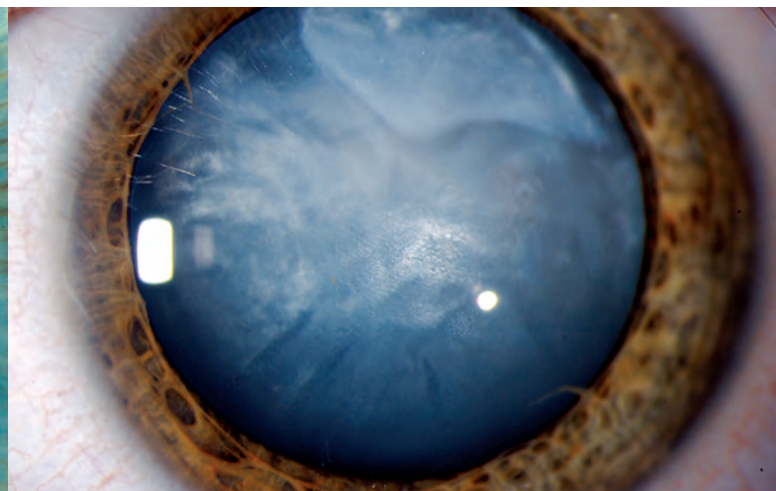
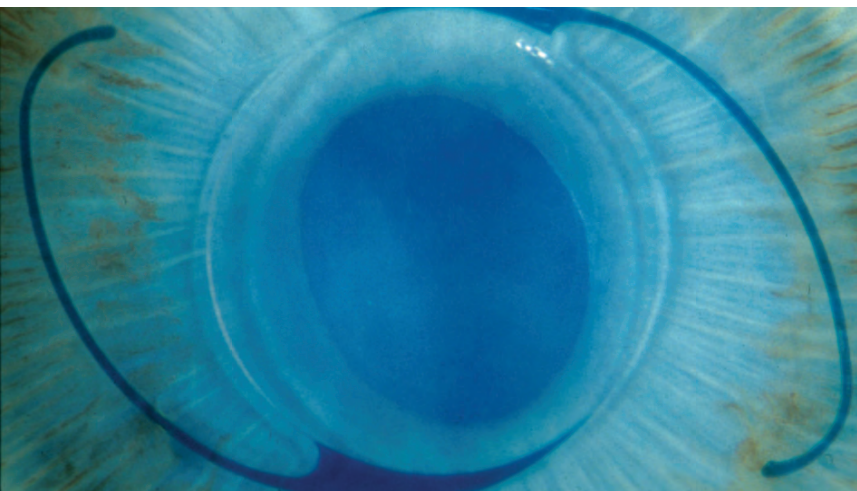
prompt laser (n=187), 0.5 mg ranibizumab + deferred (> or =24 weeks) laser (n=188), or 4 mg triamcinolone + prompt laser (n=186). Retreatment followed an algorithm facilitated by a web-based, real-time data-entry system.

MAIN OUTCOME MEASURES:

Best-corrected visual acuity and safety at 1 year.

RESULTS: The 1-year mean change (\pm -standard deviation) in the visual acuity letter score from baseline was significantly greater in the ranibizumab + prompt laser group (+9 \pm -11, $P < 0.001$) and ranibizumab + deferred laser group (+9 \pm -12, $P < 0.001$) but not in the triamcinolone + prompt laser group (+4 \pm -13, $P = 0.31$) compared with the sham + prompt laser group (+3 \pm -13). Reduction in mean central subfield thickness in the triamcinolone + prompt laser group was similar to both ranibizumab groups and greater than in the sham + prompt laser group. In the subset of pseudophakic eyes at baseline (n=273), visual acuity improvement in the triamcinolone + prompt laser group appeared comparable to that in the ranibizumab groups. No systemic events attributable to study treatment were apparent. Three eyes (0.8%) had injection-related endophthalmitis in the ranibizumab groups, whereas elevated intraocular pressure and cataract surgery were more frequent in the triamcinolone + prompt laser group. Two-year visual acuity outcomes were similar to 1-year outcomes.

CONCLUSIONS: Intravitreal ranibizumab with prompt or deferred laser is more effective through at least 1 year





compared with prompt laser alone for the treatment of DME involving the central macula. Ranibizumab as applied in this study, although uncommonly associated with endophthalmitis, should be considered for patients with DME and characteristics similar to those in this clinical trial. In pseudophakic eyes, intravitreal triamcinolone + prompt laser seems more effective than laser alone but frequently increases the risk of intraocular pressure elevation.

Randomized, sham-controlled trial of dexamethasone intravitreal implant in patients with macular edema due to retinal vein occlusion.

Author: Haller JA, Bandello F, Belfort R Jr, Blumenkranz MS, Gillies M, Heier J, Loewenstein A, Yoon YH, Jacques ML, Jiao J, Li XY, Whitcup SM; OZURDEX GENEVA Study Group. Collaborators (765)

Journal: *Ophthalmology*. 2010 Jun;117(6):1134-1146.

OBJECTIVE: To evaluate the safety and efficacy of dexamethasone intravitreal implant (DEX implant; OZURDEX, Allergan, Inc., Irvine, CA) com-

pared with sham in eyes with vision loss due to macular edema (ME) associated with branch retinal vein occlusion (BRVO) or central retinal vein occlusion (CRVO).

DESIGN: Two identical, multicenter, masked, randomized, 6-month, sham-controlled clinical trials (each of which included patients with BRVO and patients with CRVO).

PARTICIPANTS: A total of 1267 patients with vision loss due to ME associated with BRVO or CRVO.

INTERVENTION: A single treatment with DEX implant 0.7 mg (n = 427), DEX implant 0.35 mg (n = 414), or sham (n = 426).

MAIN OUTCOME MEASURES:

The primary outcome measure for the pooled data from the 2 studies was time to achieve a ≥ 15 -letter improvement in best-corrected visual acuity (BCVA). Secondary end points included BCVA, central retinal thickness, and safety.

RESULTS: After a single administration, the time to achieve a ≥ 15 -letter improvement in BCVA was significantly less in both DEX implant groups compared with sham ($P < 0.001$). The percentage of eyes

with a ≥ 15 -letter improvement in BCVA was significantly higher in both DEX implant groups compared with sham at days 30 to 90 ($P < 0.001$). The percentage of eyes with a ≥ 15 -letter loss in BCVA was significantly lower in the DEX implant 0.7-mg group compared with sham at all follow-up visits ($P < 0.036$). Improvement in mean BCVA was greater in both DEX implant groups compared with sham at all follow-up visits ($P < 0.006$). Improvements in BCVA with DEX implant were seen in patients with BRVO and patients with CRVO, although the patterns of response differed. The percentage of DEX implant-treated eyes with intraocular pressure (IOP) of > 25 mmHg peaked at 16% at day 60 (both doses) and was not different from sham by day 180. There was no significant between-group difference in the occurrence of cataract or cataract surgery.

CONCLUSIONS: Dexamethasone intravitreal implant can both reduce the risk of vision loss and improve the speed and incidence of visual improvement in eyes with ME secondary to BRVO or CRVO and may be a useful therapeutic option for eyes with these conditions.

Clinical Articles/Reports

Treatments for neuro-ophthalmologic conditions.

Author: Spencer BR Jr, Digre KB.

Journal: *Neurol Clin*. 2010
Nov;28(4):1005-35.

ABSTRACT: Neuro-ophthalmology covers disorders that fall between the cracks of Neurology and Ophthalmology. Neurologists see patients with neuro-ophthalmic disorders. Recognition of the diagnosis is difficult enough, but treatment can be challenging. This article reviews several common neuro-ophthalmic disorders, outlining their features and treatments, from retinal vascular disorders to eye movements and blepharospasm.

Idiopathic intracranial hypertension.

Author: Digre KB.

Journal: *BMJ* 2010; 341:c2836

ABSTRACT: Weight loss may be effective, but confirmation is needed from randomised trials. In the linked prospective cohort study, Sinclair and colleagues observed intracranial pressure in patients with idiopathic intracranial hypertension who follow a low energy diet. This condition is often chronic and is characterized by symptoms and signs of intracranial hypertension, with no cause found by adequate imaging studies, and normal cerebrospinal fluid. Visual loss from papilloedema is the most feared visual complication. Headaches (which are difficult to treat) and depression are common, and quality of life is often reduced.

Elimination of consult codes in neuro-ophthalmology: another blow to our subspecialty?

Author: Frohman L, Digre K.

Journal: *J Neuroophthalmol*. 2010
Jun;30(2):210-1.

ABSTRACT: There are threats to the practice of neuro-ophthalmology from many directions. These include lack of recognition in academic centers, lack of reimbursement for complex neuro-ophthalmic problems, and lack of procedures that provide income for practitioners. Now we have another threat—the loss of consultation codes from the Centers for Medicare and Medicaid Services (CMS). Yet neuro-ophthalmology is a consultative subspecialty—patients do not come to us except on another physician's request for consultation. How did this situation arise? CMS proposed discontinuing consultation codes in July 2009. The reason for the proposal was that consultations were costing Medicare/Medicaid large amounts of money and there was evidence that consultation codes were frequently used incorrectly by physicians not knowing the difference between a referral (transferring the care from one physician to another) and a consultation (rendering an opinion about a condition and sending back to the requesting physician). In October 2009, CMS published the 2010 guidelines for payment that eliminated this code. The rationale cited in the Federal Register was based on a review by the Office of the Inspector General entitled "Consultations in Medicare: Coding and Reimbursement". CMS stated that elimination of the codes would be budget neutral as the work relative value units for new and established office visits would be increased. To quote, "We believe that the rationale for a differential payment for a consultation service is no longer supported because documentation requirements are now similar across all E/M services." The long-term repercussion of this action is unknown. *Neurology Today* reported that a call to several of the private payers (Cigna, Aetna, UnitedHealthCare) revealed that they were studying whether to follow suit.



Kathleen B. Digre, MD, specializes in neuro-ophthalmology. She evaluates and treats complex visual complaints which can be due to optic nerve or brain disease. Her interests include gender differences in neuro-ophthalmic disorders, pseudo tumor cerebri, ischemic optic neuropathy, temporal arteritis, papilledema, episodic vision loss, headaches and eye pain, diplopia and Graves' Disease. She has worked with NANOS and the University Eccles Library to develop a Neuro-ophthalmology virtual educational library (NOVEL).

Dr. Digre also edited a book that just came out: Jones RE, Digre KB. *Diabetes: Focus on Women*. University of Utah 2011





Jason Goldsmith, MD, focuses on the medical and surgical management of cataracts and glaucoma. Dr. Goldsmith's research interests include the use of optical coherence tomography, an ophthalmic imaging technology, for use in screening for angle closure glaucoma.



Roger P. Harrie, MD, practices comprehensive ophthalmology and ocular surgery with a subspecialty in ophthalmic ultrasound. He is the senior instructor in the ocular ultrasound course at the annual American Academy of Ophthalmology meeting. He has carried out more than 20 medical missions, mostly training doctors in developing countries in diagnostic and therapeutic techniques.

Bilateral explantation of Visian Implantable Collamer Lenses secondary to bilateral acute angle closure resulting from a non-pupillary block mechanism.

Author: Khalifa YM, Goldsmith J, Moshirfar M.

Journal: J Refract Surg. 2010 Dec;26(12):991-4.

PURPOSE: To report a case of bilateral non-pupillary block angle closure glaucoma after Visian Implantable Collamer Lens (ICL, STAAR Surgical) surgery.

METHODS: A 35-year-old woman with high myopia, white-to-white measurements of 11.8 mm in the right eye and 11.9 mm in the left eye, and anterior chamber depths >3 mm in both eyes underwent simultaneous bilateral ICL implantation with 13.2-mm lenses.

RESULTS: Persistent, bilateral acute angle closure developed despite multiple patent peripheral iridotomies and iridectomies. Visante anterior segment optical coherence tomography (AS-OCT, Carl Zeiss Meditec) revealed profound vaulting of the ICLs and angle closure. Both ICLs were explanted. After explantation, ultrasound biomicroscopy demonstrated a sulcus-to-sulcus diameter of 10.8 mm in the right eye and 11.2 mm in the left eye.

CONCLUSIONS: The correlation between white-to-white and sulcus-to-sulcus measurements were poor in this patient, resulting in extreme vaulting of the ICL and angle closure from a non-pupillary block mechanism. Proper identification of the mechanism of angle closure is aided by AS-OCT. For non-pupillary block mechanisms, ICL extraction is necessary.

CT and Orbital Ultrasound Findings in a Case of Castleman Disease.

Author: Brubaker JW, Harrie RP, Patel BC, Davis DK, Mamalis N.

Journal: Ophthal Plast Reconstr Surg. 2010 Aug 10.

ABSTRACT: A 53-year-old man with a 2-month history of left periorbital swelling was found to have a large solid intraconal mass on CT scan. Orbital ultrasound showed that the lesion had a cavernous pattern of internal reflectivity. Histopathology revealed hyaline-vascular type Castleman disease (CD). This article represents the first reported orbital ultrasound findings in CD. The findings of CT scan and ultrasound may be useful in the preoperative evaluation of orbital hyaline-vascular type CD.

Retained nuclear fragment found during Descemet-stripping automated endothelial keratoplasty.

Author: Mifflin MD, Neuffer MC, Mamalis N.

Journal: J Cataract Refract Surg. 2011 Jan 17.

ABSTRACT: An 82-year-old man with a 2- to 3-month history of progressive visual loss due to corneal edema was referred to our center. The ocular history was significant for uneventful cataract surgery approximately 3 years earlier. Pseudophakic bullous keratopathy was diagnosed and Descemet-stripping automated endothelial keratoplasty (DSAEK) performed. During surgery, a retained nuclear fragment was discovered in the anterior chamber. The fragment was removed and the DSAEK completed successfully. At the 4-month follow-up, the symptoms had completely resolved and the uncorrected distance visual acuity in the affected eye was 20/40. **FINANCIAL DISCLOSURE:** No author has a financial or proprietary interest in any material or method mentioned.

Keratitis and Corneal Melt With Ketorolac Tromethamine After Conductive Keratoplasty.

Author: Khalifa YM, Mifflin MD.

Journal: Cornea. 2010 Nov 17.

PURPOSE: To report a case of keratitis and corneal melt after conductive keratoplasty (CK) enhancement.

METHOD: Case report.

RESULTS: A 52-year-old woman with emmetropic presbyopia had undergone previous CK for monovision and underwent CK enhancement 4 years later. Postoperatively, she was managed with ketorolac tromethamine 0.4% and developed keratitis and corneal melt.

CONCLUSIONS: This is the first reported case of keratitis and corneal melt associated with nonsteroidal anti-inflammatory topical medications in a post-CK patient.



Majid Moshirfar, MD, FACS

Softec HD hydrophilic acrylic intraocular lens: biocompatibility and precision.

Author: Espandar L, Sikder S, Moshirfar M.

Journal: Clin Ophthalmol. 2011 Jan 10;5:65-70.

ABSTRACT: Intraocular lens development is driven by higher patient expectations for ideal visual outcomes. The recently US Food and Drug Administration-approved Softec HD™ lens is an aspheric, hydrophilic acrylic intraocular lens (IOL). The hydrophilic design of the lens is optimized to address dysphotopsia while maintain-

ing biocompatibility, optical clarity, resistance to damage, and resistance to biocontamination. Aspheric lenses decrease postoperative spherical aberration. The addition of the Softec lens provides clinicians with another option for IOL placement; however, randomized comparative studies of this lens to others already on the market remain to be completed.



Nick Mamalis, MD

Toxic anterior segment syndrome: common causes.

Author: Cutler Peck CM, Brubaker J, Clouser S, Danford C, Edelhauser HE, Mamalis N.

Journal: J Cataract Refract Surg. 2010 Jul;36(7):1073-80.

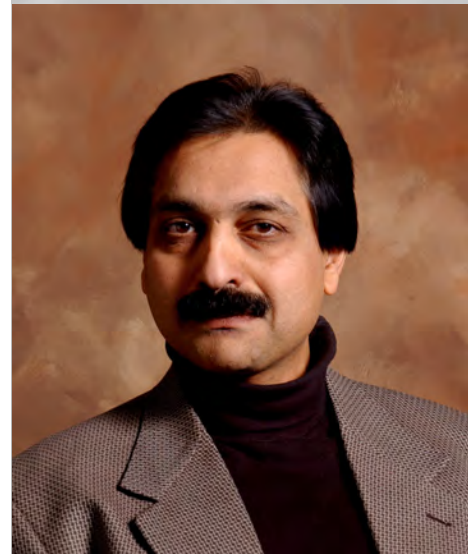
PURPOSE: To identify the most common risk factors associated with toxic anterior segment syndrome (TASS).

SETTING: Ophthalmic surgical centers in the United States, Argentina, Brazil, Italy, Mexico, Spain, and Romania.

METHODS: A TASS questionnaire on instrument cleaning and reprocessing and extraocular and intraocular products used during cataract surgery was placed on the American Society of Cataract and Refractive Surgery



Mark D. Mifflin, MD, is the Residency Program Director and Education Director for the Dept of Ophthalmology, and Medical Director, Utah Lions Eye Bank. He specializes in the medical and surgical treatment of corneal and anterior segment eye diseases. His expertise includes all types of corneal transplantation, cataract surgery, and vision correction using lasers, intra-ocular lenses, and conductive keratoplasty.



Bhupendra Patel, MD, FRCS, FRC, is an expert in the management of disorders involving eyelids, peri-orbital tissues, the lacrimal system, and facial bones including fractures. His clinical research interests include thyroid disease, optic nerve disorders, orbital and eyelid tumors, blepharospasm, lacrimal surgery and facial cosmetic surgery.



web site. A retrospective analysis of questionnaires submitted by surgical centers reporting cases of TASS was performed between June 1, 2007, and May 31, 2009, to identify commonly held practices that could cause TASS. Members of the TASS Task Force made site visits between October 1, 2005, and May 31, 2009, and the findings were evaluated.

RESULTS: Data from 77 questionnaires and 54 site visits were analyzed. The reporting centers performed 50 114 cataract surgeries and reported 909 cases of TASS. From January 1, 2006, to date, the 54 centers reported 367 cases in 143 919 procedures; 61% occurred in early 2006. Common practices associated with TASS included inadequate flushing of phaco and irrigation/aspiration handpieces, use of enzymatic cleansers, detergents at the wrong concentration, ultrasonic bath, antibiotic agents in balanced salt solution, preserved epinephrine, inappropriate agents for skin prep, and powdered gloves. Reuse of single-use products and poor instrument maintenance and processing were other risk factors.

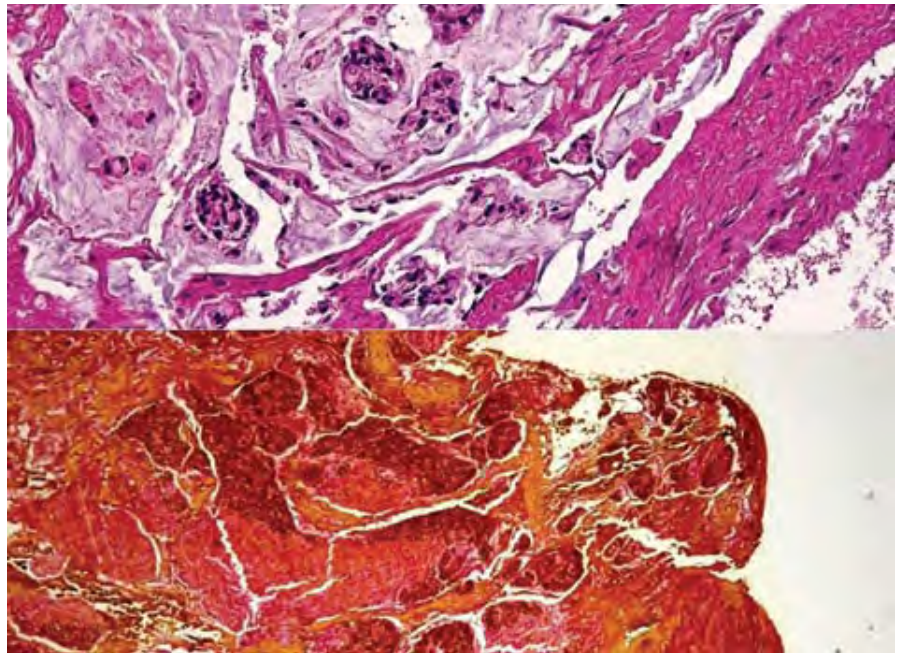
CONCLUSIONS: The survey identified commonly held practices associated with TASS. Understanding these findings and the safe alternatives will allow surgical center personnel to change their practices as needed to prevent TASS.

Metastatic mucinous adenocarcinoma of the orbit.

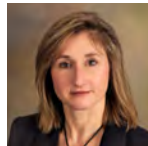
Author: Monson BK, Patel BC, Kim CH.

Journal: Orbit. 2011 Jan;30(1):18-20.

ABSTRACT: Metastatic mucinous adenocarcinoma in the orbit is extremely rare. We review the literature and report a case of metastatic mucinous adenocarcinoma of the orbit in a 37-year-old male with primary pancreatic adenocarcinoma.



Top photo. Photomicrograph of a metastatic mucinous adenocarcinoma in a 37 year-old male. Note the islands of epithelioid cells within pools of mucinous material that, in turn, are surrounded by dense fibrous tissue. (H&E; original magnification, 10X) Bottom photo. Positive mucicarmine stain for intracytoplasmic mucicarmineophilic mucin. The positive mucicarmineophilic cells and negative S100 protein favor mucinous adenocarcinoma over chordoma. (mucicarmine stain; original magnification, 2X) 68x89mm (300 x 300 DPI)



**Barbara Wirostko,
MD**

Lack of evidence for a link between latanoprost use and malignant melanoma: an analysis of safety databases and a review of the literature

Author: Tressler CS, Wiseman RL, Dombi T, Jessen B, Huang K, Kwok KK, Wirostko B.

Journal: BJO, In Press

AIM: To determine if an association exists between the use of latanoprost ophthalmic solution and malignant melanoma and to assess the evidence of a plausible biological mechanism.

METHODS: Two safety databases were reviewed: one representing all latanoprost (n=24) and fixed-combination latanoprost/timolol (n=16) clinical trials conducted from November 1992 through November 2007 and a global safety database of all spontaneous nontrial-related clinical reports

spanning 13 and 9 years for latanoprost and for latanoprost/timolol, respectively. A systematic PubMed search for studies evaluating potential mechanisms was conducted.

RESULTS: Amongst 12 880 latanoprost-treated subjects in clinical trials, no reported cases of ocular melanoma and three cases of cutaneous melanoma were identified. Of 19 940 cases recorded in the global safety database, 22 reports of ocular/cutaneous neoplasms were identified. Of these neoplasms, 11 were ocular and six were cutaneous melanomas. Possible association with latanoprost use could not be excluded in three ocular and one periorbital report. In vitro and in vivo data are consistent with a mechanism whereby the increased iris pigmentation results from stimulation of melanin synthesis by induction of tyrosinase transcription without increasing mitotic activity.

CONCLUSION: Presently, no evidence exists that establishes a link between latanoprost use and either ocular or cutaneous melanoma.

Contrast sensitivity, ocular blood flow and their potential role in assessing ischaemic retinal disease

Author: Shoshani YZ, Harris A, Rusia D, Spaeth GL, Siesky B, Pollack A, Wirostko B.

Journal: ACTA Oph, 2011, In Press

PURPOSE: To examine the definition, evaluation methodology, association to ocular blood flow and potential clinical value of contrast sensitivity (CS) testing in clinical and research settings, focusing in patients with ischemic retinal disease.

METHODS: A review of the medical literature focusing on CS and ocular blood flow in ischemic retinal disease.

RESULTS: CS may be more sensitive than other methods at detecting subtle defects or improvements in primarily central retinal ganglion cell function early on in a disease process. CS testing attempts to provide spatial detection differences which are not directly assessed with standard visual acuity chart testing. Analyzing all studies that have assessed both CS change and ocular blood flow, it is apparent that both choroidal circulation and retinal circulation may have an important role in influencing CS.

CONCLUSION: The concept that CS is directly influenced by ocular blood flow is supported by reviewing the studies involving both. Although the studies in the literature have not established a direct cause and effect relationship per se, the literature review makes it logical to assume that changes in retinal and choroidal blood flow influence CS. This raises the possibility that a subjective visual characteristic, specifically CS, may be able to be evaluated more objectively by studying blood flow. It appears appropriate to study the relationship between blood flow and CS more extensively to develop improved ways of measuring various aspects of blood flow to the eye and to best quantify early changes in visual function.



The John A. Moran Eye Center Approved for New Vision Institute

Institute status will foster multidisciplinary collaborations to accelerate research to new patient treatments



The Vision Institute at the John A. Moran Eye Center at the University of Utah is dedicated to serving our patients and the greater public health community by creating a broad-based organization focused on clinical care, caregiver education, and basic and translation research. Using a multidisciplinary approach we encourage learning from our patients and using that knowledge to create effective educational and research programs with the goal of creating new, widely available treatments for diseases shared by our patients and the global health community.

R. and Edna Wattis Dumke Clinical Pavilion



The John A. Moran Eye Center (JMEC) announces the formation of The Vision Institute. The establishment of The Vision Institute bridges research efforts across University of Utah colleges and departments to enhance and broaden the area of translational medicine. This team approach into the study of diseases will help turn research discoveries into drugs and medical devices that benefit patients.

“The Vision Institute creates an environment for sciences to work together and connects research throughout the campus,” says Randall J. Olson, M.D., professor and chair of the Department of Ophthalmology and Visual Sciences and the U of U and CEO of JMEC.

Forming The Vision Institute includes the establishment of the Moran Center for Translational Medicine. “Our goal is the acceleration of the translation of basic scientific discoveries to clinically effective diagnostics and therapies for the treatment of devastating eye disorders such as age-related macular degeneration and glaucoma, as well as other diseases with shared etiologies,” Olson said.

Gregory Hageman, Ph.D., professor of Ophthalmology and Visual Sciences, who recently came to JMEC from the University of Iowa, leads the Moran Center for Translational Medicine. “Research activities must reach the ‘marketplace’ to have

an impact on patient care. Developing partnerships through The Vision Institute is key to making this happen and they will help us to develop coordinated strategies and provide a thorough understanding of disease biology,” says Hageman.

Worldwide research, along with findings from JMEC indicates many of the most serious blinding diseases are often accompanied by the presence of a distinct set of coexisting or additional diseases, called comorbidities. Genetic study of the various diseases and their respective comorbidities shows diseases of the eye often affect multiple organ systems, rather than being limited to ocular tissues. To understand these diseases JMEC works with a variety of other research disciplines and clinical specialties.

“The scope of research and technical expertise in the JMEC now far transcends the study of vision and extends into systemic disease biology, cancer research, brain plasticity, gene therapies, new imaging technologies and new molecular tools. The collaborative relationships of our faculty range from physics and computer sciences to bioengineering and infectious diseases. It is fitting to encompass this ever-broadening scientific horizon in The Vision Institute, with its far larger scientific and translational missions,” said Robert Marc, Ph.D., Director of Research at JMEC.



The following individuals and organizations contributed to the Moran Eye Center from January 1, 2010 through December 31, 2010

Gifts of \$500,000 and Above

Bamberger-Allen Health & Education Foundation
John A. Moran

Gifts of \$100,000 and above

Allergan, Inc.
Alexander S. Bodi
Gayle L. Eschmann
Research to Prevent Blindness

Gifts of \$50,000 and above

Alcon Laboratories, Inc.

Alan J. and Berte Hirschfield
Randall and Ruth Olson

Gifts of \$25,000 and above

Abbott Medical Optics
The Boyd Henrie Family

Gifts of \$10,000 and above

Lance D. Alworth Family Trust
Anonymous
John I. and Toni F. Bloomberg
Ian and Annette Cumming
John B. and Geraldine W. Goddard
JeNeal Hatch
G. Mitchell and June M. Morris
Marcia and Gordon M. Olch
Rayner Intraocular Lenses, Ltd
Noel and Florence Rothman Family
The Semnani Family Foundation
Denise R. Sobel
University of North Carolina/Chapel Hill
Utah Lions Foundation

James W. and Jeanne Welch

Gifts of \$5,000 and above

Burningham Foundation
Anthony J. Chaudry
Margaret D. Hicks
Johnson Foundation - Jamestown, New York
Ralph and Marge Neilson
Hazel M. Robertson
Richard and Carmen Rogers

Gifts of \$1,000 and above

David R. and N. L. Anderson
Anonymous
Marvin L. Arent
Ralph L. Ashton
Richard E. Ashworth
Rodney H. & Carolyn Hansen Brady Foundation
Laura D. Byrne
Robert A. and Ann J. Carlson
Robert S. Carter Foundation
F. Burton Cassity
Whit and Fran Cluff
Julie Crandall and Alan Crandall, MD
Robert and Carol Culver
Thomas and Candace Dee Family
Katherine W. Dumke & Ezekiel R. Dumke Jr., Foundation
William and Fern England Foundation
Joan B. and John H. Firmage
Nicholas and Courtney Gibbs
Leah Hatzithanasiou and Family
Lisette and C. Charles Hetzel, III
Brad, Tracey, Sam, Jonah and Zev Katz
The Mark and Kathie Miller Foundation
Helga E. Kolb and Richard A. Normann
Edward N. and Carol Scott Robinson
William L. Rogers Foundation
Tueng T. Shen, MD
Howard S. Spurrier
Robert and Luree Welch
Louise and Norman A. Zabriskie, MD
Robert C. and Patience Ziebarth

Gifts of \$100 and above

G. Howard and C. LaRue Abplanalp
Hans and Martha Ahrens
Anita and Sylvan Alcabes
Milton and Dianne Anderson
Anonymous
Brock K. Bakewell, MD
John Bendixen
David and Margaret Bernhardt
Emmy Blechmann
Lyman and Jane Brothers
Harold W. and Violet Johnson Brown Charitable Foundation
Dolores and Raymond Buchanan
William L. and Sheral L. Calvin
Colleen F. Carter
Irene G. Casper
Pauline and George Childs
Don and Anne Christensen
Blaine and Jacquelyn Clements
CLM Marketing, LLC

Donna B. and John C. Cole
 Marjorie A. and Don A. Coleman, MD
 Nancy C. Cook and Joseph V. Cook, MD
 Taylor V. and Nancy Cooksey
 Drury W. Cooper
 Lisa Crandall and David A. Crandall, MD
 Yohannes Dagne and Negedework
 Gebreselassie
 Craig W. Dayhuff
 Larry A. Donoso, MD, PhD, JD, MBA
 Gayle and R. Michael Duffin, MD
 East Millcreek Lions Club
 Karen Ehresman
 Lavon and Richard Erickson
 Fred W. and Christine Fairclough
 Spencer P. and Barbara S. Felt
 Fidelity Charitable Gift Fund
 Peter Q. Freed
 Roger C. Furlong, MD
 D. Jay and Lynda Gamble
 Jane C. and Neil L. Getzelman
 Mickey D. Gillespie
 William A. and Claudia M. Gislason
 Kathryn A. Goodfellow, RPh
 Dee Ann Gornichec
 Robert and Joyce Graham
 Lois Guest
 Frank J. and Gloria Gustin
 William B. Hale
 Sharan and Blaine Hale
 David G. and Donna Ann Hall
 Hammi Medical Inc.
 Phyllis F. Hellar Trust
 Henry Day Ford
 Ruth A. Hensel
 Daggett H. and Sara G. Howard
 Edward and Roberta Hughes
 Gil and Thelma Iker
 Sheila O. and Lewis F. Jensen
 Frank J. and Sally Johnson
 Carol A. Jost
 Laurel D. and Charles Kay
 Drs. Robert M. and Jeryl D. Kershner
 Geraldine and Paul Kilpatrick
 William M. Kleinschmidt and Julia
 J. Kleinschmidt, PhD
 Mary G. and G. Douglas Krieger
 Irmgard and Max Kunz
 Peter G. and Geraldine S. Kypreos
 Olle S.T. and Andrea Hart Larsson
 Dixie and Larry Lehman
 Donna M. Luers and Patrick R.
 Luers, MD
 Willard Z. Maughan, MD and Rona Lee
 Maughan, PhD
 William and Julie McCarty
 Beth and Edward M. McGill, MD
 Craig and Polly McQuarrie
 Marvin A. and Renee B. Melville
 Corey A. and Nancy J. Miller
 William L. Miller
 Moab Lions Club
 William K. and Diane Moore
 Edward B. and Barbara Cannon Moreton
 Ruth A. Morey
 Marilyn Mott, RN
 David and Jann Nelson

Elizabeth Ann Nielson
 Joan J. and Charles W. Odd
 Eugene and Jean Overfelt
 D.A. and Joseph J. Palmer
 Linda Rankin
 Mervin J. and Verna B. Rasmussen
 Rita and Ralph Reese
 Carol A. and Stanley J. Riemer
 Raye C. and Joseph F. Ringholz
 Salt Lake City Lions Club
 John F. Schroll
 Susan Beatty Schulman
 Elaine and Paul Schwanebeck
 Marilyn Schwartz
 Michael R. and Loretta G. Falvo-Scott
 Suzanne M. and D. Brent Scott
 John L. and Carole Sellstrom
 Gregory J. Skedros
 Albert H. Small
 Stewart R. Smith
 James M. and Linda W. Steele
 Shirley N. Stevenson
 Carlton T. Sumsion
 Barbara Tingey
 Utah Nonprofits Association
 Valley of the Sun United Way
 Michael W. Varner, MD and Kathleen
 B. Digre, MD
 Deborah C. Walker
 Elmer M. and Beverly J. Wardell
 Judith S. and Douglas G. Waters
 Wells Fargo Dealer Services
 Bart and Marlene Wheelwright
 Mary Jo C. and J. Ross Wight
 Michael B. Wilcox, MD, PC
 Carlene A. and John C. Williams
 Donna and Carl T. Woolsey, Sr, MD
 Gerard and Dominique Yvernault

Planned Gift

The following individuals and organizations designated a planned gift to the Moran Eye Center from January 1, 2010 through December 31, 2010

Richard A. Fay and Carol M. Fay

In Memory of

Those in whose memory gifts were made to the Moran Eye Center from January 1, 2010 through December 31, 2010

David Arbuckle
 William F. Bailey
 Douglas L. Beckstead
 William S. Brown
 Kyle Carlile
 Michael Cooper
 Cecil P. Counts
 Winona H. Cowan
 Henry J. Desz
 Cortis B. Griebel

Leonard Clark Hardy
 LaVilla Shomaker Henrie
 Kim A. Howes
 Donald C. Husband
 Dr. Wallace V. Jenkins
 Joanne C. Kettner
 J. Alejandro Langford
 John H. Littlefair
 Richard P. Makoff
 Storey A. Mills
 Steven J. Nichols
 Altamae G. Niesen
 William K. Olson
 Robert S. Pattison
 Anna K. Picco
 Sarah-Jane Powell
 D. Dale Ratliff
 Frances H. Redington
 Robert L. Rees
 Jerry Rich
 Peggy Stewart Rogers
 Matthew R. Simmons
 Bartley H. Stowell
 Calvin W. Thomson
 Donald M. Willey

In Honor of

Those in whose honor gifts were made to the Moran Eye Center from January 1, 2010 through December 31, 2010

Captain Daniel M. Anderson, MD
 Alan S. Crandall, MD
 Elmer Inman
 Renee Krebs
 Warren V. Kunz
 Jean H. and Lamar Miller
 John Mills
 Sandee Mills
 Matthew R. Parsons, MD
 Geoffrey Tabin, MD
 Judith Warner, MD
 Stephen Wynn

The Moran Eye Center is very grateful for the contributions made to support our mission and goals. We have made every effort to ensure that this 2010 Donor Report is as accurate as possible. Should you find an error or wish to change your listing, please feel free to contact us at (801) 585-9700.



The John A. Moran Eye Center is committed to the goal that no person with a blinding condition, eye disease or visual impairment should be without hope, understanding and treatment.



John A. Moran Eye Center
65 Mario Capecchi Drive
Salt Lake City, UT 84132

Telephone 801.581.2352
Fax 801.581.3357

© 2011 Moran Eye Center
All Rights Reserved